

Long Island University

Digital Commons @ LIU

Selected Full-Text Dissertations 2020-

LIU Brooklyn

2021

Ex vivo dermis microdialysis: A tool for bioequivalence testing of topical dermatological drug product (Demonstration of proof of concept and testing)

Mohammad Asif Ali
Long Island University

Follow this and additional works at: https://digitalcommons.liu.edu/brooklyn_fulltext_dis



Part of the [Pharmacy and Pharmaceutical Sciences Commons](#)

Recommended Citation

Ali, Mohammad Asif, "Ex vivo dermis microdialysis: A tool for bioequivalence testing of topical dermatological drug product (Demonstration of proof of concept and testing)" (2021). *Selected Full-Text Dissertations 2020-*. 37.

https://digitalcommons.liu.edu/brooklyn_fulltext_dis/37

This Dissertation is brought to you for free and open access by the LIU Brooklyn at Digital Commons @ LIU. It has been accepted for inclusion in Selected Full-Text Dissertations 2020- by an authorized administrator of Digital Commons @ LIU. For more information, please contact natalia.tomlin@liu.edu.

**Ex Vivo Dermis Microdialysis: A Tool for Bioequivalence Testing of
Topical Dermatological Drug Product
(Demonstration of Proof of Concept and Testing)**

A DISSERTATION SUBMITTED
IN PARTIAL FULFILLMENT OF THE REQUIREMENTS
FOR THE DEGREE OF

DOCTOR OF PHILOSOPHY

WITH SPECIALIZATION IN PHARMACEUTICS

TO THE FACULTY OF THE ARNOLD & MARIE SCHWARTZ COLLEGE
OF PHARMACY AND HEALTH SCIENCES
LONG ISLAND UNIVERSITY
BROOKLYN, NEW YORK

April 2021

BY

MOHAMMAD ASIF ALI

Approval by:

Sponsoring Committee

Grazia Stagni, Ph.D., Chair

Avinash Kumar, Ph.D.,
Committee member

Yousuf Mohammad, Ph.D.,
Committee member

Lakshmi Raghavan, Ph.D.,
Committee member

Christopher Surratt, Ph.D.,
Associate Dean of Research

Dedication

To my loving parents

For their relentless sacrifices and untiring hard work to keep me comfortable with every means, they could afford. I feel pride in the persistent hope they have shown upon me.

Thanks, Mama and Papa, I finally did it!

Acknowledgment

All praise for Allah, the most merciful and beneficent.

I express my sincere regards to my Ph.D. mentor and supervisor Prof. Grazia Stagni for all her guidance and wisdom throughout this project. I am indebted to her steady support from the inception to the completion of this project. She has always been an inspiration and a source of incredible thinking, it would not have been possible without her guidance. Her insightful feedback pushed me to sharpen my thinking and brought my work to a higher level.

Special gratitude to Dr. Yousuf Mohammad for responding to my phone call and messages immediately, despite being in opposite time zones. He has not only been a great scientific advisor but also a good friend. I feel blessed to have him on my dissertation committee. Thanks to Dr. Lakshmi Raghavan for his continued support and advice. Thanks to Dr. Avinash Kumar for his insights on the project.

I would like to extend my gratitude to Dr. Kerry Weinberg for her generosity in sharing the ultrasound equipment, and for communicating her expertise in ultrasound imaging. Thanks to Dr. Rutesh Dave, former Division Director at Long Island University, and Dean Surratt for their support, mentorship, funding opportunities, and constructive criticisms. Special thanks to Aruna Kissoon, my academic advisor for being patient with me and providing us with the necessities to keep the research uninterrupted. My thanks to the entire faculty at the Arnold & Marie Schwartz College of Pharmacy and Health Sciences for their invaluable assistance and tutelage

A special thanks to my friend Dr. 'Sunshine' Kuzma, he has been a great support and collaborator during my stay in LIU. Many thanks to Rucha, Sharareh, my other labmates, colleagues, friends, and AAPS student chapter members for a cherished time spent together in the lab, and in social settings.

I wish to reserve a special credit for my guardian angel uncle, Dr. Shamim Ahmed, for standing there with me forever. When I was a child, his personal and professional achievements were an inspiration to me; and when I wanted to follow his footsteps, I always found him by my side with untiring support- protecting me from all harm. Thanks for being my scientific, professional and personal trainer.

Life in New York City is fast-paced and lonely. I would like to thank my friends from Ozone Park- Sohail and Lincoln for their moral support and happy distractions to my mind during this emotional journey. Also, I would like to thank my friends from India- Aammar, Meran, and Neha for stimulating me to pursue this journey. Thank you all for your wise counsel and sympathetic ear.

A larger share of this achievement is deserved by my hard-working parents. They have sacrificed their entire life for the better future of my younger brother and mine. They have never failed in providing unconditional love and care. I love you mom and dad, and I would not have made it this far without you two. My younger brother Arif has pressed me to pursue this emotional journey and since then he has been feeling lonely, I wanted to express how much I love him, and wanted to thank him for taking care of our parents since I left them back home.

There has been a lot of achievements in the past five years- professionally and personally. One of the best was marrying my wife- Saadiya. She has been indulgent and instrumental in instilling confidence in me. Saadiya has become my greatest support and loved me unconditionally in all my ups and downs. I thank her for her being compassionate toward me even at times when I was irritable and depressed. I am happy we have traveled this path together, we have embraced the tough times, learned, and loved each other, and strengthened our commitments.

~ Mohammad Asif Ali

Abstract

Clinical response to most topical dermatological drug products (TDDP) depends on the availability of the drug in the dermis. Dermal Microdialysis (dMD) is a sampling technique that permits measuring the concentration of a drug over time, in vivo, directly into the target tissue, the dermis. The pharmacokinetic parameters obtained from such studies may help to optimize the development of TDDP and potentially can be applied to the assessment of TDDP bioequivalence. However, these studies require several hours or even days of continuous sampling that makes it often stressful and unpractical for human subjects as well as animals. The goal of this dissertation was to develop a reliable and consistent ex-vivo dMD method to complement and assist in vivo dMD experiments.

In the first part of the project, we have developed and tested the ex-vivo dermal microdialysis method on two different experimental skin models using freshly excised porcine skin. Porcine skin was selected due to the close resemblance to human skin, it is advantageous in terms of availability and expense. For the microdialysis study, in-house dermal microdialysis probes were conveniently manufactured with controlled specifications and the microdialysis recovery process was screened with an in vitro setup to match the intended use. The in vitro microdialysis method was optimized for probe specification, analyte suitability, perfusion flow rate, and perfusate composition. A maximized, rapid, and steady recovery was demonstrated within a wide range of concentrations. For the ex vivo dermal microdialysis study, the two different skin models developed were: M1-- Full-thickness skin (≈ 0.25 cm) without subcutaneous fat layer placed on a hydrated 0.5 cm cellulose backing support, and M2 -- Full-thickness skin with subcutaneous fat layer (total thickness = 1.0 cm) placed directly on an aluminum boat, avoiding any kind of hydration. Both setups were tested on TDDP cream and gel of metronidazole

(MTZ) for which both in vivo and IVPT data are available for comparison. The two different formulations, Metronidazole cream and gel, were compared side-by-side for the rate and extent of delivery to the dermis. The latter skin model was found suitable, manifesting data comparable to the available data from in vivo pig and IVPT (human cadaver) study. The selection of the best-fit-model was based on the comparative bioavailability response from the negative control, Metronidazole gel, resulting in a lower bioavailability profile (90% CI). Using this suitable ex vivo dMD model, site-specific results of the drug can be conveniently monitored in the dermis leading to dose-dependent rate and extent in concentration-time exposure.

The M2 model was further tested for the effect of temperature of the skin on the bioavailability profile of the drug. As reported in several pieces of literature, an increase in dermal exposure is expected with the rise in skin temperature. Superficial addition of heat to the skin was not feasible as it may change the thermodynamics of the formulation leading to alteration in permeation kinetics. Thus, the physiological temperature of ex vivo pig skin explant was achieved by providing continuous heat from the ventral side using a closed water-bath system. The process of supplementation of temperature did not impact the bioavailability profile, rather unfavorable damages to the skin microstructure due to thermal degradation was observed. Further studies with the proposed model ex vivo dMD model were conducted at ambient lab temperature.

Yet another aspect of the proposed model was to test its capability to determine bioequivalence (BE). The potential of using this model for BE testing was validated by comparing the BA of MetroCream with its USFDA-approved generic Metronidazole 0.75% cream. The overall BE estimation resulted in an \ln -AUC of 91.65 (80.93, 104.88) and an \ln -C_{max} value of 87.56 (74.87,102.39). The fact that reference and test formulations can be tested simultaneously at multiple sites on a skin sample harvested from a single animal subject reduces the burden of

inter-subject variability. The experimental population size required to establish bioequivalence for topically applied drugs can be reduced.

Yet another aspect of the study was to design a mathematical model, based on the ex vivo dMD findings, to extend its predictability to in vivo outcomes. A first-of-its-kind unit impulse response method was applied in dermis tissue of skin explant to measure the absorption independent elimination parameters. The estimated parameters were employed to calculate the cumulative absorption of the drug from different topical formulations. The absorption profile of the developed model was time-scaled and absolute-scaled with a permeation scaling factor to map with available literature data on in vivo pig. The levy point-to-point regression coefficient was employed to predict the in vivo PK profile thereafter. With the current intervention, we propose a mathematical possibility to predict in vivo outcomes for a given topical dose. The studies presented were limited internal predictions only, and external validation with a different set of data is yet to be performed and to be undertaken at another time.

Overall, the studies presented in this work provides a foundation stone for an elaborate field of work that can be undertaken to minimize the use of animal in pharmacokinetic evaluations for topical and transdermal products. Ex vivo dermal microdialysis warrants testing on a plethora of drug molecules of different polarities to decide on the future of the technique. Regardless, the technique holds unmet potential and needs to be nurtured over time.

Table of content

Dedication	ii
Acknowledgment.....	iii
Abstract	v
Table of content	viii
List of Figures.....	xiii
List of Tables	xv
List of Abbreviations	xvi
Chapter 1: Introduction	1
1.1 Statement of Problem.....	2
1.2 Rationale for the Study.....	3
1.3 Specific Aims	7
1.4 Schematics of the overall goal of the research work.....	8
Chapter 2: Background	9
2.1 Skin structure and the source of variability in permeation between species	10
2.2 Permeation pathway	11
2.3 Topical dermatological drug products Bioequivalence: A regulatory perspective.....	12
2.4 Alternative approaches to the human skin model	13
2.5 Microdialysis.....	14
2.6 The current state of ex vivo dermal microdialysis studies.....	15

Chapter 3: Determination of Relative Recovery of The Dermal Microdialysis Probe And

Assessment of Influence of Perfusion Rate on The Recovery. 17

3.1	Introduction	18
3.2	Method	19
3.2.1	Microdialysis Probe.....	19
3.2.2	HPLC method.....	20
3.2.3	In vitro dose linearity study.....	20
3.2.4	In vitro flow rate optimization study.....	22
3.3	Results.....	23
3.3.1	HPLC Analytical method.....	23
3.3.2	In Vitro linearity study	24
3.3.3	Flow rate study	26
3.4	Discussion	26
3.5	Conclusion.....	28

Chapter 4: Development of An Ex-Vivo Dermal Microdialysis Model for Characterization of Dermal Disposition of Drug from Topical Dermatological Drug Products..... 29

4.1	Introduction	30
4.2	Method	32
4.2.1	Chemicals and reagents.....	32
4.2.2	HPLC Analytical method.....	32
4.2.3	Dermal Microdialysis Probe	32
4.2.4	Ex vivo experimental setup	33
4.2.5	Probe depth measurement.....	36
4.2.6	Dose-Response study	36

4.2.7	Data processing	37
4.2.8	Statistical analysis	37
4.3	Results.....	38
4.3.1	Lateral diffusion	38
4.3.2	Dermal Pharmacokinetic profile	38
4.3.3	Relationship of Permeation profile with probe depth.....	41
4.3.4	Dose-response study:.....	45
4.4	Discussion	46
4.5	Conclusions	49

Chapter 5: Effect Of Temperature On Permeation Of Formulation Using Ex Vivo Dermal

Microdialysis Method	51	
5.1	Introduction	52
5.2	Method	53
5.2.1	Chemicals and reagents.....	53
5.2.2	HPLC Analytical method.....	54
5.2.3	Experimental setup	54
5.2.4	Ultrasound measurement.....	56
5.2.5	Data processing	56
5.2.6	Statistical analysis	56
5.3	Results.....	57
5.3.1	Dermal Pharmacokinetic profile	57
5.3.2	Ultrasound Measurement.....	60
5.4	Discussions.....	61
5.5	Conclusions	62

Chapter 6: Feasibility Testing Of A Bioequivalence Study Of Metronidazole Cream

Using An Ex Vivo Dermal Microdialysis Method. 64

6.1	Introduction	65
6.2	Method	66
6.2.1	Chemicals and reagents.....	66
6.2.2	HPLC Analytical method.....	66
6.2.3	Ex vivo experimental setup	67
6.2.4	Data processing	68
6.2.5	Statistical analysis	68
6.3	Results.....	69
6.3.1	Dermal Pharmacokinetic profile	69
6.3.2	Bioequivalence testing.....	71
6.4	Discussion	72
6.5	Conclusions	73

Chapter 7: Estimation of Dermal Unit Impulse Response in Skin Ex Vivo, Absorption-Independent Drug Disposition in Dermis and Development of An Ex Vivo- In Vivo Co-relationship. 74

7.1	Introduction	75
7.2	Method	78
7.2.1	Chemicals and reagents.....	78
7.2.2	HPLC Analytical method.....	78
7.2.3	Bioavailability and dUIR experimental design.....	79
7.2.4	Retrodialysis and Microdialysis procedure.....	80
7.2.5	Estimation of dermal disposition	81
7.2.6	Ex vivo in vivo correlation (EVIVC) development	82

7.2.7	Extrapolation of ex vivo data to in vivo PK profile and validation.....	83
7.2.8	Statistical analysis	84
7.3	Results.....	85
7.3.1	Ex vivo dermal bioavailability and disposition.....	85
7.3.2	Dermis Unit Impulse Response (dUIR)	86
7.3.3	Ex vivo in vivo correlation (EVIVC) development	87
7.3.4	Extrapolation of ex vivo data to in vivo PK profile and validation.....	91
7.4	Discussion.....	93
7.5	Conclusions.....	96
Chapter 8: Conclusion and General Discussions		98
References.....		104

List of Figures

Figure 1.1: Schematic representation of the overall study	8
Figure 2.1: Drug permeation pathways in the stratum corneum	11
Figure 3.1: Sample schematics of the dMD probe placement for in vitro Relative Recovery study.	21
Figure 3.2: Sample schematics of the dMD probe placement for in vitro flow rate study.	22
Figure 3.3: Representative chromatogram from HPLC	23
Figure 3.4: Recovery of MTZ from bulk in-vitro at different concentrations.	25
Figure 3.5: Linear relationship of Steady-State Recovery of MTZ from bulk in vitro	25
Figure 3.6: Recovery of MTZ from bulk in-vitro at different flow rates	26
Figure 4.1: Schematic representation of the pig skin explant setup for ex vivo dMD study	35
Figure 4.2: Sample template of the dMD probe placement and application site for the formulations	35
Figure 4.3: Concentration-time profile of MTZ in dermis ex vivo	39
Figure 4.4: 90% confidence intervals of the ratio of the ln-AUC and ln-Cmax	39
Figure 4.5: Box plot for min & max values of skin thickness measurement.....	41
Figure 4.6: Linear relationship of PD and RPD with AUC 0-24 hr	43
Figure 4.7: Linear relationship of PD and RPD with pAUC 0-24 hr.	44
Figure 4.8: Dose-response after topical application of different dosages	45
Figure 4.9: Comparison of AUCs of Ex vivo, In vivo, and IVPT studies.	49
Figure 5.1: Schematic representation of the study of the influence of temperature	55
Figure 5.2: Effect of temperature on the concentration-time profile of MTZ	58
Figure 5.3: Effect of temperature on AUC and Cmax	58
Figure 5.4: Ultrasound images showing the effect of temperature on skin explant	60
Figure 6.1: Schematic representation of the Bioequivalence study	67
Figure 6.2: Concentration-time profile of MTZ for each donor in BE study.....	69
Figure 6.3: Overall concentration-time profile of MTZ cream RLD and Generic product.....	70
Figure 6.4: BE plot of MTZ cream RLD and generic product.	71

Figure 7.1: Schematic representation of probe placement for EVIVC study	80
Figure 7.2: Steps to design a Level A EVIVC and predict in vivo concentration-time profile	84
Figure 7.3: Concentration-time data from retrodialysis-microdialysis study.....	86
Figure 7.4: Bioavailability comparison of MTZ in In vivo and Ex vivo	89
Figure 7.5: Cumulative absorption profile of MTZ in In vivo and Ex vivo	89
Figure 7.6: Fractional Cumulative absorption profile of MTZ in In Vivo and Ex vivo	89
Figure 7.7: Levy plot for point-to-point comparison of Tin vivo and Tex vivo.....	90
Figure 7.8: Observed In vivo and mapped Cumulative Absorption Ex vivo.....	91
Figure 7.9: Predicted vs Observed concentration-time profile In vivo.....	92

List of Tables

Table 3.1: Precision and Accuracy of calibration standards of analytical method.....	24
Table 3.2: In vitro Relative Recovery (RR) of Metronidazole.....	25
Table 4.1: Pharmacokinetic parameter calculated in the dermis for methods M1 and M2..	40
Table 4.2: One-way ANOVA to compare the difference in the skin thickness between groups.	42
Table 5.1: Influence of temperature on PK parameters Metronidazole cream in derms ex vivo	59
Table 7.1: Estimated and derived parameters from retrodialysis and microdialysis in ex vivo pig skin.....	87

List of Abbreviations

Standard acronyms and definitions are listed below.

Abbreviations	Definition
µg	Microgram
µL	Microliter
APAP	Acetaminophen
AUC	Area under the curve
AUC ₀₋₂₄	AUC from the time of dosing to 24th hour
BE	Bioequivalence
CA	Cumulative amount
Cl	Dermal clearance
C _{max}	Maximum dermal concentration
CV	Coefficient of variation
dMD	Dermal microdialysis
dUIR	Dermal Unit impulse ratio
EVIVC	Ex vivo-In vivo correlation
fCA	Fractional Cumulative Absorption
G	Gram
HPLC	High performance liquid chromatography
hr	Hour
IACUC	Institutional animal care and use committee
IVIVR	In vitro in vivo relationship

IVPT	In vitro permeation test
LLOQ	Lower limits of quantitation
LOD	Limit of detection
LRS	Lactated ringer solution
mg	Milligram
min	Minute
mL	Milliliter
MTZ	Metronidazole
NCA	Non-compartmental analysis
pAUC ₀₋₂	The partial AUC between the time of dosing and 2nd hour
PD	Probe depth
PDR	Probe depth ratio
PK	Pharmacokinetics
RLD	Reference listed drug
SD	Standard deviation
sec	Second
SEM	Standard error mean
TDDP	Topical dermatological drug products
TEWL	Transepidermal water loss
T _{half}	Terminal elimination half-life
T _{max}	Time to maximum plasma concentration (C _{max})
USDA	United states department of agriculture
V _d	Volume of distribution
λ _z	The terminal phase elimination rate constant

Chapter 1: Introduction

1.1 Statement of Problem

Topical dermatological drug products (TDDP) are intended to present their therapeutic effect on the skin. Hence, the characterization of the permeability kinetics of drug molecules in the various layers of the skin would promote the development of more effective formulations and better-informed clinical use of these products. Dermis microdialysis (dMD) has emerged as a potential tool to study pharmacokinetics in vivo directly in the skin for drugs applied topically. It is an accurate, sensitive, reproducible, and efficient method to measure drug concentration in the skin. dMD has the potential to discriminate between formulation types (1) and to evaluate bioequivalence for TDDP. Currently, the bioequivalence of TDDPs is based on evidence-based clinical end-points studies; however, in the last decade, the FDA in collaboration with academia is evaluating quantitative approaches like dMD or dermal open flow microperfusion (dOFM) as more efficient tests to demonstrate bioequivalence of TDDP. While these techniques provide promising results, one thing became clear: the assessment of dermal pharmacokinetics from TDDP is a lengthy process that requires several hours or even days for the complete characterization. Thus, these experiments can be very onerous for the participants also considering that the sampling probes must stay implanted in their skin for the entire duration of the experiment restricting their freedom of movement or, in animal studies, requiring continuous sedation.

1.2 Rationale for the Study

Clinical response to dermal products is a function of the availability of the drug at the site of action, often located in the dermal region. The evaluation of permeability and availability of the drug candidate in the dermal compartment is pivotal to the drug discovery and development process. The estimation of the dermal drug concentration-time profile during product development would help to optimize the selection of the most successful formulation composition.

Dermal microdialysis (dMD) allows the measurement of the analyte concentration at the site of action without disturbing the surrounding tissue, thereby making it possible to monitor the concentration-time course of the active pharmacological ingredient (API) in vivo directly in the dermal compartment (2,3). Dermal microdialysis studies could be potentially useful in the animal model during preclinical studies to understand critical experimental details before proceeding to clinical studies in humans. Such preclinical studies for TDDP are usually conducted in hairless minipigs, an animal model that is recognized as the most predictive of human permeability for a wide spectrum of molecules (4). Swindle et al. reported the structural similarity of porcine skin with human skin. Similarity includes epidermal thickness and dermal-epidermal thickness ratios. Also, pig skin is relatively hairless, has a fixed subcutaneous layer, and dermal hair follicles density similar to humans (5). However, working with live pigs has some disadvantages. Given the length of the experiments and the fragility and complexity of the dMD technique, animals must be continuously sedated. Besides, studies involving livestock require dedicated housing and specialized procedural facility, certification from USDA, approval from IACUC, trained personnel for handling and proper biohazard disposal, and many other unaccounted financial and management issues.

In this current study, we have laid down the fundamentals to develop an ex vivo model using porcine skin explant harvested from domestic pigs to test and tune-up dMD conditions and

experimental parameters. Porcine skin would easily be available to purchase from a local meat shop. The feasibility and reliability of the ex vivo model were thoroughly evaluated for the model to provide robust data supporting the study design of subsequent pre-clinical or clinical studies. Ultimately, it may even become a surrogate for clinical endpoints.

Fresh porcine skin explant with high moisture content has been reported as a suitable alternative to fresh human skin (6). Various approaches to maintain this hydration of skin explant were undertaken and evaluated to develop a meaningful and reproducible model. Variables tested and optimized include

- level of hydration,
- skin thickness,
- occlusion,
- backing support, and
- temperature.

The experimental conditions were tested and optimized for the following criterion:

- Specificity: A proposed model will be considered selective only if the drug concentration detected via dMD at a dosing site is free of interferences by the analyte from the neighboring test sites. The specificity of the dMD method can be tested by probing the lateral diffusion of the test analyte in the skin at known distances from the application site. Optimization of the minimum distance between the application/test site would help to maximize the utilization of the skin sample.

- Sensitivity: The ability of the devised dMD method to record dose-dependent responses to TDDP will ensure the sensitivity of the method. Linear dose-response with high regression coefficient will determine the degree of sensitivity of the model.
- Discriminatory: The ability of the devised dMD method to selectively discriminate between formulations that are known to have different pharmacokinetic profiles.
- Reproducibility: The ability of the devised dMD method to provide similar results in different subjects will determine the reproducibility of the method.

Commercial Metronidazole (MTZ) TDDP formulations were used as a model drug to test the ex vivo model. MTZ is an approved topical treatment for rosacea since 1995. The site of action is believed to be the dermis layer of the skin. MTZ being a hydrophilic molecule with low protein binding (7,8), and having a molecular mass of 207.61 g/mol presents as a good substrate for microdialysis recovery. Yet another reason for selecting MTZ as our model drug is the availability of in vivo permeation data of MTZ products on the Yucatan mini-pig model which in turn provided us a basis for reference.

Once the model was developed, bioequivalence (BE) of commercially available MTZ generic products was tested in comparison to its reference listed drug (RLD) product. According to the current accepted criteria, two formulations are deemed bioequivalent to each other when the ratio of log-normal AUC of the test formulation is between 0.8 and 1.25 of reference formulation, at a confidence of 90% (9).

Additionally, we presented a method to study the dermal pharmacokinetics of metronidazole (MTZ) independently of its absorption from topical administration. While, the study design mentioned above can measure changes in the dermal concentration-time profile, the

absolute absorption, and the intrinsic distribution/elimination data are inseparable. For systemic administrations, the absorption process can be elucidated by deconvolution of the plasma concentrations with the unit impulse response (UIR). A plasma UIR is usually estimated from intravenous administration, a type of administration that by-pass the absorption process. In our research group, we have earlier proposed a retrodialysis/microdialysis approach to deliver metronidazole (MTZ) directly to the dermis (intra-dermally) to estimate the dermis unit impulse response (dUIR). The dUIR provides a measure of dermal disposition independent of the absorption process. The dUIR was then applied to estimate the flux into the dermis and the cumulative amount (CA) absorbed via numerical deconvolution of the dermal concentration profiles detected at the topical formulation administration sites (10). In the present project, the same approach was applied ex vivo by comparing the ex vivo flux and the cumulative amount absorbed into the dermis with the in vivo skin permeation testing data (IVPT) to develop an Ex Vivo In Vivo Correlation (EVIVC). Since the major difference between the in vivo and ex vivo experiments is the absence of blood flow, this approach may help to sort out the influence of in vivo blood elimination on the dermis PK profile.

1.3 Specific Aims

Overall Aims:

To develop an ex vivo dermal microdialysis (dMD) method on excised pig skin to predict the pharmacokinetics of topical dermal products.

Background work:

- Validation of HPLC method from the existing in-house method for Metronidazole (MTZ).
- In vitro microdialysis and retrodialysis study- optimization of flow rate and establishment of linearity in probe recovery.

Specific Aim 1: Identify the experimental conditions that make the excised skin model a robust environment for the assessment of dermal pharmacokinetics using dMD.

Specific Aim 2: Test the model developed to determine the bioequivalence of commercial generic topical drug product of MTZ to its reference listed drug product.

Specific Aim 3: Determine the dermis MTZ disposition independent of the formulation by dermal infusion of MTZ, thereby, estimating the dermal unit impulse response and development of an EVIVC (Ex Vivo In Vivo Correlation) on pig skin with available in vivo permeation testing data for prediction of dermal drug exposure.

1.4 Schematics of the overall goal of the research work

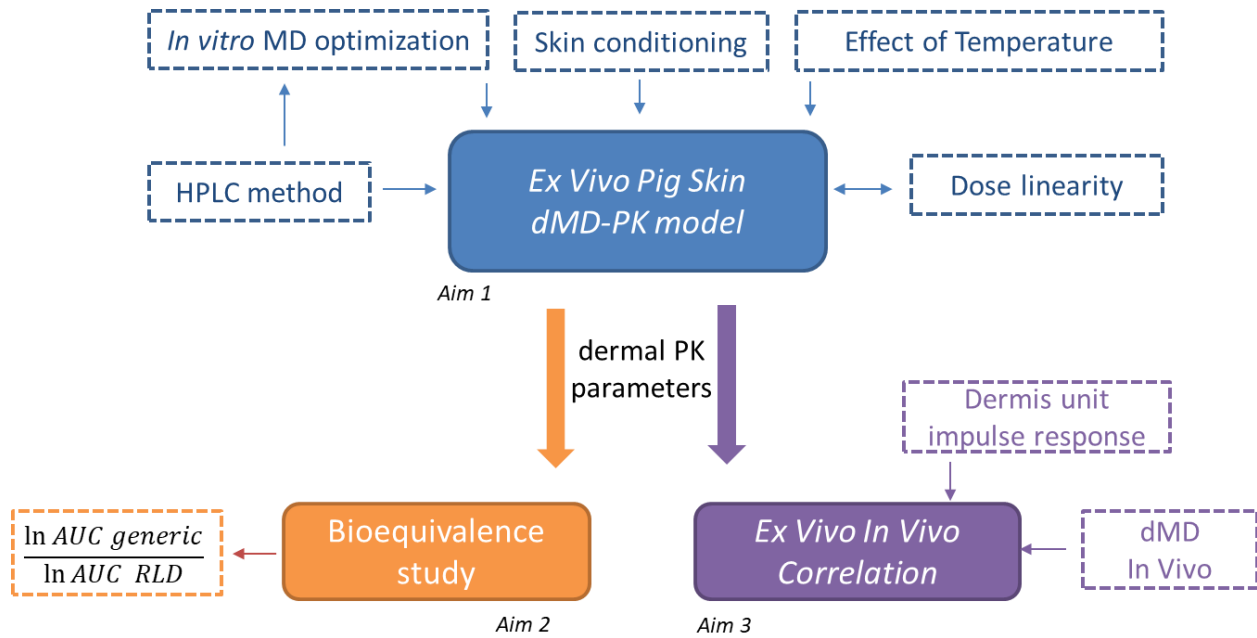


Figure 1.1: Schematic representation of the overall study- development of an ex vivo model (Aim 1), testing the model for Bioequivalency (Aim 2), and understanding the disposition of the drug in the target tissue (Aim 3).

Chapter 2: Background

2.1 Skin structure and the source of variability in permeation between species

Skin can be defined as the partition layer between the body and the outside environment. It serves as an important interface through which the body interacts with the surrounding in a controlled physiological process. This ability to finely regulate the exchange of substances makes the skin selectively permeable. It is highly selective as to what it lets into or out of the body and at what rate. This introduces a challenge for delivering drugs across the skin into the body (11).

Full-thickness mammalian skin broadly comprises three distinct layers of cell structures-epidermis, dermis, and deeper subcutaneous fat & connective tissues. The outermost layer of the skin known as the epidermis is made of proliferating basal and differentiated supra-basal epithelial keratinocytes held tightly by surrounding lipid-enriched extracellular components to represent a brick and mortar design (11). The outermost layer of the epidermis, stratum corneum, is about 10-15 layers of terminally differentiated keratinocytes called corneocytes. These non-living corneocytes have a cornified envelope instead of the plasma membrane and are surrounded by a lipid coat which contributes to the hydrophobic barrier function of the skin and exceptionally low permeability to water-soluble drugs (12). These variations in the membrane structure and lipid composition provide the structural and biochemical basis for intra-subject, inter-subject, and inter-species differences in permeability of drugs.

The avascular epidermal layer of the skin is supported and nourished by the diffusion of intracellular fluids from the vascular dermal layer beneath. The dermis is composed of a dense extracellular matrix that supports the cutaneous vasculature, sensory nerve cells, sweat glands, and hair follicles. The collagen fiber from the dermis is responsible to bind water and contributes to the hydrophilicity of the skin.

2.2 Permeation pathway

Drug molecules are expected to permeate through the skin via either the transepidermal pathway (diffusing across the stratum corneum) or the appendageal route (diffusion through hair follicles and/or sweat ducts). These pathways are not mutually exclusive, and a combination of pathways is taken by most drugs.

The transepidermal route can be classified into the paracellular route (=passing through the intercellular space) and the transcellular route (=through a cell). In the paracellular route, the drug navigates the convoluted path within the extracellular matrix, avoiding passing through the cells. While this route occupies a small portion of the entire epidermal layer, it provides a continuous path through the epidermis into the dermis and the hypodermis.

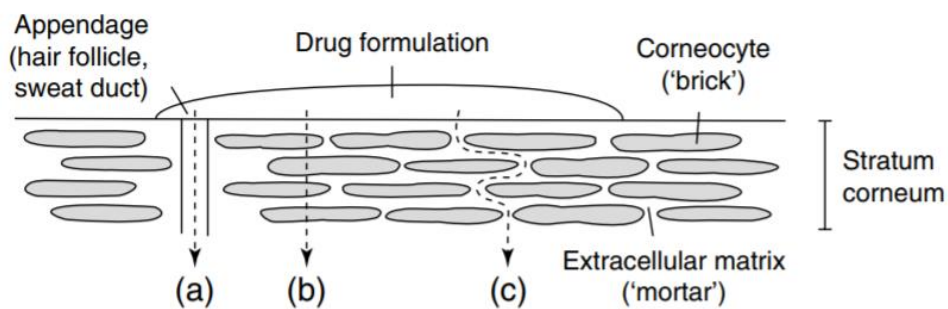


Figure 2.1: Drug permeation pathways in the stratum corneum: (a) the appendageal route, (b) the transcellular route, and (c) the paracellular route (11).

Corneocytes in the transcellular route contain an intracellular keratin matrix that is relatively hydrated and thus polar in nature. Permeation through the transcellular route requires repeated partitioning between this polar environment and the lipophilic domains. The transcellular pathway is lesser preferred of the two pathways. Overall, the transepidermal pathway is the primary route

of drug permeation in the skin (11,13). Thereby, diffusion across the stratum corneum is the rate-limiting step that governs the flux of a drug through this pathway.

Due to the sparse existence of appendages on the skin surface (hair follicles or sweat ducts), percutaneous transport through appendages is usually minor.

2.3 Topical dermatological drug products Bioequivalence: A regulatory perspective

Topical dermatological drug products (TDDP) are intended to act locally in the skin. Thus, local tissue concentrations at the site of action are critical components in determining bioequivalence (BE) for such products. However, such data is not readily available or even measured for most products. Additionally, topical administration of drug products typically does not lead to quantifiable drug concentrations in the systemic circulation, rendering bioequivalence evaluation a challenging process for these complex dosage forms in the absence of local drug pharmacokinetic data.

The Food and Drug Administration (FDA) draft guidance on topical dermatological drug products of 1998 introduced a dermatopharmacokinetic (DPK) approach to develop the kinetic relationship of the TDDP after topical application in vivo in humans (14,15). Briefly, the stratum corneum (SC) layer at the application site was removed by sequential tape-stripping, and subsequently, the drug was extracted for quantification. Topical products that produced comparable SC drug quantity versus time profiles were deemed bioequivalent (16). FDA eventually withdrew the guidance as the DPK method was not only exclusive for products that are intended for therapeutic effectiveness at the SC but also provided conflicting results between laboratories (17).

FDA ensures that high-quality topical dermatological generic drug products are made available to consumers. On that note, the FDA has taken multiple research initiatives to evaluate the feasibility of alternative, scientifically valid methods for evaluating the therapeutic equivalence for these TDDPs (18). Such research projects are intended to explore the development of appropriate in vitro and in vivo approaches that have the potential to support BE studies based upon cutaneous PK approaches. FDA is also funding institutional researchers working to develop dMD and dOFM based pharmacokinetic methods to evaluate the rate and extent to which a topically applied compound becomes available in the dermis, at or near a site of action within the skin, and to evaluate the relative sensitivity of dermal pharmacokinetic methods to discriminate differences in drug concentrations in the skin. The goals of these research initiatives include developing appropriate and relevant study conditions to evaluate the BE of topical drug products and developing predictive models to help evaluate topical BE.

2.4 Alternative approaches to the human skin model

Human skin for research is available in limited amounts and can only be sourced from clinics performing cosmetic surgeries or harvested from cadavers. In comparison, animal skin is easily available. Some of the most commonly used animal models for biological research are rodents like mice, rats, and guinea pigs. These animals are easy to handle and relatively inexpensive, but the structure of their skin is not comparable to humans (19). Rodents are often referred to as loose-skinned animals due to their lack of strong adherence to the underlying structures, which provides a bias for comparison (20). Furthermore, the presence of thick fur on the skin and non-comparable skin thickness to humans presents a challenge to mimic the human skin permeation model. To obtain a reliable prediction of the PK profile of a drug that is indicative of human skin, physiological differences between human and test species skin need to be minimized. Conversely, porcine skin is attached to the underlying subcutaneous fat like in humans, it possesses

comparable morphology, and has a similar hair density. In the late 70s, Yorkshire pig or the domestic pig was considered the only animal to have morphological and functional characteristics comparable to human skin (21); thus, meeting the requirements of a model for human skin; however, with advancing research smaller porcine species (e.g., Gottingen, Yucatan, and Bama mini-pigs) gained popularity given their ease of handling. Gore et al, demonstrated that the in vitro permeation characteristics of dorsal domestic pig skin are closer to human cadaver skin than the Yucatan pig skin and thus suggested the domestic pig model to be a better and more economical model to study transdermal permeation of drugs in vitro (22). Likewise, Qvist et al reported similarity in the permeation rate between cadaver and dorsal domestic pig skin. Their study also concluded that the variance in the result is least in domestic pig compared to human and Gottingen pig skin (23).

2.5 Microdialysis

Microdialysis (MD) is a semi-invasive sampling technique that allows continuous sampling of a target analyte in an organ matrix. MD probe containing a semipermeable segment is introduced into the organ at the target site and an isotonic solution is perfused through the probe. A diffusion-based process drives the influx of analyte from the concentration-rich target tissue into the perfusate according to the concentration gradient between the outside sample space and the perfusion fluid.

The microdialysis technique came into use in the 1980s and was soon adapted into pharmacological research. The number of publications per year involving MD reached 700-800 in the late 90s and since then balanced out to about 400-500 publications per year. Although the majority (about 70%) of these publications are in the field of neurotransmitter studies and brain research (24); a range of other applications of MD in different fields of biological research has also been illustrated (25). In the last 25, years over 800 papers have been published on skin

microdialysis (26), mostly on the pharmacology of skin diseases and their medicinal interventions. Dermal Microdialysis (dMD) has since its introduction been instrumental in improving the understanding of drug distribution into tissues in vivo and thereby makes it possible to determine extracellular unbound drug concentrations over time at the site of action as a function of dose. The method has substantially improved drug pharmacokinetic measurements from depending on discrete plasma and whole tissue samples to better-informed pharmacological results.

2.6 The current state of ex vivo dermal microdialysis studies

In the context of TDDPs, the difference between in vitro and ex vivo testing is not clearly defined. Generally, the term in vitro permeability is used to describe experiments performed with dermatomed skin i.e., cryopreserved human cadaver skin, 0.5-0.9 mm thick, obtained from a skin bank and stored at -80 °C until use. Alternative animal models are skin from pig inner ears, and nude mice or rats of similar thickness and similarly preserved. These types of experiments are conducted using Franz diffusion cell apparatus (22,23), where the dermatomed skin is the membrane separating the donor and the receiver compartments. Conversely, the term ex vivo is used for experiments performed on fresh specimens obtained for example from cosmetic surgery on otherwise healthy individuals. A large number of documented methods are available on the use of human and animal skin ex vivo for percutaneous permeability studies (27); however, there is a limited number of reports available on the use of dMD ex vivo for TDDP permeation studies.

In one of the earliest report, Ault and his group (28) evaluated the feasibility of dMD in Sprague Dawley rat skin ex vivo where the excised skin flap (cleaned of excess connective tissue and adipose tissue, hydrated in Dulbeccos modified phosphate buffer saline) was implanted with an MD probe to monitor the drug flux in the dermis from topically applied 5-fluorouracil cream. The group observed a rapid increase in flux for the first six hours after which a steady-state level was achieved. One of the key observations was an increase in flux due to minor disruption of the

skin microstructure from the insertion of guide cannula for dMD probe. These adverse effects can be minimized by a reduction in the size of the cannula itself.

Leveque et al (29), used dMD on abdominal skin fragments from female donors to monitor the intrinsic dermal level of ascorbic acid followed by quantification of the skin penetration of ascorbic acid and its degradation products from their topical formulation. In another report (30), researchers used dMD on human skin explant to compare an in-house formulation of dexamethasone and compared its dermal penetration with its marketed formulation.

From our preliminary literature survey, we understand, dMD on human or animal skin ex vivo was performed either to explore the permeation of model drugs in the skin or quantify the drug permeation from any in-house TDDPs of respective labs. There is one report on the comparison of dMD and dOFM performance of two model drugs of opposite polarity using skin explant (31). Since then dMD and dOFM have been reported in various scientific articles and conference proceedings to develop in vivo bioequivalence between TDDPs. Exploration and development of a statistically meaningful comparative ex vivo dMD method will contribute to the FDAs Critical Path Initiative (32) for preclinical development of generic TDDPs that are generally difficult to demonstrate bioequivalent (33).

Chapter 3: Determination of Relative Recovery of The Dermal Microdialysis Probe And Assessment of Influence of Perfusion Rate on The Recovery.

3.1 Introduction

Microdialysis is a tissue sampling technique used for continuous measurement of free, unbound analyte concentrations in the extracellular fluid with the help of implanting a probe containing a semipermeable exchange window of the desired length directly into the tissue matrix. The exchange of analyte molecules occurs at the junction of the tissue matrix and the semi-permeable membrane of the dialysis probe. The ability of this probe to recover the analyte of interest from the target tissue matrix or interstitial fluid is vital to the selection of an experimental design. Some parameters of importance in this procedure are the perfusate flow rate, temperature, characteristics of the semipermeable membrane, probe geometry, surface of the semipermeable membrane, membrane length, perfusate composition, and tubing characteristics (34). Parameters related to the exchange membrane selection have been extensively studied by Kuzma, et al where Gambro AN 69 HF from a PrismaFlex System with 17mm probe window were found optimal for Metronidazole.

The binding of the analyte to the probe wall, connector tubing, or any component of the microdialysis system may lead to an initial lag time or erroneous estimation of the drug analyte in vivo (24), and thus needs to be evaluated in the experimental design. One general practice to determine the binding is to conduct a series of in vitro microdialysis experiments with all the proposed components of the methods. It is performed by accounting for gain in analyte concentration with time in the microdialysis probe when immersed in a known concentration of the bulk sample. The in vitro microdialysis studies not only help to determine the binding but also helps to assess the linearity of the method with changing analyte concentration. The slope of steady-state recovery (gain) and the bulk concentration of the analyte will give the Relative Recovery (RR) of the analyte, specific to the experimental conditions. The RR in vitro is different

from the RR in vivo since the tissue resistance is much greater than the resistance in a solution (35).

The in vitro recovery is inversely dependent on the flow rate of the perfusate. With a faster process, the recovery is reduced. Ultraslow microdialysis has been used in the past to increase recovery (36). However, the method resulted in initial lag time and very low sample output. The microdialysis experimental design must include an optimum flow rate that will balance the recovery as well as the sample volume.

In the present chapter, we have conducted in vitro microdialysis to determine the linear response of our in-house microdialysis probe for Metronidazole, established the in vitro relative recovery (RR), determined the optimum perfusate flow rate, and optimized our microdialysis system for downstream ex vivo studies.

3.2 Method

3.2.1 Microdialysis Probe

Disposable linear dermal Microdialysis probes (will be referred to as dMD probes here onward) were made in-house using a modified Stagni et al method (37). The probe has two non-permeable arms, a semi-permeable membrane, and a stainless-steel wire support. Briefly, a 25 mm long tubular piece of semipermeable polyacrylonitrile membrane of molecular weight cut-off value of 50 KDa (Gambro AN 69 HF from a PrismaFlex System, M100, Baxter, Int., Inc.) was cut and two arms of 75 mm segments of polyimide tubings (0.127 mm ID x 0.165 mm OD, Nordson Medicals, Marlborough, MA) were introduced into the membrane and glued with Loctite Cyanoacrylic glue (Henkel Corp, Hartford, CT) leaving an exchanged window of 17 mm on the membrane. Eventually, a stainless-steel guide wire (0.0381 mm diameter, Molecu-Wire Corp., Wall Township, NJ) was inserted in the probe to provide support from bending and stretching. Tygon ND 100-80

Polytetrafluoroethylene tubing (0.25 mm ID x 0.76mm OD, Saint Gobain, Akron, OH) was glued to one end of the probe using Loctite glue. The probes were made no more than 2 days before the experiment and stored in a heat-sealed pouch. Before connecting to the pump, all probes were quality checked for dimensional similarity and flushed with LRS to check for leak or blockage.

3.2.2 HPLC method

The concentration of analyte was measured using an Agilent 1100 series HPLC-UV apparatus (Agilent Technologies, Santa Clara, CA) and the results were integrated using Agilent ChemStation. Briefly, the system consists of a degasser, quaternary pump, temperature-controlled autosampler with a 50 μ L sampling loop, a temperature-controlled column compartment, and a DAD Detector. The column compartment was fitted with an Xbridge C18 3.0x50mm 5 μ m reverse phased column (Waters Corp. Milford, MA) and was set at 25°C. The mobile phase consisted of deionized water (DI) and acetonitrile (ACN) at the ratio of 90:10 and an isocratic flow was maintained at 0.3 mL/min. The detection wavelength was 325 nm (bandwidth \pm 4nm) and the reference wavelength was set at 400 nm (bandwidth \pm 5nm). The autosampler was maintained at 5°C.

Intra-day precision calculations were performed on four batches of calibration standards on the same day. Inter-day precision calculations were based on intra-day for 3 different days. Results for intra-day and inter-day precision experiments were represented as Mean \pm SD. Accuracy data of all the intra-day and inter-day runs were pooled together and presented as % Error from theoretical concentration.

3.2.3 In vitro dose linearity study

The relative recovery of Metronidazole (MTZ) was investigated for a range of concentrations by the following scheme (Figure 4.1). Four linear dMD probes, with a 1.7 cm diffusion window, were

placed in a jacketed beaker (maintained at 32 ± 0.5 °C) and fixed at the rim to keep the adjacent probes at least 1 cm apart. Three such jacketed beakers were set up and filled with 0.5, 2.0, and 6.0 $\mu\text{g}/\text{mL}$ of MTZ in Lactated ringer solution (LRS) respectively. Two of the four probes were perfused with LRS (Blank) and the other two with internal standard Acetaminophen (APAP) 1.0 $\mu\text{g}/\text{mL}$ in LRS (Blank + APAP) at 0.5 $\mu\text{L}/\text{min}$ using Chemyx Fusion 400 Pump (Chemyx, Inc.; Stafford, TX). The dialysate was collected every 60 minutes and analyzed in HPLC. In vitro study at different concentrations was repeated on three different days and the recovered dialysate concentration of MTZ was plotted against time. Data were represented as Mean \pm SEM). Alpha errors less than 0.05 were considered significant.

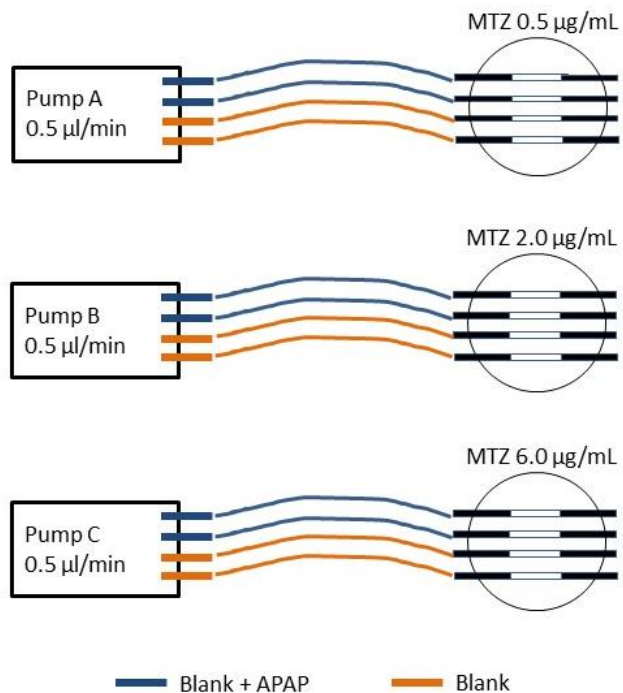


Figure 3.1: A sample schematics of the dMD probe placement for in vitro Relative Recovery study. The rectangular boxes represent the pump and the flow rate of the microdialysis system. Tubing for perfusate with APAP is drawn in blue and tubing for perfusate without APAP in orange. The circle represents individual jacketed beakers containing bulk metronidazole solutions of known strength as mentioned above each circle. Samples are collected at the open end of the probe at every hour interval for 4 hours.

3.2.4 In vitro flow rate optimization study

Four (4) in-house linear dMD probes were placed in a jacketed beaker as mentioned in section 4.2.3. Three such jacketed beakers were filled with a bulk solution of 100 µg/mL of MTZ in Lactated ringer solution (LRS) respectively (Figure 4.2). Two of the four probes in each beaker were perfused with LRS (Blank) and the other two with internal standard Acetaminophen (APAP) 100 µg/mL in LRS (Blank + APAP). Perfusate flow rates for each of the three jacketed beakers were set at 0.5, 1.0, and 1.5 µL/min respectively using Chemyx Fusion 400 Pump (Chemyx, Inc.; Stafford, TX). The dialysate was collected every 60 minutes and analyzed in HPLC. In vitro study flow rate study was repeated on three different days and the recovered dialysate concentration of MTZ was plotted against time. Data were represented as Mean ± SEM. Alpha-errors less than 0.05 were considered significant.

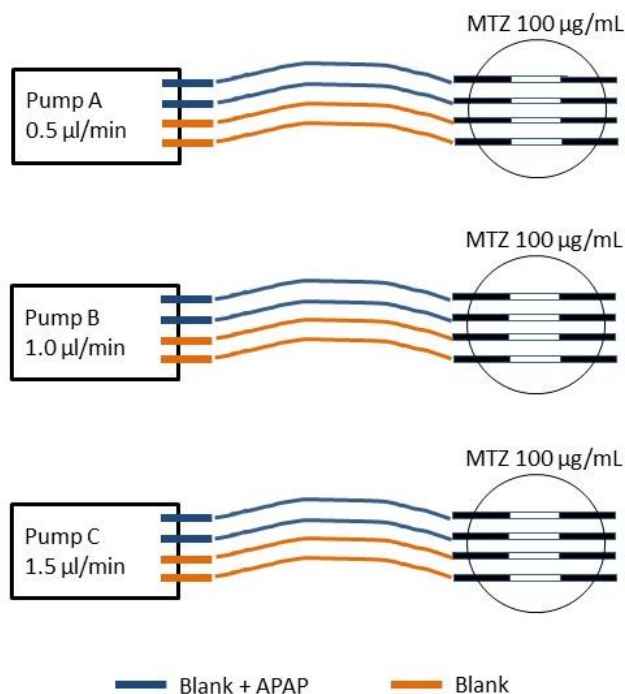


Figure 3.2: A sample schematics of the dMD probe placement for in vitro flow rate study. The infusion pumps were operated at three different flow rates of 0.5, 1.0 and 1.5 µL/min. Tubing for perfusate with APAP is drawn in blue and tubing for perfusate without APAP in orange. The circle represents individual jacketed beakers containing bulk solution of 100 µg/mL of Metronidazole in Lactated ringer solution (LRS). Samples are collected at the open end of the probe at every hour interval for 4 hours.

3.3 Results

3.3.1 HPLC Analytical method

With an auto-injection of 20 μL of the blank (LRS) spiked with MTZ, a typical chromatogram showed a sharp and symmetric peak at a retention time of 2.1 ± 0.1 min. No interfering noise was detected within 0.5 min from the retention time of the analyte in the blank (LRS) as well as the blank dialysate from ex vivo skin (Figure 6.1). The LOD of the method was < 10 ng/mL; however, the LLOQ selected was 125 ng/mL. A typical workflow included a seven-point calibration in the beginning and at the end of the experiment. The calibration curve, in the range of 125 - 10000 ng/mL, showed a linear response in all experiments, $R^2 = 0.99$. The precision and accuracy data obtained from intra-day ($n=4$) and inter-day ($n=3$) study are tabulated in table 6.1. The CV% were less than 15% at any instance of calibration standards and QCs (HQC, MQC, and LQC standards were 8000, 4000, and 400 ng/mL respectively). Carryover was not observed in any carryover-blank samples.

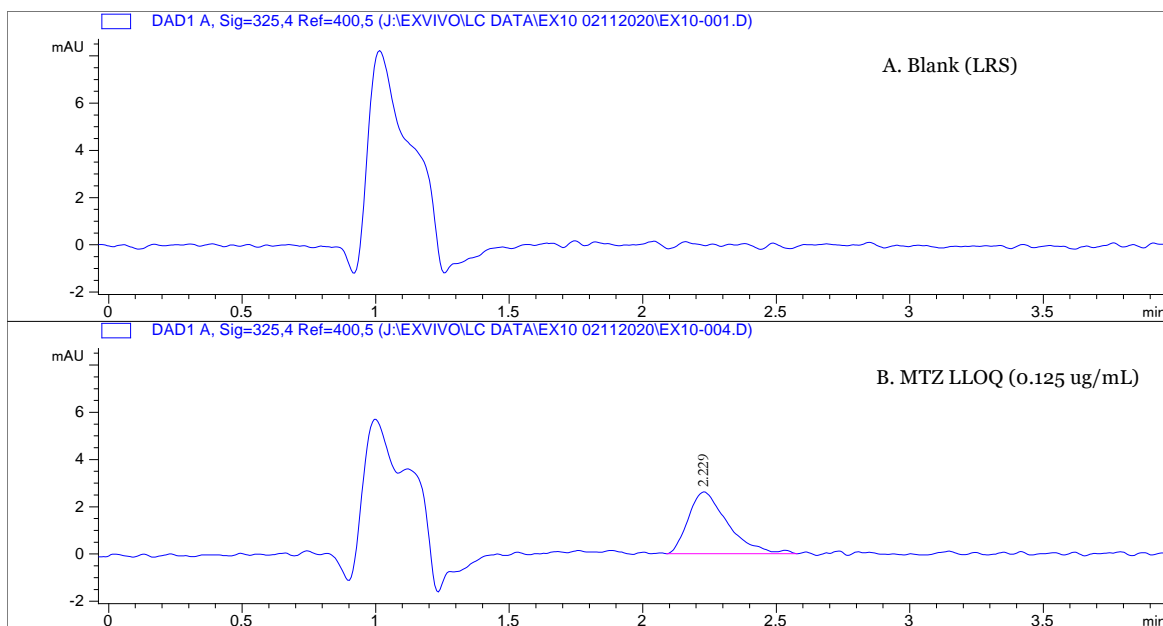


Figure 3.3: Representative chromatogram from Agilent 1100 HPLC with DAD detector at 325 ± 4 nm with a reference band at 400 ± 5 nm. (Top) Chromatogram for a blank sample. (Down) Chromatogram for Metronidazole lower limit of quantitation 0.125 $\mu\text{g}/\text{mL}$ at a peak retention time of 2.229 min.

Table 3.1: Precision and Accuracy of calibration standards at intra-day and inter-day run. (Mean \pm SD).

Calibration Standards	Precision				Accuracy
	Intra-day (n=4)		Inter-day (n=3)		(n=12)
ng/mL	ng/mL	CV %	ng/mL	CV %	Error %
125	126.63 \pm 4.59	3.62	126.63 \pm 3.13	2.62	-1.30
250	252.14 \pm 7.63	3.03	252.14 \pm 3.25	1.29	-0.86
1250	1254.19 \pm 18.62	1.48	1254.19 \pm 13.95	1.11	-0.33
2500	2505.38 \pm 24.32	0.97	2505.38 \pm 8.59	0.34	-0.22
5000	5032.13 \pm 62.63	1.24	5032.13 \pm 27.14	0.54	-0.64
7500	7515.12 \pm 107.63	1.43	7515.12 \pm 86.15	1.15	-0.20
10000	10055.27 \pm 120.27	1.20	10051.52 \pm 64.94	0.65	-0.55

3.3.2 In Vitro linearity study

Assessment of linearity and relative recovery of MTZ in the dMD probes was performed by placing the probes in jacketed beakers containing 0.5, 2.0, and 6.0 $\mu\text{g/mL}$ MTZ bulk solutions, with circulating water at 37 ± 0.5 $^{\circ}\text{C}$, as illustrated in Figure 3.1, (n=3). The perfusate with and without the presence of APAP was perfused at a flow rate of 0.5 $\mu\text{L/min}$. In vitro microdialysis recovery was close to 100% of bulk concentration at the first-hour sampling, and thereafter a steady-state in the concentration was observed until the end of the study (Figure 3.4). The presence of APAP as an internal standard in the perfusate had no significant difference in the percentage recovery of MTZ at different concentrations (non-parametric, one-sided, t-test, $p = 0.5464, 0.0972, \text{ and } 0.3547$, respectively). The recovery of MTZ from bulk solution at different concentrations shows a linear relationship (Figure 3.5), and the %RR is tabulated in Table 3.2.

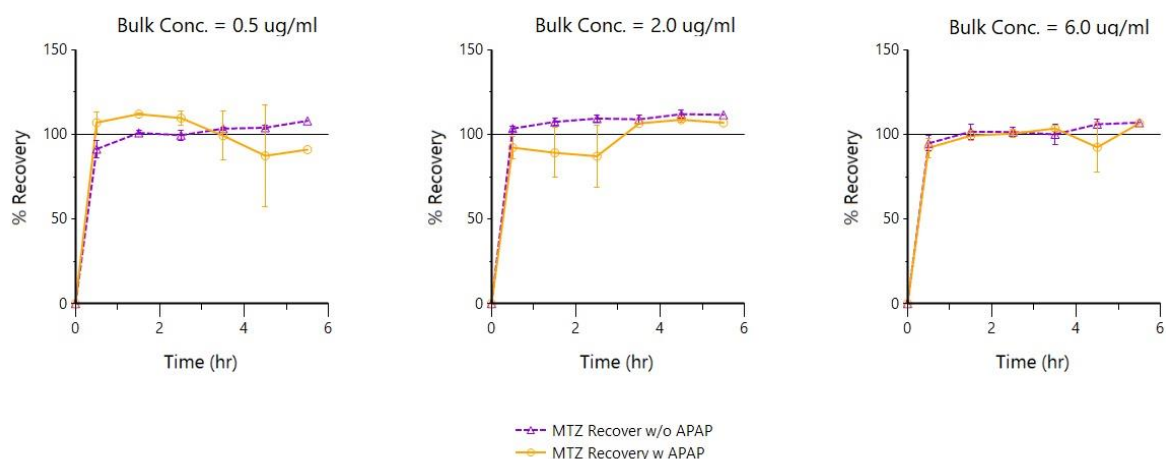


Figure 3.4: Recovery of MTZ from bulk in-vitro at three different concentrations (0.5, 2.0, and 6.0 $\mu\text{g/mL}$). Purple- recovery of MTZ in absence of APAP; Orange- recovery of MTZ in presence of APAP in the perfusate. (Mean \pm SEM, n=3). The presence of APAP as an internal standard in the perfusate had no significant difference in the percentage recovery of MTZ at different concentrations (p = 0.5464, 0.0972, and 0.3547, respectively).

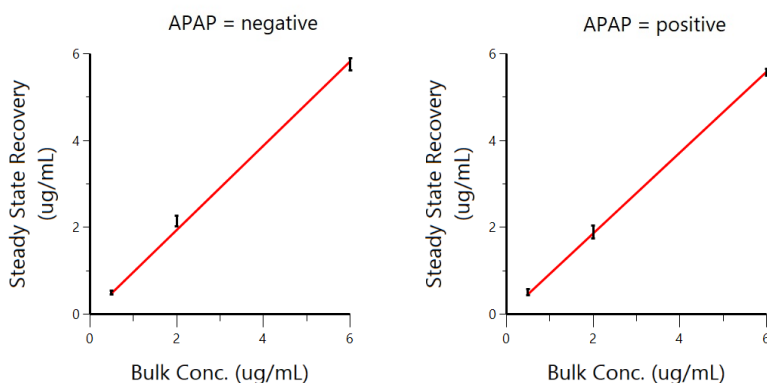


Figure 3.5: Linear relationship of Steady-State Recovery of MTZ from bulk in vitro at three different concentrations (0.5, 2.0, and 6.0 $\mu\text{g/mL}$). Left- recovery of MTZ in absence of APAP; Right- recovery of MTZ in presence of APAP in the perfusate. (Mean \pm SEM, n=3).

Table 3.2: In vitro Relative Recovery (RR) of Metronidazole calculated from the slope of linear regression of response of dMD recovered at variable concentration. The influence of the internal standard APAP on the RR of MTZ was verified. No significant difference was observed with or without APAP. (Mean \pm SEM, n=3, $\alpha = 0.05$).

	Relative Recovery of Metronidazole	Correlation Factor (R^2)
Perfusate without internal standard APAP	97 %	0.9988
Perfusate with internal standard APAP	93 %	0.9999

3.3.3 Flow rate study

The recovery of MTZ at a flow rate of 0.5 $\mu\text{L}/\text{min}$ was close to 100% of the bulk concentration during the first-hour sampling and remained steady till the end of the study. The recovery of MTZ substantially reduced with an increase in the flow rate (Figure 3.6). No significant difference in the recovery of MTZ with and without APAP was observed at a flow rate of 0.5 $\mu\text{L}/\text{min}$ (non-parametric, one-sided, t-test, $p=0.0663$). At higher flow rates of 1.0 $\mu\text{L}/\text{min}$ and 1.5 $\mu\text{L}/\text{min}$, the recovery of MTZ with and without APAP changed significantly (non-parametric, one-sided, t-test, $p= 0.0001$ and 0.0002 respectively).

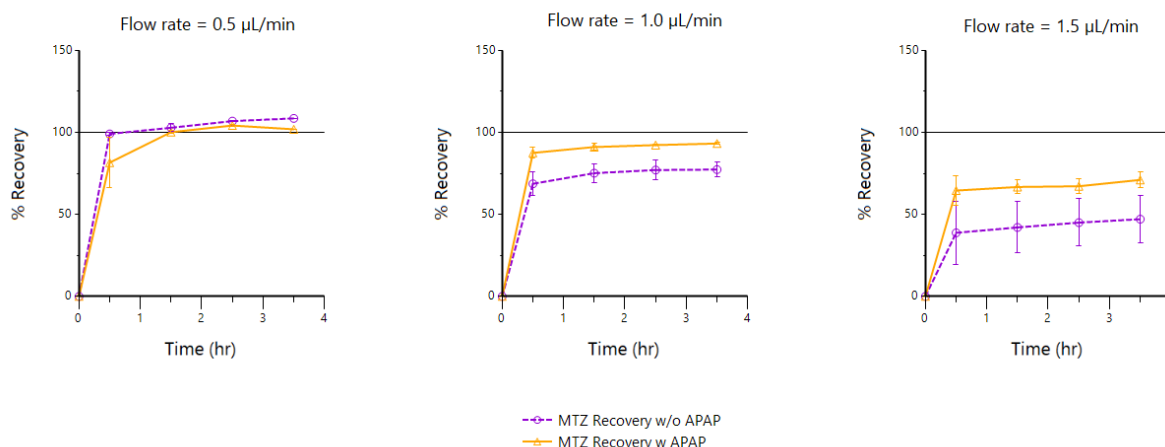


Figure 3.6: Recovery of MTZ from bulk in-vitro at 3 different flow rates (0.5, 1.0, and 1.5 $\mu\text{L}/\text{min}$). Purple-recovery of MTZ in absence of APAP; Orange- recovery of MTZ in presence of APAP in the perfusate (Mean \pm SEM, $n=3$). At 0.5 $\mu\text{L}/\text{min}$ there was no significant difference ($p=0.0663$) in the recovery of MTZ with/without the presence of APAP in the perfusate. At flow rates of 1.0 and 1.5 $\mu\text{L}/\text{min}$, a significant difference ($p= 0.0001$ and 0.0002 respectively) in MTZ recovery was observed between APAP and without APAP groups.

3.4 Discussion

At such a low sample volume, any form of evaporation will inflate the data and will present confounding results. The volume of dialysate was verified by weighing the sampling inserts before and after sample collection, at every time interval during the flow rate study (section 3.2.4) and

no discrepancies were observed. This observation relieved us of the extra measure that needs to be taken during the sampling; however, precautionary measures were taken to seal the sampling inserts immediately after collection and were analyzed at the earliest.

In-vitro microdialysis recovery (gain) study was performed to maximize our in-house dMD probe performance and optimize the recovery of MTZ during our ex vivo studies. We observed that the in-vitro relative recovery of MTZ was independent of drug concentration and the presence of probe calibrator (APAP), at a slow perfusion rate of 0.5 $\mu\text{L}/\text{min}$. The concentration of bulk MTZ for in-vitro MD linearity study was selected based on our expected concentration from ex vivo studies; however, during pilot studies, the concentration of MTZ recovered from ex vivo studies was significantly higher than the ULOQ of the analytical method. Analysis of such a highly concentrated analyte sample could be addressed by dilution of the sample immediately before injection into the HPLC. Another way would be to reduce the relative recovery of the analyte during the dialysis by increasing the flow rate of the dialysis. This warrants the study of the effect of flow rate on MTZ recovery. In a different set of in-vitro studies, MTZ recovery was assessed at three different flow rates (0.5, 1.0, and 1.5 $\mu\text{L}/\text{min}$) with an elevated bulk concentration of 100 $\mu\text{g}/\text{mL}$ of MTZ. The dialysate was similarly collected every 60 minutes and analyzed in HPLC. We observed that the in vitro relative recovery of MTZ was independent of drug concentration and the presence of probe calibrator (APAP), at a slow perfusion rate of 0.5 $\mu\text{L}/\text{min}$. However, with increasing the flow rate of perfusion, an anomaly of recovery was observed between the groups with & without APAP. It is clear from the above results, transfer of molecules across the semi-permeable membrane is a function of the time and physicochemical nature of the drug, and surely the flow rate is a rate-limiting factor for drug diffusion, directly affecting the recovery.

In an in vitro setting, analytes are free to move in a solution. The rate of removal of the analyte inside the probe is in equilibrium with the rate at which molecules appear at the external

surface of the probe. In an in vivo setting, where the tissue provides resistance to analyte flow, the rate of analyte removal from the inside of the probe is higher than the rate of analyte replaced at the probe membrane surface (38). We can anticipate that the in vivo results will vary from our in vitro findings. However, by correcting the microdialysis recovery of MTZ from the skin tissue with the loss in APAP (probe calibrator) from perfusate, as originally proposed by Larsson (39), we could get the nearest estimation of MTZ in the dermal tissue.

3.5 Conclusions

A dose-linear recovery of Metronidazole from bulk was verified using in vitro microdialysis. The microdialysis method was thus optimized for the in vitro process for probe specification, analyte suitability, flow rate, perfusate composition (Lactated ringer isotonic solution, and Acetaminophen). A maximized, rapid, and steady recovery of MTZ was possible at 0.5 $\mu\text{L}/\text{min}$ perfusions within a wide range of concentrations (0.5 to 100 $\mu\text{g}/\text{mL}$). Thus, 0.5 $\mu\text{L}/\text{min}$ perfusion with APAP as probe calibrator was decided to be used for MTZ recovery from dermis ex vivo dermal bioavailability studies.

Chapter 4: Development of An Ex-Vivo Dermal Microdialysis Model for Characterization of Dermal Disposition of Drug from Topical Dermatological Drug Products

4.1 Introduction

The therapeutic efficacy of a drug product is challenged by the availability of the active constituent at the site of action. Pharmacokinetic (PK) methods are generally employed to measure the unbound drug concentration in the plasma and the tissue to properly evaluate the pharmacodynamic (PD) nature of the drug. Likewise, the rate and extent of percutaneous permeation of molecules is a key step in the evaluation of topical dermatological drug products (TDDP). The gold standard for therapeutic evaluation of topical products would be a human study in vivo (40); however, in the case of TDDPs, it may not be always feasible to measure the unbound drug levels in plasma and correlate the drug concentration at/near site of action (dermis), rendering bioequivalence evaluation a challenging process for these complex dosage forms in the absence of local drug pharmacokinetic data. Thus, there is an unmet need for an alternate method for assessment of these products that will produce permeation kinetics, produce local bioavailability data, and can be translated to human equivalent results.

The Food and Drug Administration (FDA) draft guidance on topical dermatological drug products of 1998 introduced a dermatopharmacokinetic (DPK) approach to develop the kinetic relationship of the TDDP after topical application in vivo in humans (14,41). Briefly, the stratum corneum (SC) layer at the application site was removed by sequential tape-stripping, and subsequently, the drug was extracted for quantification. Topical products that produced comparable SC drug quantity versus time profiles were deemed bioequivalent (16). FDA eventually withdrew the guidance as the DPK method was not only exclusive for products that are intended for therapeutic effectiveness at the SC but also provided conflicting results between laboratories (17). The progress in conversion of branded TDDPs to their generic counterpart has not proceeded at the same pace as for other drug products (42), and may be contributed to the lack of a proper pharmacokinetic method. To address this issue, the Hatch-Waxman Act was

amended in 2003 for the evaluation of bioequivalence of drugs that are not intended for systemic absorption (43). Yet, alternative methods accepted for the evaluation of bioequivalence for TDDPs have remained limited.

Measuring the unbound drug concentration in the tissue has been made possible (28) in the past three decades by the advancement in dermal Microdialysis (dMD) techniques. In a typical dMD study, a linear thin hollow capillary with a central piece made of a semipermeable membrane of known length and porosity is implanted directly in the dermis traversing a designated section of the skin. The hollow capillary with membrane, commonly known as dMD probe, is perfused with a sterile isotonic physiological buffer at a fixed flow rate using an infusion pump. The probe capillary may be compared to a tissue vasculature where the probe window helps in diffusion or exchange of free molecules across the diffusion gradient between the perfusate and the tissue and delivered out with the dialysate to be analyzed. The unique feature of microdialysis is thus that it samples local unbound concentrations, thereby making it possible to directly reflect tissue concentrations to pharmacological effects (24). The concentration over time at the dermis can lead to a more meaningful pathway for the development of safe and efficacious medications and their dosing regimens. The ability to understand the PK of a drug at or near the site of action will provide the key for effective use of medications.

In the present chapter, we have tried to explore the feasibility of using the dermal microdialysis process to assess the bioavailability of Metronidazole 0.75 topical product on pig skin ex vivo model. The microdialysis probes and experimental specifications developed in chapter 3 (by in vitro studies) were evaluated on skin ex vivo. A study design was proposed, tested, and optimized for estimation of bioavailability, selectivity of performance by testing two different formulation types, and eventually testing the dose sensitivity (linearity) of the model to different dosing.

4.2 Method

4.2.1 Chemicals and reagents

Metronidazole (99%) (MTZ) was purchased from Beantown Chemical (Hudson, NH). Lactated Ringer Solution (LRS, NDC- 0338011703, Baxter Healthcare Corp., Deerfield, IL), Metronidazole 0.75% Cream (NDC- 0168032346, Fougera Pharmaceutical Inc., Melville, NY), Metronidazole 0.75% Gel (NDC- 0115147446, Impax Generics, Hayward, CA) and all other medical supplies were purchased from Henry Schein (Melville, NY). LC Grade acetonitrile, water, and other supplies were purchased from Fisher Scientific (Fair Lawn, NJ, USA).

4.2.2 HPLC Analytical method

The concentration of the analyte in the dialysate was measured using an Agilent 1100 series HPLC-UV apparatus (Agilent Technologies, Santa Clara, CA) and the results were integrated using Agilent ChemStation. Briefly, the system consists of a degasser, quaternary pump, temperature-controlled autosampler with a 50 μ L sampling loop, a temperature-controlled column compartment, and a DAD Detector. The column compartment was fitted with an Xbridge C18 3.0x50mm 5 μ m reverse phased column (Waters Corp. Milford, MA) and was set at 25°C. The mobile phase consisted of deionized water (DI) and acetonitrile (ACN) at the ratio of 90:10 and an isocratic flow was maintained at 0.3 mL/min. The detection wavelength was 325 nm (bandwidth \pm 4nm) and the reference wavelength was set at 400 nm (bandwidth \pm 5nm). The autosampler temperature was maintained at 5°C.

4.2.3 Dermal Microdialysis Probe

Disposable linear dermal Microdialysis (dMD) probes were made in-house using a modified Stagni et al method (37). The probe has two non-permeable arms, a semi-permeable membrane, and a stainless-steel wire support. Briefly, a 25 mm tubular piece of a semipermeable membrane of

molecular weight cut-off value of 50 KDa (0.240 mm ID x 0.340 mm OD, GambroAN69-HF Hospal-Gambro, Inc, CA) was cut and two arms of 75 mm segments of polyimide tubings (0.127 mm ID x 0.165 mm OD, Nordson Medicals, Marlborough, MA) were introduced into the membrane and glued with Loctite Cyanoacrylic glue (Henkel Corp, Hartford, CT) leaving an exchanged window of 17 mm on the membrane. Eventually, a stainless-steel guide wire (0.0381 mm diameter, Molecu-Wire Corp., Wall Township, NJ) was inserted in the probe to provide support from bending. One end of the probe was introduced into Tygon ND 100-80 Polytetrafluoroethylene tubing (0.25 mm ID x 0.76mm OD, Saint Gobain, Akron, OH) and glued with Loctite glue. Before connecting the Tygon tubing to the pump, all probes were quality checked for dimensional similarity and flushed with LRS to check for leak or blockage. The other end of the probe was left open to be inserted into the skin and the dialysate will be collected from this end into plastic vials. The probes were made no more than 2 days before the experiment and stored in a heat-sealed pouch.

4.2.4 Ex vivo experimental setup

Skin explants were harvested from fresh slaughtered female Yorkshire pig belly purchased from a local meat shop. The harvested skin was used to develop two different ex vivo experimental setups (M1 and M2). The experiments differ principally in the skin thickness and presence/absence of external hydration.

M1 — Hydrated skin model: Four, square Ancare Nestlets (Bellmore, NY) of 5 cm at the edge, were placed side-by-side on an aluminum tray of 1 cm height. A total of 60 mL (15 mL per testing site) of Lactated ringer solution (LRS) was poured and evenly spread on top of the nestlets and allowed to hydrate the setup until the TEWL measurement was constant. These hydrated nestlets act as physical backing support as well as a water reservoir providing hydration from the vascular side of the skin. A full-thickness pig skin explant (thickness \approx 0.25 cm), cleaned of the underlying

subcutaneous fat layer was placed on top of the hydrated backing support and allowed to hydrate until the TEWL measurement on the top of the skin is constant (Figure 4.1, top).

M2 — A full-thickness pig skin explant with the underlying subcutaneous fat layer (total thickness \approx 1 cm) was placed on an aluminum tray. No additional LRS or external hydration was applied in this method. The skin explant was allowed to equilibrate until the TEWL measurement on the top of the skin was constant (Figure 4.1, bottom).

A total of six skin explants from different animal subjects ($n=3$, for M1 and M2 respectively), each of dimension 5 x 20 cm was used. On each skin strip, four different application sites (5 x 5 cm) were marked and a parallel four-period full-replicate (RTRT) design was employed (Figure 4.2). These application sites were visually inspected for damages or discoloration. Skin pieces with defects or deviation of TEWL more than 20% within the application sites were excluded from the study. On each application site, a circular (2.5 cm diameter) location, towards the center, was selected and two dMD probes, 1 cm apart, were inserted into the dermis with the help of a guide cannula (a total of eight probes per skin strip), and one lateral diffusion probe was inserted in the dermis toward the center of the skin at a distance of 2 cm from the adjacent test probes.

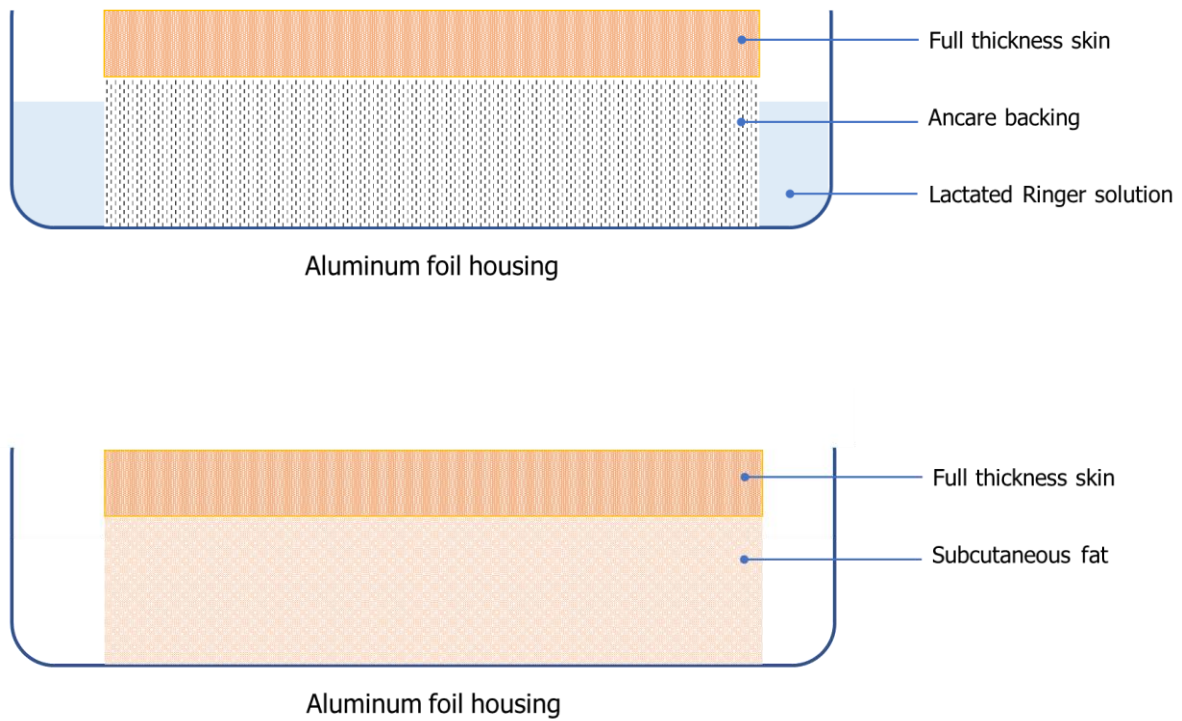


Figure 4.1: Schematic representation of the pig skin explant setup for ex vivo dMD study — Method 1 for hydrated skin using full-thickness skin without underlying subcutaneous fat layer (top), Method 2 for full-thickness skin with underlying subcutaneous fat layer (bottom).

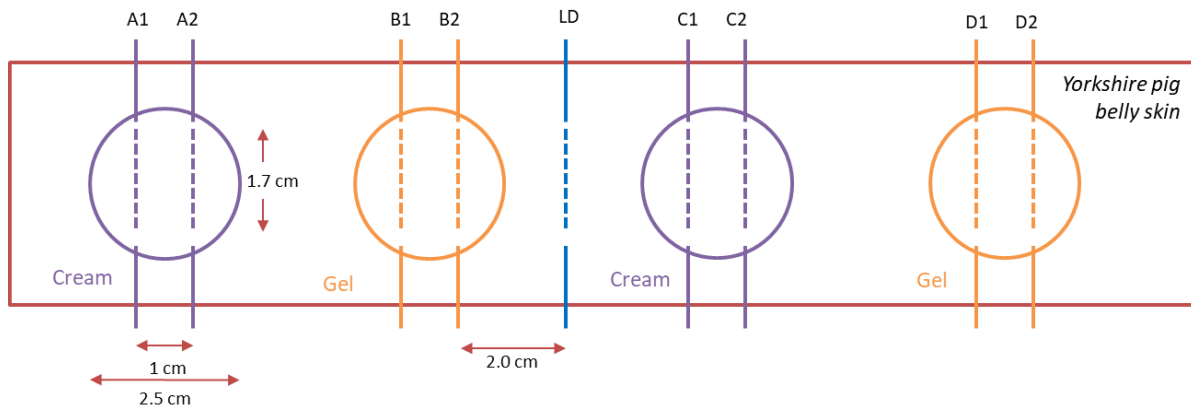


Figure 4.2: A sample template of the dMD probe placement and application site for the formulations on the skin. The probe and application site for MTZ cream is marked with purple and MTZ gel with orange. The application sites are circular (diameter 2.5 cm) and the probes in each site are 1cm apart. The lateral diffusion probe (blue) is 2 cm apart from adjacent probes.

On one end of the probe arm, Tygon tube connected to Chemyx Fusion 400 Pump (Chemyx, Inc.; Stafford, TX) was attached. The entire probe tubing was flushed with LRS perfusate to remove any air bubbles. After flushing, the perfusate was set to a perfusion rate of 0.5 μ L/min. A 3M double-sided tape (3M, Minneapolis) with a circular hole (2.5 cm diameter) punched out, was placed on the top of the application area as a guide for formulation application, and commercially available generic Metronidazole 0.75% topical cream and Metronidazole 0.75% topical gel were applied alternately on the four marked sites of the skins (Figure 4.2). In each circular application site (area = 4.9 cm^2), 10 mg/cm^2 of the formulation was carefully administered with a positive displacement pipette (Gilson Distriman, Middleton, WI) and rubbed in a circular motion with the rubber head of 1ml BD syringe plunger for 15 sec. The time of application of formulation is noted and samples were collected at the end of each hour in HPLC inserts for eight hours and terminally at 24th hours and analyzed immediately.

4.2.5 Probe depth measurement

The role of the dMD probe depth on the local microenvironment (AUC) of the drug in the skin was determined using a 20 MHz ultrasound machine (Logiq E7, GE Healthcare, Chicago, IL) at the end of each study. Briefly, the 1.5 cm ultrasound probe was placed over the skin where the dMD probe is placed (the entry and exit of dMD probe serve as a guide), and three images from each probe were captured to calculate the mean probe depth (PD) and the ratio of probe depth over the thickness of the dermis, called as relative probe depth (RPD) was calculated.

4.2.6 Dose-Response study

In a separate set of experiments, the dose-response relationship of the best fit ex-vivo dMD method was evaluated. Typically, fresh Yorkshire pig belly skin was harvested and cut to a dimension of 5 x 30 cm. Six different dose application sites were marked and experimental steps

(as mentioned in the ex vivo microdialysis section) were followed. MTZ 0.75% cream was applied at the dose of 5.0, 10, and 30 mg/cm² on the application site (two sites per dosing), and the dMD scheme was applied. The concentration calculated from the dialysate sample collected hourly for 8 hours and terminally at the 24th hour was plotted against time and NCA was performed to estimate the dose-response relationship. The experiment was repeated three times.

4.2.7 Data processing

The calculated concentration of MTZ in the samples was plotted against mid-sample interval time using PhoenixWinNonlin 8.2 (Certara; Princeton, NJ). A non-compartmental analysis (NCA) was used to obtain pharmacokinetic parameters and the log ratio of the geometric mean of PK parameters (AUC, C_{max}) between cream and gel was established. For the selection of the best-fit model, the log-ratio data were compared with reported in-vivo Yucatan minipig data (44) and IVPT data for cadaver skin (calculations performed on available data of (45)). Occasional plotting of data was performed using Prism 8 (GraphPad, San Diego, CA)

4.2.8 Statistical analysis

For ex vivo studies, a two-stage analysis approach was employed. The first stage of the approach involves estimating the PK parameters from individual dense concentration over time data (taking mid-points of the sampling intervals) using noncompartmental methods in PhoenixWinNonlin. Individual parameter estimates obtained during the first stage were used as input data for the second-stage calculation of descriptive summary statistics on the sample, typically, mean parameter estimates, SEM, median, and range. The non-parametric, unpaired Mann-Whitney test was used to compare the descriptive statistical differences (GraphPad Prism Software, San Diego, CA). ANOVA was done to check if there is any difference in the mean of data between two or more groups of data. The definition of statistical significance was set at an alpha error of less

than 0.05. The NCA outcomes were used for ranking of formulation in the Bioequivalence function of WinNonlin taking cream as the reference formulation in a parallel study. For linear regression of the dermal bioavailability and dose study, the Mean (SD) was plotted for each dose and linear line fitting was generated.

4.3 Results

4.3.1 Lateral diffusion

Lateral diffusion probes were strategically placed between two adjacent dosage application sites, one for cream and the other for gel. If there was any potential lateral diffusion from any of the formulations, it would have been detected in the probe. In all the studies, the signal for MTZ in the lateral diffusion probe was below the LLOQ of the analytical method and could not be conclusively determined.

4.3.2 Dermal Pharmacokinetic profile

Following the topical application of the MTZ cream and gel, a rapid rise in the dermal penetration was observed, and C_{max} was achieved within the first 2 hrs in both methods M1 and M2 (Figure 4.3). The AUC₀₋₂₄ of MTZ gel was significantly higher than the cream treatment in M1 (unpaired, non-parametric, t-test, p value=0.0294). The higher permeability of gel ex vivo in M1, leads to higher relative bioavailability, the ratio of ln-AUC = 1.27 (90% CI: 1.06-1.53) (Figure 4.4).

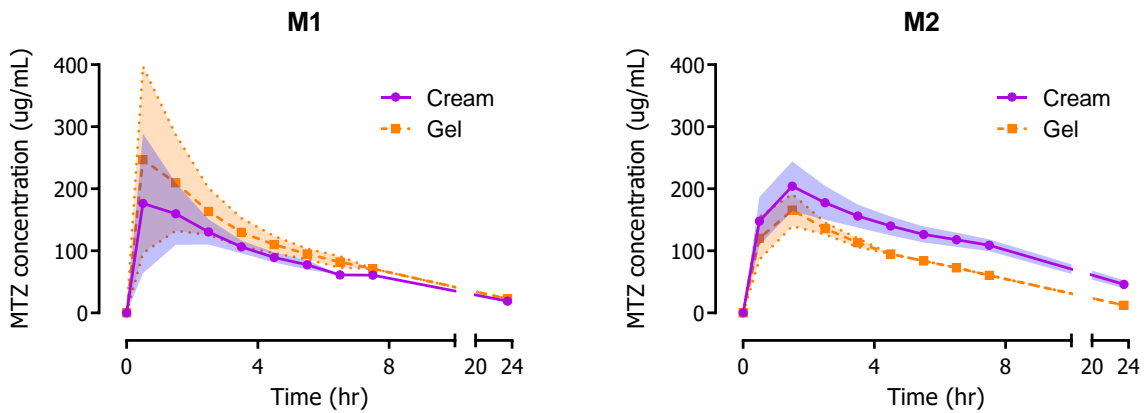


Figure 4.3: Concentration-time profile of MTZ in the dermis after topical administration of formulations in two different experimental conditions M1 (left) and M2 (right). Purple- profile after treatment with MTZ 0.75% topical cream and, Orange- profile after treatment with MTZ 0.75% topical gel. (Mean \pm SEM, n=3).

An opposite response was observed in the studies performed by the M2 method. The overall permeation profile of cream was significantly higher than the gel (unpaired, non-parametric, t-test, p value=0.0005). The ratio of ln-AUC from M2 was reduced to 0.58 (90% CI: 0.45–0.74) and the ratio of ln-C_{max} was 0.81 (90% CI: 0.58–1.12) (Figure 4.4). The effect of the M2 method is supported by the observations in vivo in pig (1). The descriptive statistics of PK parameters from either method are tabulated in Table 4.1.

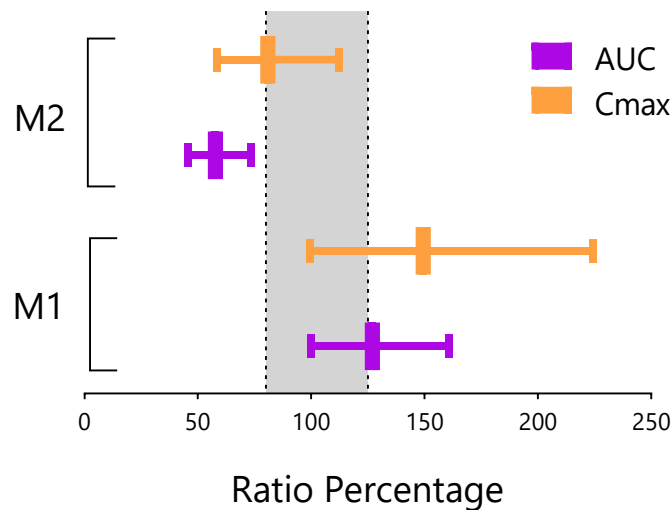


Figure 4.4: 90% confidence intervals of the ratio of the ln transformed AUC (purple) and C_{max} (orange). The reference is the cream while the test is the gel. The dashed lines indicate the bioequivalence limits of 80-125% CI.

Table 4.1: Pharmacokinetic parameter calculated in the dermis for both methods M1 and M2. (n=3).

PK parameters	Units	Formulation	M1	M2
			Median (Range)	Median (Range)
AUC₀₋₂₄	<i>hr*ug/ml</i>	Cream	1422.02 (1355.58)	2525.98 (2064.72)
		Gel	1654.44 (2603.94)	1260.43 (1680.4)
C_{max}	<i>ug/ml</i>	Cream	154.46 (471.29)	220.22 (248.57)
		Gel	251.1 (560.49)	149.79 (243.75)
T_{max}	<i>hr</i>	Cream	1.5 (4)	1.5 (4)
		Gel	1.5 (5)	1.5 (3)
λ	<i>1/hr</i>	Cream	0.069 (0.049)	0.051 (0.067)
		Gel	0.07 (0.042)	0.10 (0.085)
T_{half}	<i>hr</i>	Cream	10.03 (7.35)	13.74 (16.6)
		Gel	9.96 (6.02)	6.91 (6.75)

4.3.3 Relationship of Permeation profile with probe depth

Benfeldt et al. in a study reported, at the end of a comparative study of lidocaine formulations, the skin thickness at the site of application of ointment was thicker compared to a cream (46). Owing to the fact that ointments are more occlusive, the author explained higher thickness at the ointment site as the result of the higher skin hydration compared to the cream application site. In our experimental setup, external hydration did not affect the thickness of the skin (comparison between M1-hydration method and M2-non-hydrated method) but an expected change in thickness was observed in the gel application sites (Figure 4.5). This change between gel and cream could be attributed to the higher occlusivity of the cream formulation. When one-way ANOVA followed by Tukey's comparison test was performed within the groups, skin thickness observed by the ultrasound measurement was not significantly different (Table 4.2).

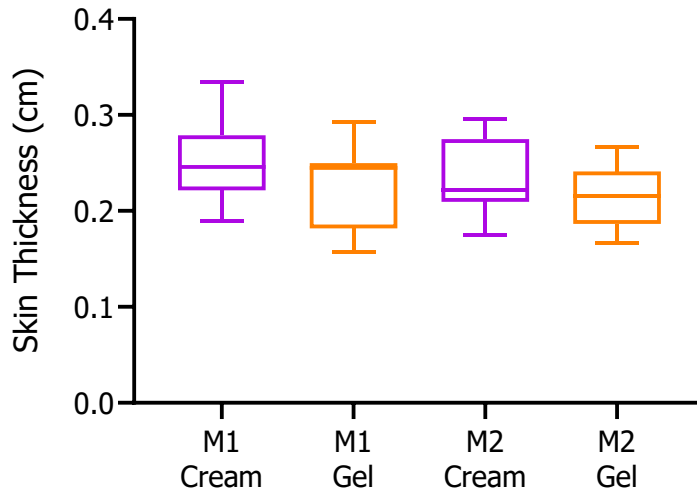


Figure 4.5: Box plot with whiskers showing the mean with min & max values of skin thickness measurement (cm) from Ultrasound recordings of either M1 and M2 methods. The cream is marked in purple and gel in orange. No significant difference in thickness was observed. [n=12 for each group]

Table 4.2: One-way ANOVA followed by Tukey's multiple comparison test shows no significant difference in the skin thickness (cm) between the groups.

Tukey's multiple comparisons test	Mean 1	Mean 2	Summary	P Value
M1 Cream vs. M1 Gel	0.2512	0.2298	ns	0.4081
M1 Cream vs. M2 Cream	0.2512	0.2343	ns	0.6508
M1 Cream vs. M2 Gel	0.2512	0.2165	ns	0.0919
M1 Gel vs. M2 Cream	0.2298	0.2343	ns	0.9897
M1 Gel vs. M2 Gel	0.2298	0.2165	ns	0.796
M2 Cream vs. M2 Gel	0.2343	0.2165	ns	0.6529

From the ultrasound skin thickness and probe depth measurements, the AUC_{0-24} values for either formulation were plotted against PD and RPD. Although the figures for all combinations of AUC, PD, and RPD from either method (M1 and M2) are represented in Figure 4.6, we were more interested in the results from the method M2 since it has the most favorable outcome (as discussed earlier). Inverse relation of PD with AUC_{0-24} was observed and the slopes for cream and gel were not significantly different ($p= 0.7335$, AUC vs PD; $p=0.6523$, AUC vs RPD). However; the coefficient of linear regression observed were very poor ($R^2_{PD-cream}= 0.03655$, $R^2_{PD-gel}= 0.04961$, $R^2_{RPD-cream}= 0.0012$, $R^2_{RPD-gel}= 0.0893$).

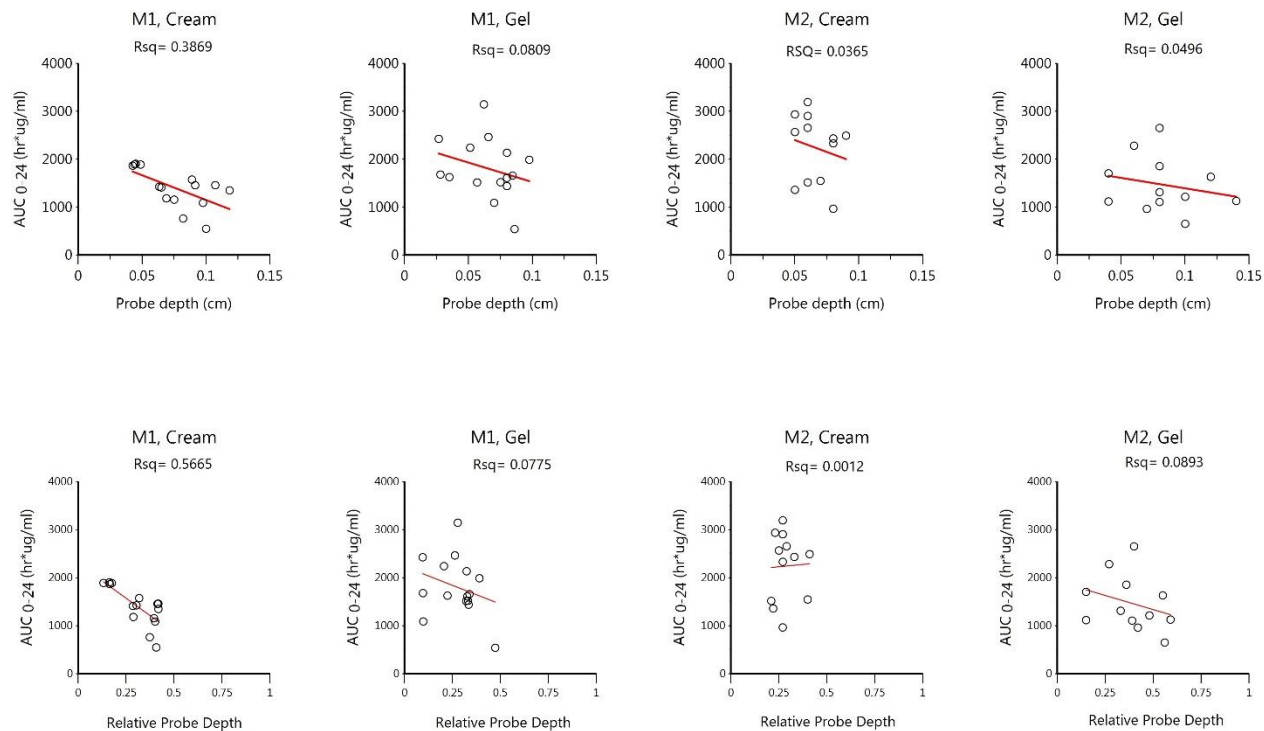


Figure 4.6: (Top) AUC of MTZ between 0 and 24 hrs (AUC_{0-24}) plotted against average probe depth for Cream and Gel treatments in either method M1 and M2. (Bottom) AUC of MTZ between 0 and 24 hrs (AUC_{0-24}) against average relative probe depth for Cream and Gel treatments in either method. The line of linear regression is drawn in red, the Rsq value indicates poor correlation.

A slight relationship between PD or RPD and the partial area from time zero to 2 hours, $pAUC_{0-2}$ was observed (Figure 4.7). During the first 2 hours, the exposure would be maximum and a better relationship between PD and AUC might be captured.

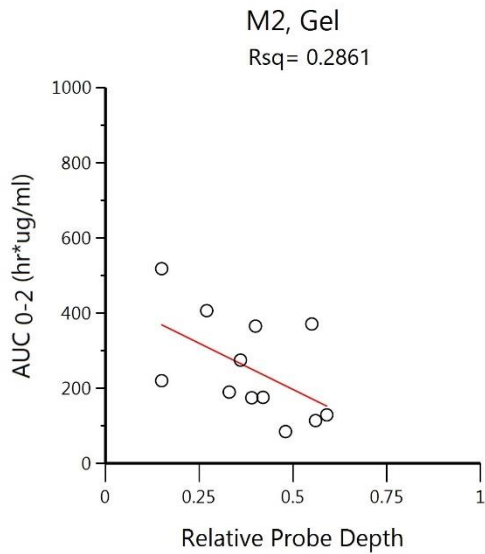
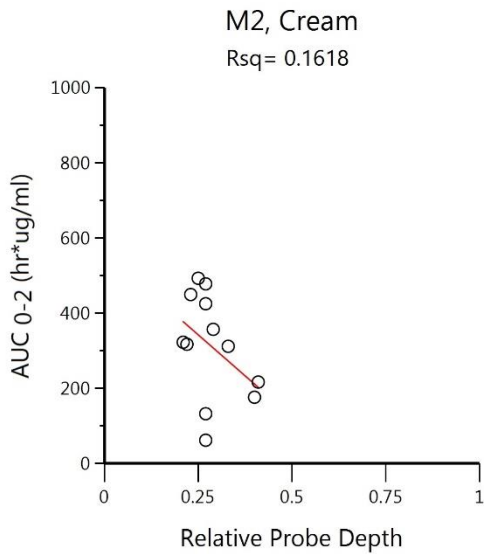
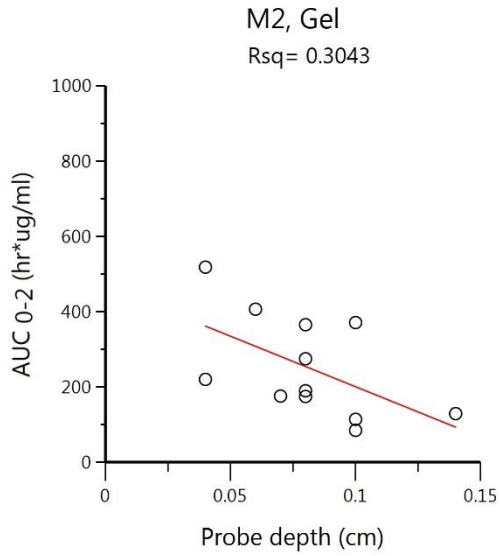
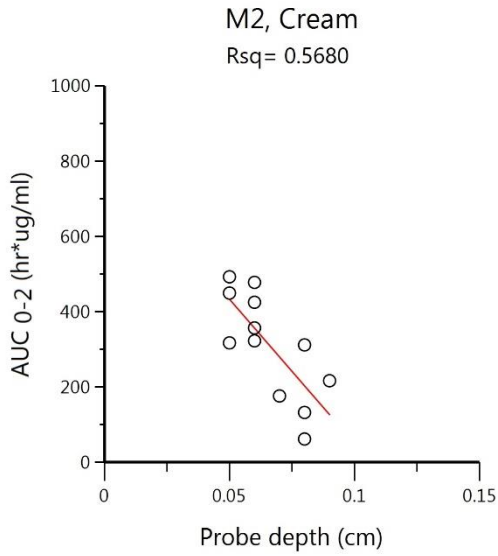


Figure 4.7: (Top) Partial AUC between 0 and 2 hrs (pAUC0-2) plotted against average probe depth for Cream and Gel treatments using method M2. (Bottom) pAUC0-2 plotted against average probe depth ratio for Cream and Gel treatments using method M2. The line of linear regression is drawn in red, the Rsqr value indicates poor correlation.

4.3.4 Dose-response study:

In a separate set of dose sensitivity experiments, Metronidazole 0.75% topical cream applied on two sites for each dosing of 5, 10, and 30 mg/cm², demonstrated a linear response (AUC) to dosing ($R^2=0.9995$, Figure 4.8). This demonstrates a good sensitivity of dMD method to detect differences in the concentration of drug at the target tissue.

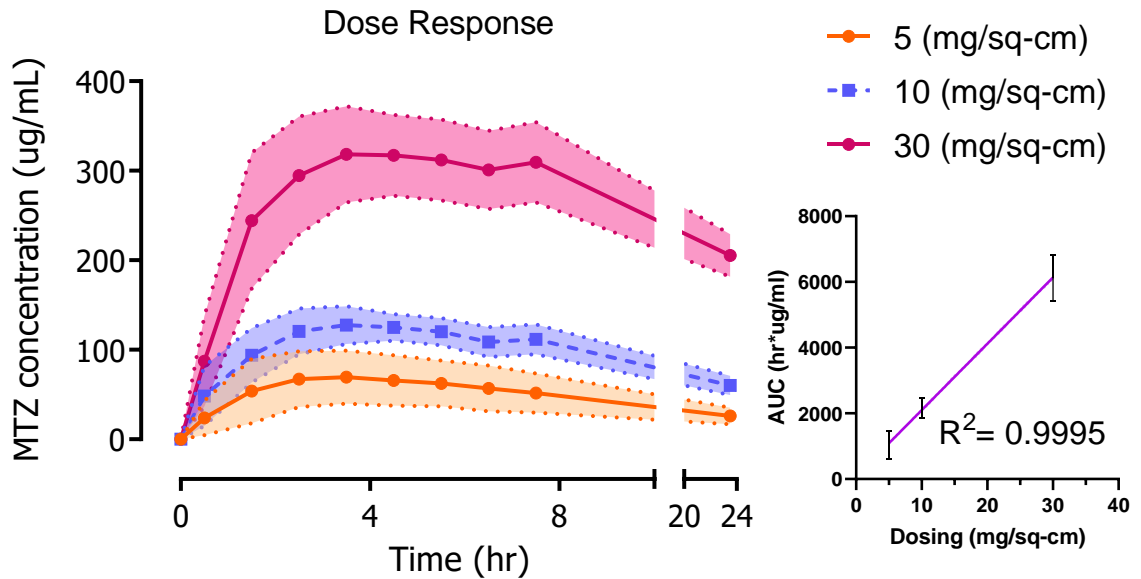


Figure 4.8: Concentration-time profile in the dermis after topical administration of MTZ 0.75% Cream at three different dosages 5, 10, and 30 mg/cm² using strategy M2. (Inset) Linear regression of AUC₀₋₂₄ with dose, $R^2=0.9995$. [Mean (SD), n=12 probes]

4.4 Discussion

The present investigation was performed to check the feasibility of undertaking an ex vivo permeation study with topical application of commercial pharmaceutical products and the likelihood to determine the bioequivalence of such products. Ex vivo dermal microdialysis (dMD) studies have been performed in the past (29,47,48) to investigate cutaneous permeation of drug in solution; yet, we were interested in designing a first of its kind ex vivo skin model to discriminate between formulations and establish it as a routine bioequivalence tool. Various factors that were pertinent to the ex vivo dMD process needed to be understood and standardized. In the previous chapter, we have discussed and standardized the dMD probe, perfusion rate, and sampling frequency. In this chapter, we have focused on our goal to select an appropriate skin model and test the system for specificity, selectivity, and sensitivity.

Outcomes of our ex vivo experiments could be translated to in vivo conclusions only when the in vivo variables are mapped to our ex vivo studies. During the initial pilot study, the full-thickness skin without subcutaneous fat layer (0.25 cm), in absence of a backing hydration reservoir, was observed to get dry with time and bent inwards toward the stratum corneum side. This phenomenon was resolved with a mechanistic approach of the addition of a backing hydration support/reservoir. A range of cellulosic fiber and Styrofoam sheets were evaluated and eventually, the Ancare Nestlet (mentioned in the M1 method section) was selected as backing material due to its wicking capacity suitable for our purpose. The backing material provided a cushion for the skin and when moistened with a surplus amount of lactated ringer solution (LRS) it acted as a reservoir that continuously provided moisture from the ventral side of the skin throughout the experiment. The TEWL of the skin was monitored often during the ex vivo MD study and LRS was added to the peripheral wall of the aluminum boat as and when required to keep the TEWL level within $\pm 20\%$ of the value recorded at the start of the experiment. Also, the

skin was occluded with a parafilm layer after application of the formulations. With these modifications, the skin at the end of the 24 hrs study was visually similar to the skin before the starting.

Historically, dermal microdialysis research has been jeopardized by high variability in inter-subject results (46,49). Fact that the intra-subject variability reported in these studies was lower than 20%, same skin explant from a single donor could be employed for four-period full-replicate two formulation design for BE study, as suggested by the latest USFDA Guideline on Statistical Approaches to Establishing Bioequivalence (9). In all experiments, fresh porcine skin strip (5 cm by 20 cm) from the belly of female donors was harvested. A total of six ex vivo experiments were conducted, three for either method (M1 and M2). Each time, a Parallel Four-period Full Replicate (RTRT) design approach was followed and nine dMD probes were inserted in the dermis of a skin strip. The reference (R) formulation was Metronidazole 0.75% topical cream (Fougera), and the test (T) formulation was Metronidazole 0.75% topical gel (Impax), and one additional lateral diffusion probe. Lateral Diffusion data shows no sign of analyte. This is first-hand proof that the signal observed in the probe beneath the application site into the dermis is not influenced by the analyte permeated from the adjacent application site and the crosstalk of dMD probes from these application sites should be rejected. The response obtained from the dMD probes confirms specificity to the respective application site. Also, Ex vivo full-thickness skin sample can be compared to a vasoconstricted system (50). Due to the lack of vascular circulation, the distribution-redistribution mechanism was assumed to be absent. This presents a strategical advantage and justifies our scheme of testing the reference and the test formulation simultaneously adjacent to each other on the same skin sample harvested from a single animal subject and reduces the burden of inter-subject variability.

The MTZ dermis PK profile observed by the M1 dMD method is not consistent with the results from reported in vivo pig data where the gel has always underperformed compared to cream (1). The results were supported with evidence that the gel formulation dries out comparatively faster and permeates slower than the cream (45). Both over-hydration and occlusion, have been reported to significantly increase the percutaneous absorption of compounds (51). This explains the anomaly in the increased exposure from gel formulation in our study method M1 and the probable reason for bioavailability profile reversal.

A repeat study was performed without occlusion of the application site, this time the ratio of In-AUC reduced to 0.94 but the 90% CI was still higher (0.60–1.49). The investigation from the concentration-time profile curve of the no-occlusion study revealed a substantial difference in the initial absorption phase. The ratio of In-Cmax reduced from 1.64 to 1.29. This gives us the idea that occlusion at the application site in synergy with other underlying factors (probably hydration) was leading to increased absorption of MTZ in gel treatments. Eventually, the concentration-time profile from the experimental method M2 proved the anomaly in absorption for gel treatment was due to over-hydration in the earlier experiments. Changes in the hydrodynamics of the skin modulate the permeation profile yet the dMD model was selective enough to discriminate between the formulation differences.

Comparing M1 and M2 methods, the former needed complicated hydration steps that may present errors due to the operator and needed constant monitoring of TEWL. Whereas the M2 method was a simple 'old school' type without any complex conditioning or monitoring steps, yet it produced the desirable results (mimic permeability profile of in vivo and IVPT, Figure 4.9). The sensitivity of the M2 dMD was assessed using various increasing doses of formulations. The three doses tested (3, 10, and 30 mg/cm²) displayed different dermal bioavailability profiles to permit noticeable discrimination between the doses and demonstrated the sensitivity of the dMD to

detect changes in MTZ's local bioavailability. All the doses were applied in duplicate on a single strip of skin explant from the same pig subject to eliminate any statistical bias and produce meaningful correlations. While a 30 mg/cm² dose application is quite large, yet at this high dose the response was linear and dose saturation was not observed.

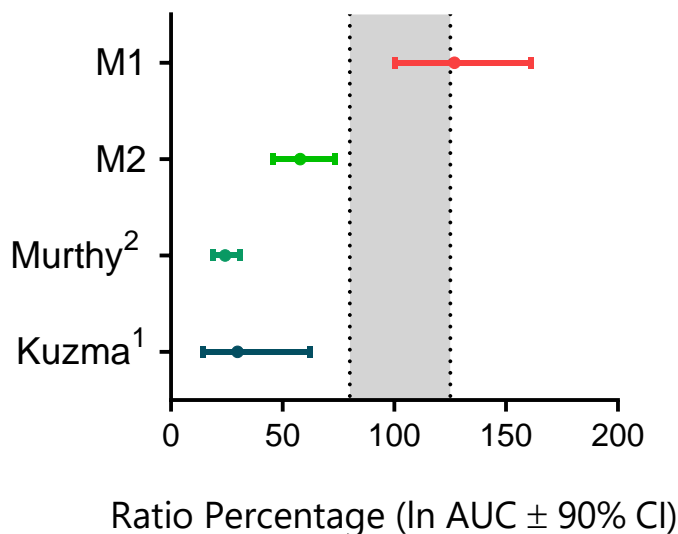


Figure 4.9: Comparison of AUCs between Gel formulation (negative control) and reference Cream formulation. The outcome of the ex vivo dMD method is consistent with in vivo data from Yucatan minipig (1), and IVPT data from a human cadaver (calculations performed on available data from Murthy et al (45)).

4.5 Conclusions

The lack of signal in the lateral diffusion rejects any possible cross-talk of dMD probes and indicates the probes implanted underneath a designated formulation application site is specifically measuring their local bioavailability. The ex vivo M2 dMD method selectively captured the differences in bioavailability between the cream and the gel and was sensitive to variable doses for which a linear dose-response was observed. The fact that reference and test formulations can be tested simultaneously, the experimental population size required to establish bioequivalence for TDDPs can be reduced. It is efficient on time and resources and mimics more closely the permeability behavior observed in vivo. This current experimental setup may provide a

convenient, reliable, cost-effective, table-top, and quantitative approach to evaluate the percutaneous drug permeability of TDDP.

Chapter 5: Effect of Temperature on Permeation of Formulation Using Ex Vivo Dermal Microdialysis Method

5.1 Introduction

In the previous chapters, we have defined a suitable dMD method using pig skin ex vivo whereby we have sequentially explored the effect of hydration, occlusion, and thickness of the skin in the bioavailability profile of gel and cream formulations. The M2 method was useful in manifesting a concentration-time profile of drugs relevant to in vivo outcomes, and also the method was found to be linear. While the sole intention of the study was to explore the feasibility of an ex vivo dMD method and optimize the parameters, the study was performed at ambient laboratory temperature of 25.1 ± 1.2 °C and warrants us to explore the pharmacokinetic performance of the formulations using the M2 dMD method at the physiological temperature.

The three major events in the drug permeation process, namely- release of drug from TDDP, drug partitioning in stratum corneum, and the drug diffusion/permeation through the skin; are all affected by the modulation of the temperature of the skin. With the increase in temperature, activation-energy-related changes in the formulation are attributed to the changes in the permeation profile of formulations. An early report by Scheuplein in the 1960s demonstrated the changing relationship of the permeation of water through the skin at different temperatures (52). In yet another report, Blank et al. investigated the effects of temperature on the transport of nonelectrolytes across the skin and found that polar and nonpolar molecules appeared to diffuse through the epidermis by different molecular mechanisms characterized by different activation energies (53).

In the last two decades, considerable work has been done to understand the effect of temperature on the permeant and the cellular components. Although, there are mixed opinions on the increased permeation of drug with temperature, the change in the structure of the skin with increasing temperature has been well documented (54). In an expert review, Hao et al (55), summarized outcomes from a myriad of in vivo studies of transdermal and topical drug products

under elevated temperatures. The review also tabulated the levels of increase in permeability with temperature changes. However, in their opinion, *in vitro* and *in vivo* methods reported in the literature to study heat effects of transdermal/topical drug products are based on inconsistent study conditions, and *in vitro* models require better characterization. An increase in the local bioavailability of any drug in the dermis may be attributed to the drug's lipophilicity, the solubility of the drug in the formulation, skin permeation pathway, activation energy, presence of hydrogen bonding groups (56). Thereby it is essential to understand the actual mechanism behind the permeation of the drug in the skin and may require careful consideration while designing a dermal bioavailability experiment. In this chapter, we will explore the effect of skin temperature on the permeation profile of metronidazole using *ex vivo* dMD.

In absence of a vasculature system in our *ex vivo* experimental method, thermoregulation is not possible. To mimic a physiological temperature, we are limited to provide heat from the ventral side of the skin explant since providing heat from the top might alter the thermodynamics of the formulation and affect the stratum corneum.

5.2 Method

5.2.1 Chemicals and reagents

Metronidazole (99%) (MTZ) was purchased from Beantown Chemical (Hudson, NH). Lactated Ringer Solution (LRS, NDC- 0338011703, Baxter Healthcare Corp., Deerfield, IL), Metronidazole 0.75% Cream (NDC- 0168032346, Fougera Pharmaceutical Inc., Melville, NY), Metronidazole 0.75% Gel (NDC- 0115147446, Impax Generics, Hayward, CA) and all other medical supplies were purchased from Henry Schein (Melville, NY). LC Grade acetonitrile, water, and other supplies were purchased from Fisher Scientific (Fair Lawn, NJ, USA).

5.2.2 HPLC Analytical method

The concentration of the analyte in the dialysate was measured using an Agilent 1100 series HPLC-UV apparatus (Agilent Technologies, Santa Clara, CA) and the results were integrated using Agilent ChemStation. The system consists of a degasser, quaternary pump, temperature-controlled autosampler with a 50 μ L sampling loop, a temperature-controlled column compartment, and a DAD Detector. The column compartment was fitted with an Xbridge C18 3.0x50mm 5 μ m reverse phased column (Waters Corp. Milford, MA) and was set at 25°C. The mobile phase consisted of deionized water (DI) and acetonitrile (ACN) at the ratio of 90:10 and an isocratic flow was maintained at 0.3 mL/min. The detection wavelength was 325 nm (bandwidth \pm 4nm) and the reference wavelength was set at 400 nm (bandwidth \pm 5nm). The autosampler temperature was maintained at 5°C.

5.2.3 Experimental setup

A general-purpose water bath of dimension 14x10 inch (Thermo Scientific, Waltham, MA) was filled with 3L distilled water and set at 50°C. The bath was covered with a stainless-steel (SS) sheet and kept 'ON' overnight to attain a temperature of 40°C at the surface of the sheet. The following day, skin explants were harvested from fresh slaughtered female Yorkshire pig belly purchased from a local meat shop. A full-thickness pig skin explant with the underlying subcutaneous fat layer (total thickness \approx 1 cm) was placed on an aluminum foil tray (refer M2 ex vivo dMD method, chapter 4), and placed on top of the SS sheet to equilibrate (Figure 5.1).

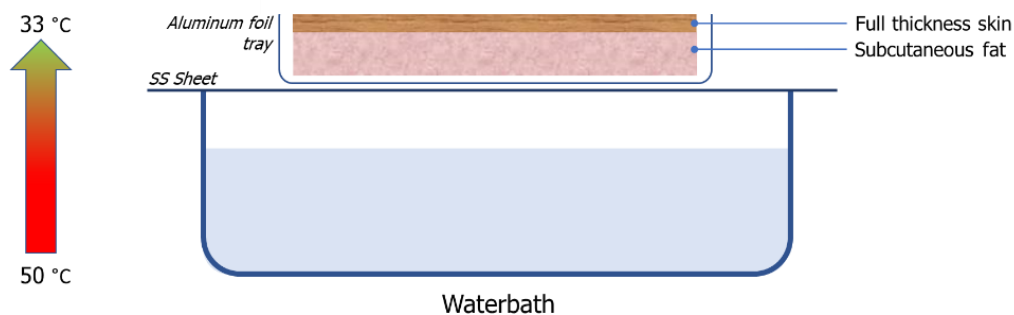


Figure 5.1: Schematic representation of the setup for the study of the influence of temperature on the ex-vivo dMD study using pig skin explant. Briefly, a water bath, filled with distilled water, covered with a stainless-steel plate is setup at 50°C. Pig skin explant housed in an aluminum foil tray is heated from the ventral side when placed on top of the steel plate over the water bath. The arrow on the left shows the gradient of heat from 50°C at the bath to 33°C at the surface of the skin.

For dermal microdialysis, disposable linear dMD probes were inserted in the skin as discussed earlier for M2 dMD setup in chapter 5. On one end of the probe arm, Tygon tube connected to Chemyx Fusion 400 Pump (Chemyx, Inc.; Stafford, TX) was attached. The entire probe tubing was flushed with LRS perfusate to remove any air bubbles. After flushing, the infusion pump was set at a flow rate of 0.5 μ L/min. A 3M double-sided tape (3m, Minneapolis) with a circular hole (2.5 cm diameter) punched out, was placed on the top of the application area as a guide for formulation application, and commercially available generic Metronidazole 0.75% topical cream and Metronidazole 0.75% topical gel were applied alternately on the four marked sites of the skins. In each circular application site (area = 4.9 cm²), 10 mg/cm² of the formulations was carefully administered with a positive displacement pipette (Gilson Distriman, Middleton, WI) and rubbed in a circular motion with the rubber head of 1ml BD syringe plunger for 15 sec. The time of application of formulation is noted and samples were collected at the end of each hour in HPLC inserts for eight hours and terminally at 24th hours and analyzed immediately.

TEWL (VapoMeter, Delfin Technologies, Miami, FL) measurement at the surface of the skin was measured before placing the skin on the SS sheet and after the equilibration of the skin.

Temperature of the SS sheet on the water bath, aluminum foil, and the skin tissue was routinely monitored using an Infrared Thermometer (Fluke Corporation, Everett, WA).

5.2.4 Ultrasound measurement

The role of the dMD probe depth on the local microenvironment (AUC) of the drug in the skin was determined using a 20 MHz ultrasound machine (Logiq E7, GE Healthcare, Chicago, IL) at the end of each study. Briefly, the 1.5 cm ultrasound probe was placed over the skin where the dMD probe is placed (the entry and exit of dMD probe serve as a guide), and three images from each probe were captured to calculate the mean probe depth (PD) and the ratio of probe depth over the thickness of the dermis, called as relative probe depth (RPD) was calculated.

5.2.5 Data processing

The calculated concentration of MTZ in the samples was plotted against mid-sample interval time using PhoenixWinNonlin 8.2 (Certara; Princeton, NJ). A non-compartmental analysis (NCA) was used to obtain pharmacokinetic parameters. Occasional plotting of data was performed using GraphPad Prism (GraphPad Software, San Diego, CA.)

5.2.6 Statistical analysis

A two-stage analysis approach was employed, the first stage of the approach involves estimating the PK parameters from individual dense concentration over time data (taking mid-points of the sampling intervals) using noncompartmental methods in Phoenix WinNonlin. Individual parameter estimates obtained during the first stage were used as input data for the second-stage calculation of descriptive summary statistics on the sample, typically, mean parameter estimates and SEM. Non-parametric, unpaired Mann-Whitney test (GraphPad Prism Software, San Diego, CA). was used to compare the descriptive statistical differences. The definition of statistical significance was set at an alpha error of less than 0.05.

5.3 Results

5.3.1 Dermal Pharmacokinetic profile

In an attempt to mimic the physiological temperature of skin explant, we have provided the heat from the ventral side of the skin. For this, a water bath with a flat steel top was used. Although, the surface temperature of the SS plate was stabilized to about 40 °C, when the aluminum tray containing the skin was placed on top of the SS plate, it took several hours before the surface temperature of the skin reached the physiological temperature. Correspondingly, the TEWL of the skin was increased and the surface became dry before sample application. To speed up the process to attain the physiological temperature of the skin explant, the temperature of the water bath was increased to 60 °C; however, this approach had to be discontinued because the subcutaneous fat layer of the skin explant, in contact with the heat, began to melt. The subcutaneous fat layer, in a way, failed to conduct the heat to the dermis and underwent a thermal degradation at a higher temperature. Thus, although time-consuming, the slow attainment of temperature was preferred for ex vivo pharmacokinetic study. The mean temperature of the skin before the application of the dosage was 33°C and drifted approximately +0.1 °C every hour as the study progressed.

Following the topical application of the MTZ cream and gel, under a controlled temperature of the skin, a rapid rise in the dermal penetration was observed, and C_{max} was achieved within the first 2 hrs. The overall permeation profile of cream was significantly higher than the gel (unpaired, non-parametric, Mann, p value=0.0005) but there was no significant difference in C_{max} between cream and gel (unpaired, non-parametric, t-test, p value=0.8428) (Figure 5.2). The change in mean AUC of MTZ cream (n=3 replicates with 4 probes for each formulation on different days) at elevated temperature compared to laboratory temperature shows no significant difference (p=0.2575) but the temperature has a significant effect on the mean AUC of MTZ gel

($p=0.0236$). No statistically significant effect of temperature was found in C_{max} of cream and gel formulation ($p=0.4868$ and 0.2675 respectively, $n=3$ replicates with 4 probes for each formulation on different days) (Figure 5.3). Fold increase in the AUC and C_{max} value at physiological temperature compared to dMD performed at laboratory temperature (chapter 4) is tabulated in Table 5.1.

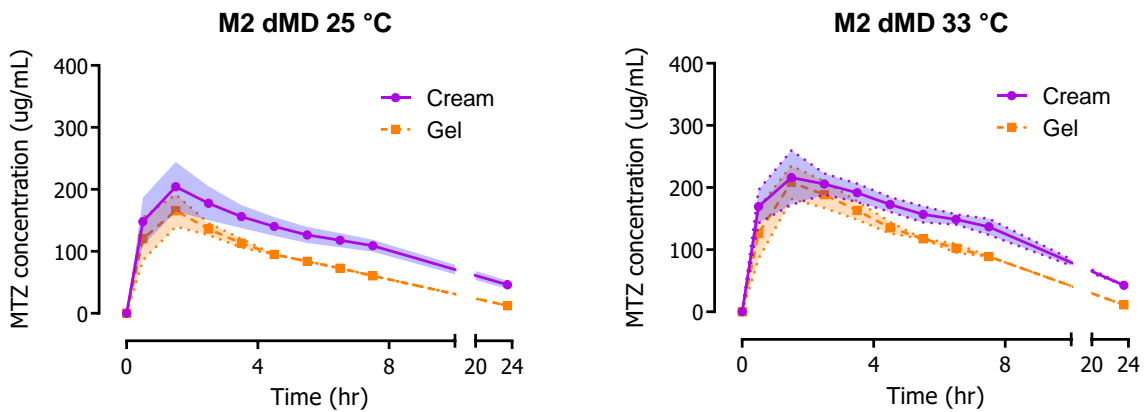


Figure 5.2: Concentration-time profile of MTZ in the dermis after topical administration of formulations in two different experimental conditions M2 at ambient laboratory temperature 25°C (left) and M2 controlled physiological temperature 33°C (right). Purple- profile after treatment with MTZ 0.75% topical cream and, Orange- profile after treatment with MTZ 0.75% topical gel. The AUC of Cream is higher than Gel at both temperature settings, but the C_{max} for Cream and Gel at 33°C was equivalent. (Mean \pm SEM, $n=3$ replicates with 4 probes)

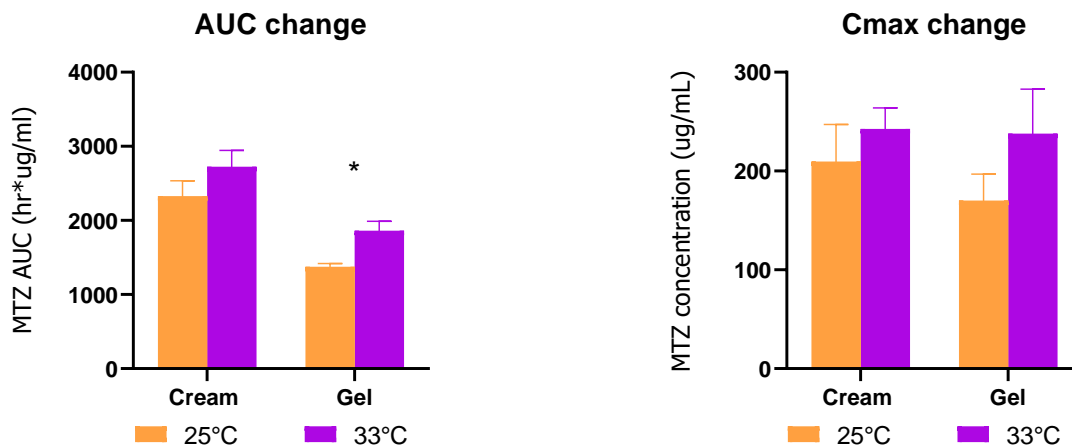


Figure 5.3: (Left) Change in mean AUC of MTZ Cream and Gel formulations between ambient laboratory temperature (25°C, orange) and physiological temperature (33°C, purple). * A significant rise in AUC for Gel formulation is observed at the elevated temperature ($p=0.0236$). (Right) Change in mean C_{max} of MTZ Cream and Gel formulations at two different temperatures. No significant change in C_{max} was observed ($p=0.4868$, 0.2675). (Mean \pm SEM, $n=3$ replicates with 4 probes for each formulation on different days).

Table 5.31: AUC and Cmax values of MTZ Cream and Gel formulation at two different experimental temperature in ex vivo dermal microdialysis. (Mean ± SEM, n=3 replicates with 4 probes for each formulation)

	AUC			Cmax		
	Laboratory Temp (25°C)	Physiological Temp (33°C)	Fold Increase	Laboratory Temp (25°C)	Physiological Temp (33°C)	Fold Increase
Cream	2329.5±205.9	2725.4±218.3	1.17	209.6±37.5	242.6±21.3	1.16
Gel	1374.7±43.3	1860.2±129.7*	1.35	170.2±26.8	237.8±45.2	1.40

5.3.2 Ultrasound Measurement

Ultrasound measurements, to verify proper probe placement in the dermis and record structural deformities of the probe, were performed terminally at the end of 24 hours of sampling. During this time, the surface of the skin was found to be visually different from the initial setup. By this time, the skin has lost a lot of its surface moisture, shrunken in size (about 10% linear reduction), and has warped on the surface. Due to these proceedings, ultrasound measurement was unsatisfactory (refer to Figure 5.4), thereby, no fruitful correlation between the probe depth and the AUC could be developed.

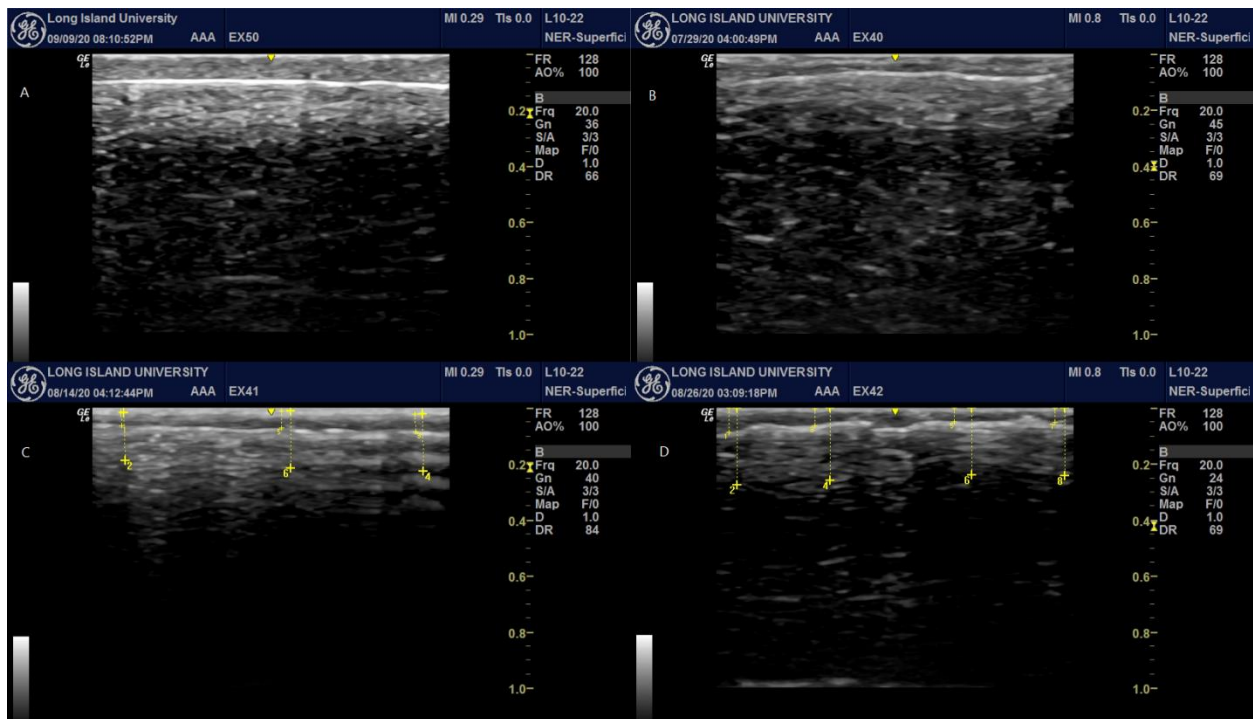


Figure 5.4: Ultrasound images captured using GE-Logiq E7 with 20 MHz probes at Nerve-Superficial setting. (A) Image captured from pig skin explant using M2 method after 24 h sampling at ambient temperature. The epidermis layer is smooth, and the probe is linear (bright horizontal line) without any wavy interferences. The dermis layer is distinct and continuous. (B) Image captured from pig skin kept at 33°C shows deformed epidermis making probe depth calculation with some errors. (C) Image captured from pig skin kept at 33°C shows wavy interferences. With time the skin shrinks and becomes warped, the ultrasound probe fails to make smooth contact with the skin resulting in wavy interferences and gives inadequate imaging; probe depth and skin thickness estimations are unrealistic. (D) The warping of the skin results in deeper tissue deformation and bending of the probe; measurement of probe depth or skin thickness from such images is not possible.

5.4 Discussions

Andersen et al., in a study investigated the physiological thermoregulation effect in pigs housed in kennels with low temperatures. With the lowering of ambient temperature to freezing and sub-freezing conditions, the core body temperature remained unchanged, but the body surface temperature decreased with decreasing temperatures. The author explains this reflex as a heat conservation mechanism by peripheral vasoconstriction (57). Also, the thicker fat layer in adult pigs enables them to limit the heat flow from the body core to the surroundings (58). The ex vivo skin explant in our study could also be compared to a vasoconstricted system with a thick subcutaneous fat layer that restricts the conduction of heat provided from the bottom to the dermis and upwards. As a result, the surface of the skin was colder, and the fat layer underneath was melting. Superficial addition of heat was also not feasible as it may change the thermodynamics of the formulation leading to alteration in permeation kinetics. Thus, the dilemma is to select an appropriate method to maintain the physiological temperature of the skin ex vivo.

Early in the 60s, in a series of pioneering works, Robert Scheuplein proposed a mechanistic relationship of the flux of permeant across the human epidermal membrane with temperature. He observed about 2 fold increase in the flux of tritiated water when the receptor temperature was raised from 25 to 35°C (52,59). In a similar experiment with another polar molecule (caffeine), Akomeah et al reported about 2 fold increase in flux across the human epidermis with every 7-8 °C rise in temperature of the cell (56). In our ex vivo pig skin study, using a polar permeant (MTZ), we expected a significant increase in the permeation profile when compared between ambient laboratory conditions and physiological temperature. However, the increase in the AUC values of MTZ after 24 hrs of microdialysis sample from the dermis suggests that the model is not sensitive for MTZ to respond to changes in temperature.

Elevated skin temperature would not only bring structural changes in the skin morphology but also leads to the drying of formulations. Such metamorphosis of the formulation may lead to a reduction in the aqueous phase due to evaporation, precipitation, or even crystallization of the drug on the skin surface and change in the diffusion constant of the entire product (60). In one trial experiment, the surface temperature of skin was intentionally elevated and the formulation (cream and gel both) drying was monitored with a microscope every hour until the end of the study. No crystal precipitation on the surface of the skin was observed throughout the study. Microscopic images of the formulation at the application sites during the microdialysis experiments were randomly monitored and no physical formulation change other than gradual drying was observed. This observation at physiological temperature is visually the same as that at ambient laboratory conditions, thus no changes based on the temperature of the testing method can be concluded.

Any temperature-related activation-energy or permeation changes of individual components of the formulations are beyond the scope of the study and were not addressed.

5.5 Conclusions

The physiological temperature of ex vivo pig skin explant was achieved by providing continuous heat from the ventral side using a closed water bath system. The process of attainment of the temperature is labor-intensive and adds several extra hours of pre-experimental set-up time; regardless, at the cost of thermal-degradation of the sub-cutaneous fat layer. After 24 hours of sampling duration, the skin is visually different, shrunk 10% in each dimension, and warped at the surface. The difference in the permeation profile of MTZ cream as well as gel formulations at physiological temperature is not apparent and may be attributed to the physiochemical nature of the permeant (MTZ). The present study methodology might be applied in the future with another model drug with different physiochemical properties (logP, polarity, etc.) to test the limits of the

method. However, with the current outcomes in place, the ex vivo dMD method developed yet should be used at ambient laboratory temperature (around 25°C) for the Bioequivalence estimation of Metronidazole 0.75% cream generic with regards to its RLD commercial product.

Chapter 6: Feasibility Testing of A Bioequivalence Study of Metronidazole Cream Using An Ex Vivo Dermal Microdialysis Method.

6.1 Introduction

In the preceding chapters, we have designed and tested a dMD method using pig skin ex vivo system to estimate dermal bioavailability of topically administered products; whereby, the method was successfully employed to discriminate within the kinetic profiles of the gel and cream formulations. The method was not able to discriminate the effects of temperature and manifested a concentration-time profile of the drug which was relevant to similar in vivo study data. Importantly, the method was found to be linear with dose-response. A worthwhile intention of the development of the model was to explore the feasibility of the model to be used in the bioequivalence study of topically applied pharmaceutical products.

The FDA requires that drug manufacturers demonstrate, among other things, Bioequivalence (BE) between the generic product and its corresponding reference listed drug (RLD) product (61). One of the parameters that the generic drug is considered bioequivalent to the RLD if they do not show significant differences in their rates and extents of absorption. The rate and extent of drug absorption are determined from the following PK endpoint parameters namely peak concentration (C_{max}) and the area under the concentration-time curve (AUC), respectively. The average bioequivalence calculation is based on the 90% confidence interval for the geometric least-squares mean ratio of the test formulation over the reference formulation for C_{max} and AUC, and must fall between the BE limits, set from 80% to 125% (9).

In the present chapter, we propose to evaluate the ex vivo dMD model developed thus far for the bioequivalence (BE) estimation between RLD (reference listed drug product) and its generic TDDP of Metronidazole. The BE will be determined by comparing the ratio of log-normal AUC of the generic formulation with its RLD formulation, at a confidence of 90%. The RLD Metrocream (Galderma) and its generic product Metronidazole 0.75% topical cream (Fougera) will be applied topically on pig skin ex vivo as discussed earlier in the method M2 (chapter 4)

using the same parallel four-period full-replicate design and the PK parameters will be compared to test the bioequivalence. The data thereby obtained will be compared to available literature or studies from other groups to ascertain the reliability of the new method.

6.2 Method

6.2.1 Chemicals and reagents

Metronidazole (99%) (MTZ) was purchased from Beantown Chemical (Hudson, NH). Lactated Ringer Solution (LRS, NDC- 0338011703, Baxter Healthcare Corp., Deerfield, IL), MetroCream (Metronidazole topical cream 0.75%, NDC-0299386545, Galderma Pharmaceutical company, Lausanne, Switzerland), Metronidazole 0.75% Cream (NDC-0168032346, Fougera Pharmaceutical Inc., Melville, NY) and all other medical supplies were purchased from Henry Schein (Melville, NY). LC Grade acetonitrile, water, and other supplies were purchased from Fisher Scientific (Fair Lawn, NJ, USA).

6.2.2 HPLC Analytical method

The concentration of the analyte in the dialysate was measured using an Agilent 1100 series HPLC-UV apparatus (Agilent Technologies, Santa Clara, CA) and the results were integrated using Agilent ChemStation. The system consists of a degasser, quaternary pump, temperature-controlled autosampler with a 50 μ L sampling loop, a temperature-controlled column compartment, and a DAD Detector. The column compartment was fitted with an Xbridge C18 3.0x50mm 5 μ m reverse phased column (Waters Corp. Milford, MA) and was set at 25°C. The mobile phase consisted of deionized water (DI) and acetonitrile (ACN) at the ratio of 90:10 and an isocratic flow was maintained at 0.3 mL/min. The detection wavelength was 325 nm (bandwidth \pm 4nm) and the reference wavelength was set at 400 nm (bandwidth \pm 5nm). The autosampler temperature was maintained at 5°C.

6.2.3 Ex vivo experimental setup

Skin explants were harvested from fresh slaughtered female Yorkshire pig belly purchased from a local meat shop. A full-thickness pig skin explant with the underlying subcutaneous fat layer (total thickness ≈ 1 cm) was placed on an aluminum foil tray (M2 ex vivo dMD method, chapter 4). A total of three skin explants from different animal subjects, each of dimension 5 x 20 cm were used. On each skin strip, four different application sites (5 x 5 cm) were marked and a parallel four-period full-replicate (RTRT) design was employed. These application sites were visually inspected for damages or discoloration. Skins with defects or deviations of TEWL more than 20% within the application sites were excluded from the study. On each application site a circular (2.5 cm diameter) location, towards the center, was selected and two dMD probes, 1 cm apart, were inserted into the dermis with the help of a guide cannula (a total of eight probes per skin strip), and one lateral diffusion probe was inserted in the dermis toward the center of the skin at a distance of 2 cm from the adjacent test probes (Figure 6.1).

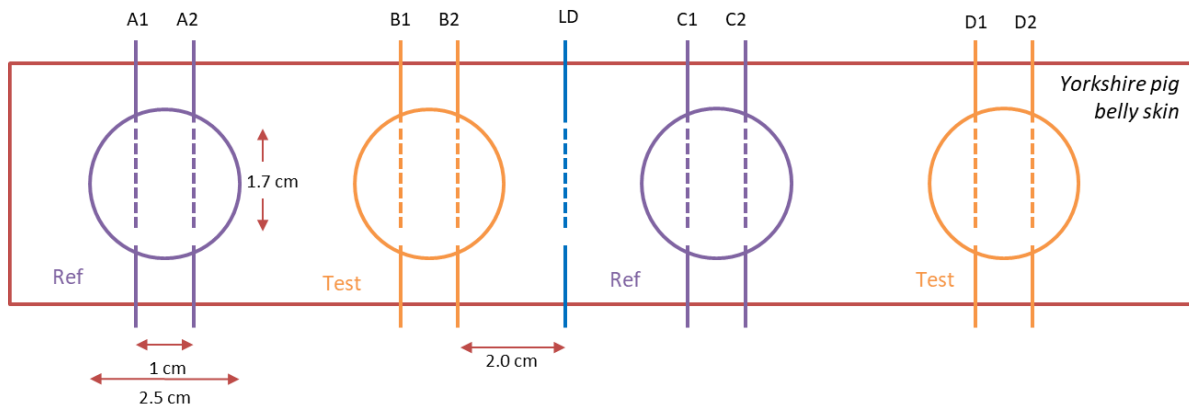


Figure 6.1: A sample template of the dMD probe placement and application site for the formulations on the skin. Probe and application site for RLD MTZ cream is marked with purple and marketed generic MTZ cream with orange. The application sites are circular (diameter 2.5 cm) and the probes in each site are 1 cm apart. The lateral diffusion probe (blue) is 2 cm apart from adjacent probes.

On one end of the probe arm, Tygon tube connected to Chemyx Fusion 400 Pump (Chemyx, Inc.; Stafford, TX) was attached. The entire probe tubing was flushed with LRS perfusate to remove any air bubbles. After flushing, the infusion pump was set at 0.5 uL/min. A 3M double-sided tape (3m, Minneapolis) with a circular hole (2.5 cm diameter) punched out, was placed on the top of the application area as a guide for formulation application, and RLD of Metronidazole 0.75% topical cream and its approved marketed generic were applied alternately on the four marked application sites of the skins (Figure 6.1). In each circular application site (area = 4.9 cm²), 10 mg/cm² of the formulations was carefully administered with a positive displacement pipette (Gilson Distriman, Middleton, WI) and rubbed in a circular motion with the rubber head of 1ml BD syringe plunger for 15 sec. The time of application of formulation is noted and samples were collected at the end of each hour in HPLC inserts for eight hours and terminally at 24th hours and analyzed immediately.

6.2.4 Data processing

The calculated concentration of MTZ in the samples was plotted against mid-sample interval time using PhoenixWinNonlin 8.2 (Certara; Princeton, NJ). A non-compartmental analysis (NCA) was used to obtain pharmacokinetic parameters. The Bioequivalence Module of PhoenixWinNonlin was used to determine the 90% confidence interval for the ratio of the geometric mean of the PK endpoint parameters of generic and its RLD, and plotting of data was performed using GraphPad Prism (GraphPad Software, San Diego, CA).

6.2.5 Statistical analysis

A two-stage analysis approach was employed, the first stage of the approach involves estimating the PK parameters from individual dense concentration over time data (taking mid-points of the sampling intervals) using noncompartmental methods in Phoenix WinNonlin. Individual parameter

estimates obtained during the first stage were used as input data for the second-stage calculation of descriptive summary statistics on the sample, typically, mean parameter estimates and SEM. The in-built Bioequivalence module of PhoenixWinNonlin was used for the BE estimation. Relevant data plotting was performed using Graph Pad (GraphPad Prism Software, San Diego, CA). The definition of statistical significance was set at an alpha error of less than 0.05.

6.3 Results

6.3.1 Dermal Pharmacokinetic profile

The dermal concentration kinetic profile of the formulations from three different skin samples with the RTRT design (as discussed in the method section above) is represented in Figure 6.2. The dermal exposure of the RLD and generic product of Metronidazole cream was similar across the study but for the second skin donor where the mean and standard deviation of the approved generic product was lesser throughout all sampling points. The overall study results indicate that the exposure of the test formulation measured at the dermis is equivalent to the reference product at 90% CI (Figure 6.3).

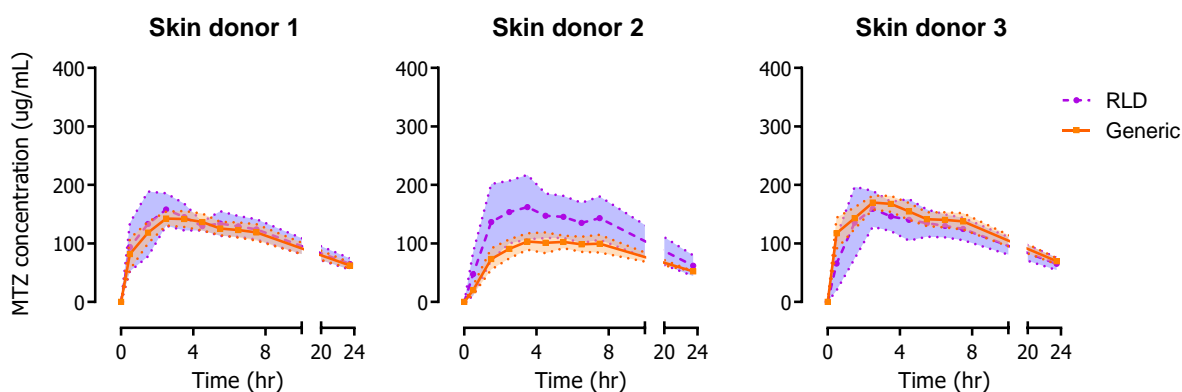


Figure 6.2: Concentration-time profile of MTZ in the dermis after topical administration of formulations in three different skin donors. Purple- profile represents treatment with RLD and, Orange- profile represents treatment with approved commercial generic MTZ 0.75% topical cream. Data represented in Mean (SD) for duplicate probes in RTRT design for each skin.

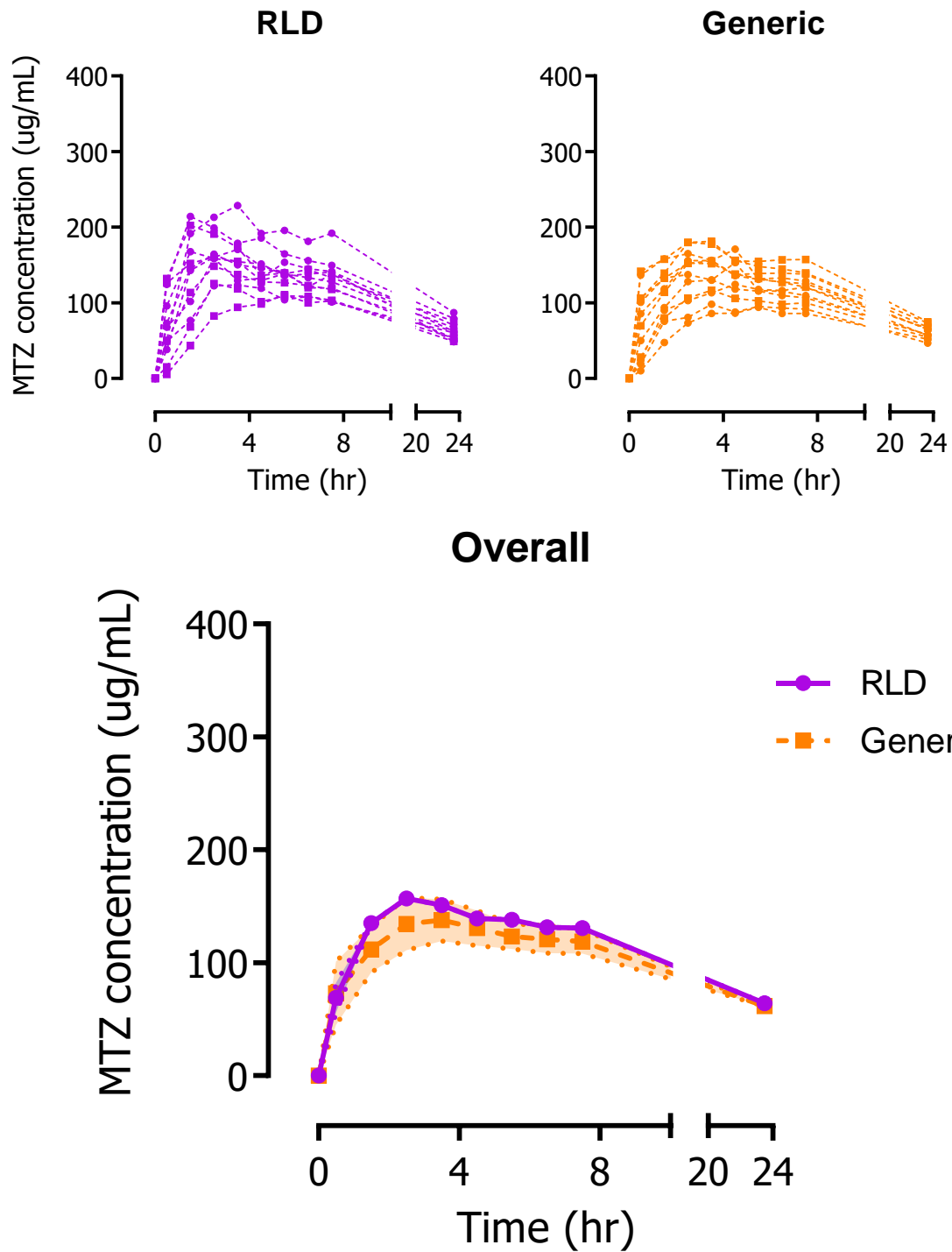


Figure 6.3: Concentration-time profile of Metronidazole 0.75% cream from individual probes under application site of (top left) RLD and (top right) Generic product, n=12. (Bottom) Mean (SEM) concentration-time profile of MTZ in the dermis after topical administration of formulations, purple-profile represent treatment with RLD and, orange- profile represent treatment with approved commercial generic of Metronidazole 0.75% topical cream.

6.3.2 Bioequivalence testing

A non-compartmental analysis (NCA) was used to obtain pharmacokinetic parameters and the log ratio of the geometric mean of PK parameters (AUC, Cmax) between the RLD and the generic cream was established. The NCA outcomes were used for ranking of formulation in the Bioequivalence function of PhoenixWinnonlin taking cream as the reference formulation in a parallel study. Due to the lower dermal PK profile of the generic cream in the second skin sample, the log ratio of AUC, as well as Cmax, was found lower on the bioavailability limit. The overall data from the three different skin samples resulted in an In-AUC of 91.65 (80.93, 104.88) and an In-Cmax value of 87.56 (74.87,102.39). The overall bioequivalent outcome of the generic cream compared to the 90% confidence interval (CI) of the RLD PK parameters is represented in Figure 7.4.

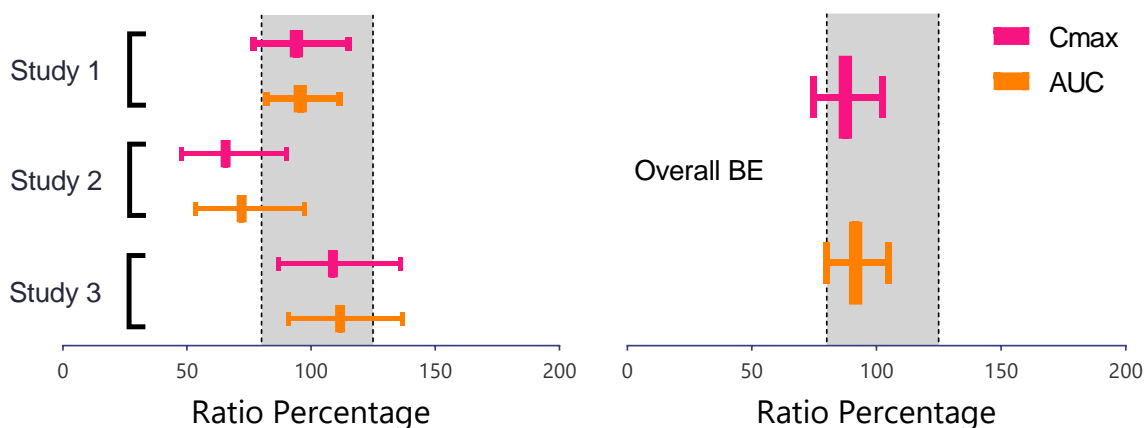


Figure 6.4: 90% confidence intervals of the ratio of the ln transformed AUC (purple) and Cmax (orange). The reference is the cream while the test is the gel. The dashed lines indicate the bioequivalence limits of 80-125% CI. From the overall study (left), the rate and extent of the generic formulation are similar to the RLD product.

6.4 Discussion

The study presented in this chapter was part of a series of experimental undertakings to check the feasibility of dermal microdialysis (dMD) sample technique on pig skin *ex vivo* and thereby estimate the permeation of commercially available topical formulation of a model drug metronidazole. The end goal of the study was to develop a dMD based test method suitable for bioequivalence (BE) estimation of the generic product of our model drug to its reference listed drug (RLD) product. The study was inspired by a similar study done on Yucatan pigs *in vivo* (1), with the intention to miniaturize the test method.

In the previous chapters, we have discussed the likelihood and developed an *ex vivo* dMD method and optimized experimental conditions for downstream BE study. In this chapter, we have provided the proof-of-concept of the possibility of developing a robust *ex vivo* dMD method. In two out of three skin samples, following a parallel full replicate design, we have observed an overlapping permeation profile of the generic formulation with its RLD. In a similar study, to explore the BE of TDDP on rabbit skin *in vivo*, the Test/Reference ratio of AUC and C_{max} was about unity, yet the limits of 90% CI were reported to be outside the 80-125 permissible range (62).

The permeation in the skin sample, where the test and the reference PK profile did not overlap, could be related to intra and inter-species variation. Such variations in permeation profile across the skin membrane have been widely reported (49,63,64). Skin samples within a species vary in their micro-structure, vasculature, and biochemical function (12,65). With the employment of skin *ex vivo*, it is appropriate to comment that the vasculature and biochemical component of the skin on permeation are neutralized, and the resulting permeation is the function of micro-structure in the skin. The demographic, age, Body-mass index, and genetic differences affect the structure of the skin (66,67). Since we used pig skin harvested from the same source,

thus the demographic variation can be ruled out, yet the age (68) and genetic make of the animal is expected to have a large impact leading to variability in permeation.

To obtain the BE results with higher confidence, we need to redesign the study with a larger number of subjects. We firmly believe, increasing the sample size to a larger number, the power and the statistical confidence in the result can be improved.

6.5 Conclusions

In the current study, we have presented a hypothesis to estimate the Bioequivalence (BE) of RLD (reference listed drug product) and its generic TDDP of Metronidazole using dermal microdialysis on pig skin ex vivo and reported the proof-of-concept respectively. The method employed for the current BE evaluation has demonstrated discriminatory results between two formulations differing in their Q1/Q2 and produced overlapping concentration-time profile in the dermis with FDA-approved bioequivalent products. Although the 90% CI of the Test/Reference ratio of PK parameters (AUC, C_{max}) was skewed toward the lower end of the limits (80%-125% permissible range), yet the data is promising considering the study was performed at a pilot-scale where the sample size was small (n=3). Increasing the sample size, the study design can be implemented for preliminary formulation selection during the development of drug products and other early phase preclinical studies.

Chapter 7: Estimation of Dermal Unit Impulse Response in Skin Ex Vivo, Absorption-Independent Drug Disposition in Dermis and Development of An Ex Vivo- In Vivo Co-relationship.

7.1 Introduction

Kinetics of Topical dermatological drug products (TDDP) is a complex interplay between the active substance, the formulation, and the skin. Generally, *in vitro* and *in vivo* studies are widely employed to evaluate drug release and permeation characteristics of such products. Understanding the rate-limiting steps that determine dermal permeation, i.e. drug release, diffusion across stratum corneum (SC), ability to bind to the SC or form skin reservoir, and/or other formulation-related aspects could benefit the development of a better product. An *in vitro*–*in vivo* correlation (IVIVC) is a predictive mathematical model often employed to describe the relationship between an *in vitro* property of a dosage form and a relevant *in vivo* response (69). A validated IVIVC model can be used to predict BA/BE based on *in vitro* data that are already available.

Similar to solid oral products, as described in the FDA IVIVC Guidance for extended-release oral dosage forms (70), Level A IVIVC correlates *in vitro* drug permeation across the skin in Franz cell setup, and *in vivo* absorption in the skin could be established. The static nature of Franz diffusion cells from *in vitro* studies could be substituted with the use of real-time drug monitoring capabilities of dermal microdialysis (dMD) in *ex vivo* studies. Dermal Microdialysis studies help in the estimation of the actual free drug concentration in the dermis and provide meaningful evidence of drug available for actual therapeutic effect. In contrast, drug concentration measured by *in vitro* Franz diffusion studies reflects the entire fraction of the drug that has permeated over time. *Ex vivo* dMD study would eventually be used to compare with *in vivo* results. The only shortcoming of using *ex vivo* dMD for estimation of drug kinetics is the absence of a vasculature system which is present in the *in vivo* environment and helps in comparatively faster clearance of the drug. However, we expect the effect of vasculature will be constant and intend to capture in the correlation factor used for translation of *ex vivo* data to its corresponding *in vivo* outcome.

In the current chapter, we have explored the feasibility of developing an Ex vivo-in vivo correlation (EVIVC), and if successfully achieved, it would be the first study of its kind. Drug concentration estimated in dermis over time in pig skin ex vivo by dermal microdialysis would be compared with the respective data obtained from available in vivo data (1), and a mathematical model would be developed to obtain the correlation factor. Such explorative study will not only provide means to extrapolate ex vivo data to in vivo outcome but will also offer a mechanistic understanding of the drug disposition independent of any absorption process (discussed in a later section).

In a dynamic situation, the concentration-time profile is the integration of an absorption function and a disposition function (71). The concept of unit impulse response would be used to initially estimate the disposition parameters, namely elimination constant and inverse volume of distribution. Once we can design a method to quantify the absorption independent disposition of the drug, it is mathematically possible to estimate the absolute absorption or permeation parameters of a drug into the skin, namely input rate, cumulative amount, and fractional input.

In the current investigation, we propose to introduce a drug in the dermis by retrodialysis (equivalent to a dermal infusion). Once the microenvironment around the dialysis probe in the dermis is saturated with the drug (steady-state), the dialysis perfusate could be switched to an isotonic solution, and a microdialysis process would be undertaken. In turn, the input function will be shunt and the elimination from the microenvironment will be captured in the dMD probe. The elimination kinetics thus achieved could be considered as the dermal unit impulse response (dUIR).

At the steady-state, the number of molecules leaving the probe is equal to the number of molecules being eliminated from the dermis. The exact dose delivered for a determined time interval can be calculated by subtracting the concentration in the perfusate minus the

concentration detected in the dialysate, at steady state, and then multiplied by the volume perfused for that time interval (Equation 7.1).

$$Dose_{t1-t2} = (C_{in-perfusate} - C_{out-ss})_{t1-t2} \times V_{perfused\ t1-t2}$$

Equation 7.1 Calculation of the dose administered where $C_{in-perfusate}$ is the concentration in the perfusate, C_{out-ss} is the concentration in the dialysate at a steady-state, and $V_{perfused}$ is the volume perfused for that time interval.

Infusion of the drug into the dermis microenvironment by dMD would be independent of any absorption process that may confound the clearance of the drug. The dermis clearance of the drug can be estimated by the ratio of the dose delivered divided by the area under the curve (AUC) for that time interval (Equation 7.2).

$$CL_{dermis} = \frac{Dose_{t1-t2}}{AUC_{t1-t2}}$$

Equation 7.2 The calculation of dermis clearance, where the dose is calculated using Equation 7.1 and the area under the curve AUC is estimated using a non-compartmental approach for the specified time interval.

During the microdialysis process, the drug elimination phase would be characterized. The drug concentration-time profile will be used to identify the number of phases in the dermis distribution, the terminal elimination rate constant, and the corresponding half-life. The volume of distribution within the dermis can be calculated using Equation 7.3.

$$V_{dermis} = \frac{CL_{dermis}}{\lambda_z}$$

Equation 7.3: Calculation of Volume of distribution in the dermis where CL_{dermis} is the dermis clearance, λ_z is the terminal elimination rate, and V_{dermis} is the volume of distribution within the dermis

For the dermal unit impulse response (dUIR) function calculation, the volume of distribution from above can be rearranged as Equation 7.4, where A is the inverse of V.

$$dUIR = A \cdot e^{-\lambda_z t}$$

Equation 7.4: Equation for Dermis Unit Impulse Response (dUIR) calculation where A is the inverse of V_{dermis} the volume of distribution within the dermis, and λ_z is the terminal elimination rate.

The concentration-time profile from topical administration of dermal products (refer to chapter 4) can be deconvolved using the dUIR function, and the absorbed (or input) function can be estimated. At this point, the fractional absorbed from topical administration ex vivo ($F_{\text{ex vivo}}$) will be compared with fraction absorbed using human skin in vivo ($F_{\text{in vivo}}$) studies. A typical Levy plot is expected to be constructed to align $F_{\text{in vivo}}$ and $F_{\text{ex vivo}}$ into a linear regression with a correlation factor.

7.2 Method

7.2.1 Chemicals and reagents

Metronidazole (99%) (MTZ) was purchased from Beantown Chemical (Hudson, NH). Lactated Ringer Solution (LRS, NDC- 0338011703, Baxter Healthcare Corp., Deerfield, IL), Metronidazole 0.75% Cream (NDC- 0168032346, Fougera Pharmaceutical Inc., Melville, NY), Metronidazole 0.75% Gel (NDC- 0115147446, Impax Generics, Hayward, CA) and all other medical supplies were purchased from Henry Schein (Melville, NY). and all other medical supplies were purchased from Henry Schein (Melville, NY). LC Grade acetonitrile, water, and other supplies were purchased from Fisher Scientific (Fair Lawn, NJ, USA).

7.2.2 HPLC Analytical method

The concentration of the analyte in the dialysate was measured using an Agilent 1100 series HPLC-UV apparatus (Agilent Technologies, Santa Clara, CA) and the results were integrated using

Agilent ChemStation. Briefly, the system consists of a degasser, quaternary pump, temperature-controlled autosampler with a 50 μ L sampling loop, a temperature-controlled column compartment, and a DAD Detector. The column compartment was fitted with an Xbridge C18 3.0x50mm 5 μ m reverse phased column (Waters Corp. Milford, MA) and was set at 25°C. The mobile phase consisted of deionized water (DI) and acetonitrile (ACN) at the ratio of 90:10 and an isocratic flow was maintained at 0.3 mL/min. The detection wavelength was 325 nm (bandwidth \pm 4nm) and the reference wavelength was set at 400 nm (bandwidth \pm 5nm). The autosampler temperature was maintained at 5°C.

7.2.3 Bioavailability and dUIR experimental design

Skin explants were harvested from fresh slaughtered female Yorkshire pig belly purchased from a local meat shop. Two different pieces of full-thickness pig skin explant from the same animal were selected (each of dimension 5 x 20 cm), such that the skin samples were devoid of any observable defects and deviation of TEWL measurement were not more than 20% on the selected study sites. The full-thickness pig skin pieces with underlying subcutaneous fat layer (total thickness \approx 1 cm) were placed on an aluminum foil tray (M2 ex vivo dMD method, chapter 5). On the first skin, four different application sites (5 x 5 cm) were marked and a parallel four-period full-replicate (Cream-Gel-Cream-Gel) design for routine bioavailability study was planned, discussed earlier in chapter 4 and 5. On the other skin piece, four different probes were inserted into the dermis with the help of a guide cannula 4 cm apart, and one lateral diffusion probe was inserted in the dermis toward the center of the skin at a distance of 2 cm from the adjacent test probes for the proposed dUIR investigation (Figure 7.1).

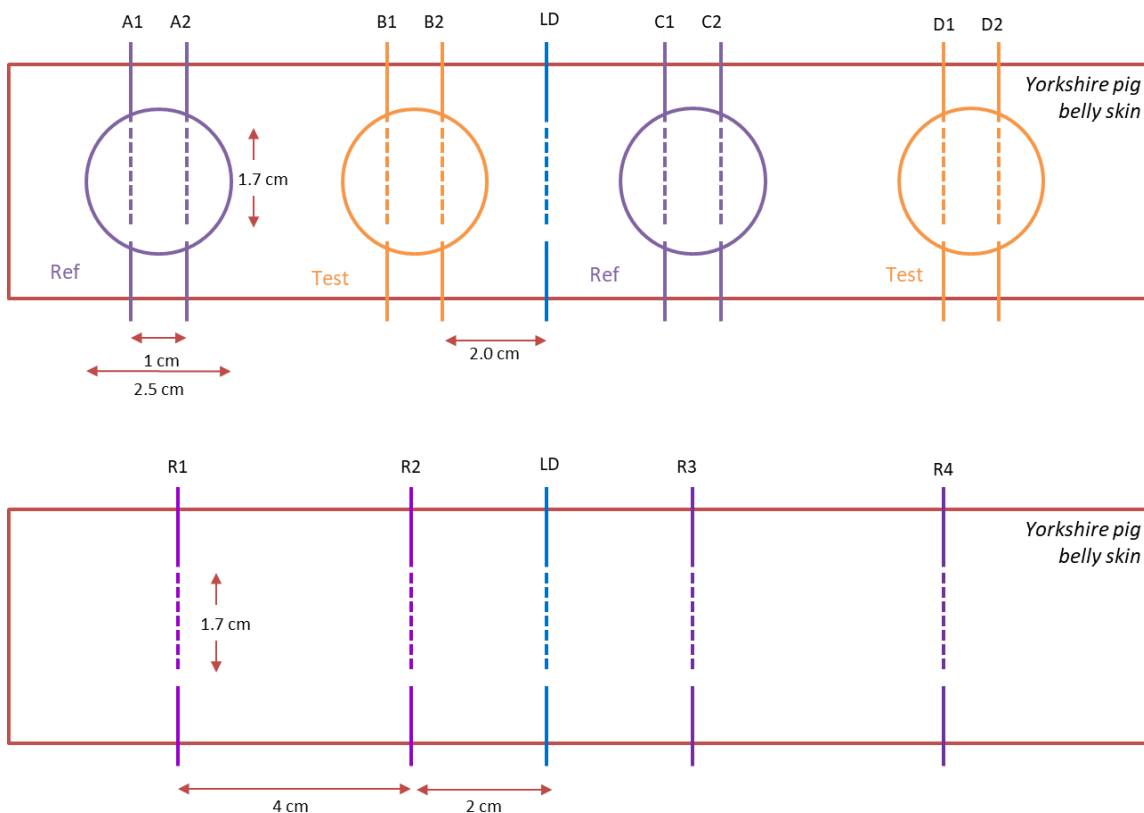


Figure 7.1: (Top) A sample template of the dMD probe placement and application site for the formulations on the skin. The probe and application site for MTZ cream is marked with purple and MTZ gel with orange. The application sites are circular (diameter 2.5 cm) and the probes in each site are 1 cm apart. The lateral diffusion probe (blue) is 2 cm apart from adjacent probes. (Bottom) A sample template of the retrodialysis-microdialysis probe (purple) and lateral diffusion probe (blue) placement on the skin. The probes in each site are 4 cm apart, and the lateral diffusion probe is 2 cm apart from adjacent probes.

7.2.4 Retrodialysis and Microdialysis procedure

Bioavailability of Metronidazole 0.75% Cream (NDC- 0168032346, Fougera Pharmaceutical Inc., Melville, NY), Metronidazole 0.75% Gel (NDC- 0115147446, Impax Generics, Hayward, CA) was performed on the first skin explant, discussed earlier in chapter 4. The dUIR investigation was performed on the second skin explant as described in Figure 7.1 (bottom). System suitability trials with a range of concentration of drug solution were performed (for retrodialysis-microdialysis optimization) to determine the drug loss on retrodialysis on each skin strip, determine the infusion time to reach steady-state in the dermis, and optimize the sampling time to capture the

elimination phase during microdialysis at a higher resolution. Once the experimental setup was verified with a certain level of investigator's confidence, the retrodialysis-microdialysis study was performed on fresh skin. Metronidazole (MTZ) at a concentration of 100 ug/mL in LR was found suitable during the initial trials. The loss for metronidazole in the retrodialysis step was calculated to be about 60% at a perfusion rate of 0.5 uL/min. In an optimized process, the probes were flushed with 100 ug/mL at a flow rate of 25 uL/min for 10 min and then perfused at 0.5 uL/min for 8 hrs. Samples were collected at every hour to determine the loss due to the retrodialysis process. At the end of 8 hours, the infusion pump was switched to LR (blank perfusate) and the probe lines were flushed with LR at a flow rate of 25 uL/min for 10 min. The perfusion rate was lowered down to 0.5 uL/min and the perfusate was discarded for the first 10 min, followed by continuous sampling at every 20 min until the next 4 hours.

7.2.5 Estimation of dermal disposition

The amount of drug delivered (dose) into the dermis at the steady-state was calculated from Equation 7.5. The dose delivered was calculated for each probe.

$$X_{2.5-7.5} = (C_{\text{perfusate}} - C_{\text{ss}}) \times V_{\text{perfused (2.5-7.5)}}$$

Equation 7.5: Where X is the dose administered at a steady-state between 2.5 and 7.5 hr, C_{perfusate} is the concentration in the perfusate, C_{ss} is the concentration (ug/ml) in the steady-state portion of retrodialysis phase, and V_{perfused} is the volume of solution perfused for the duration of steady-state, between 2.5 and 7.5 hrs.

Clearance of MTZ from the dermis at the steady-state phase was calculated as per equation 7.2 where T₁ and T₂ were 2.5 and 7.5 hrs respectively. Similarly, the volume of distribution in the dermis was calculated using equation 7.3, where λ_z was the terminal elimination rate constant estimated from the Non-compartmental analysis of the microdialysis data. The inverse value of the volume of distribution was then applied for the calculation of the dermis unit impulse response (dUIR).

7.2.6 Ex vivo in vivo correlation (EVIVC) development

The bioavailability data of metronidazole: In our current bioavailability study using pig skin ex vivo, regular sampling was continued until 8 hrs and terminally at 24 hrs. Data for the missing time points between 8th and 24th hrs were bootstrapped by spline analysis from the mean of the profile from all probes. The available in vivo bioavailability data from the pig (10) was considered as the reference in the study here onwards, and the 48 hr PK data was trimmed at 24 hr to match our ex vivo study design. The dUIR parameters from both ex vivo and in vivo studies were employed to deconvolute individual PK data (from each donor/probes) for the estimation of the cumulative absorption (CA) kinetics. Mean CA from cream as well as gel products was generated for both ex vivo and in vivo population, later fractional cumulative absorption (fCA) was generated for either method. Mean permeation time (MPT) of the active molecules in the pig skin in vivo was determined using the PhoenixWinNonlin Dissolution module (MPT is the same as Mean Dissolution Time, MDT, in the software module). Two different permeation models (Hill, and Weibull) were used, and the MPT values thus obtained, were employed to investigate the time-scaling (TS) of the ex vivo mean fractional Cumulative Absorbtion (fCA) profile. Eventually, the scaled time of ex vivo fCA data was compared to in vivo time for corresponding fCA, and the Levy plot was constructed. The selection of either the Hill model or the Weibull model was be determined from the slope and Rsq value of the Level A Correlation of the Levy plots. The formulas used in the mathematical conversion are listed below:

$$Xt = \frac{Finf \cdot t^b}{MPT^b + t^b}$$

Equation 7.6: Hill equation of dissolution to calculate the amount (Xt)of drug absorbed at time t, where, Finf is the fraction of drug absorbed in the system at infinity, MPT is the mean of permeation time and b is a shape factor.

$$X_t = F_{inf} \left[1 - \exp \left(\frac{-t}{MPT} \right)^b \right]$$

Equation 7.7: Weibull equation of dissolution to calculate the amount (X_t) of drug absorbed at time t, where, F_{inf} is the fraction of drug absorbed in the system at infinity, MPT is the mean of permeation time and b is a shape factor.

$$t = \left(\frac{X \cdot MPT^b}{F_{inf} - X} \right)^{1/b}$$

Equation 7.8: The formula to calculate the inverse of the Hill equation. This formula is generally useful for reverse calculation of the time taken for a quantity of drug (X) to absorb, where F_{inf} is the fraction of drug absorbed in the system at infinity, and the MPT and shape factor b value is known.

$$t = -\ln \left(1 - \frac{X}{F_{inf}} \right)^{\frac{1}{b}} \cdot MPT$$

Equation 7.9: The formula to calculate the inverse of the Weibull equation. This formula is generally useful for reverse calculation of the time taken for a quantity of drug (X) to absorb, where F_{inf} is the fraction of drug absorbed in the system at infinity, and the MPT and shape factor b value is known.

7.2.7 Extrapolation of ex vivo data to in vivo PK profile and validation

The regression values of scaled time from the appropriate Levy plot were matched to fCA and original CA of ex vivo study and an absolute scaling (scaling the cumulative absorption with a hypothetical factor) was used to match the extent of in vivo CA profile. Thereafter, the absolute scaled ex vivo profile was convoluted with its dUIR parameters using PhoenixWinNonlin Convolution module to estimate the in vivo PK profile. Whenever required, a spline analysis was applied to bootstrap data from the convoluted profile for a better fit. The PK parameters (C_{max}, AUC) from the ex vivo convolution data were compared to the in vivo bioavailability data to determine the percentage predictability error (%PE) in the prediction profile from ex vivo data. A

general flowchart of the EVIVC development, in vivo PK profile prediction, and validation is provided in the scheme below (Figure 7.2).

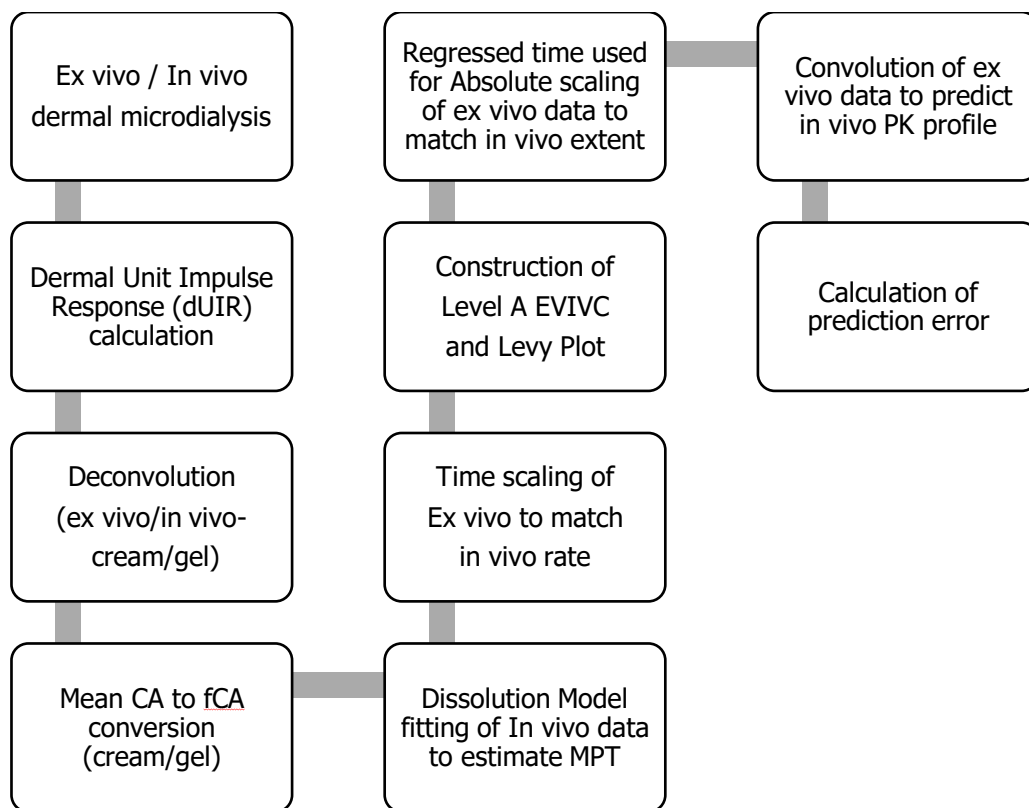


Figure 7.2: A sample algorithm to design a Level A EVIVC and predict in vivo concentration-time profile from ex vivo dMD data.

7.2.8 Statistical analysis

A two-stage analysis approach was employed, the first stage of the approach involves estimating the PK parameters from individual dense concentration over time data (taking mid-points of the sampling intervals) using noncompartmental methods in PhoenixWinNonlin (Certara; Princeton, NJ). Individual parameter estimates obtained during the first stage were used as input data for the second-stage calculation of descriptive summary statistics on the sample, typically, mean parameter estimates and SEM. Bootstrapping of data from spline analysis, and other statistical

calculations was GraphPad Prism (GraphPad Software, San Diego, CA). Prediction fold error was calculated using Equation 7.10.

$$\%PE = \left(\frac{(P_{obs} - P_{pred})}{P_{obs}} \right) \cdot 100$$

Equation 7.10: Percentage prediction error (%PE) calculation to calculate prediction accuracy. P_{obs} is the observed value and P_{pred} is the predicted value.

7.3 Results

7.3.1 Ex vivo dermal bioavailability and disposition

The dermal microdialysis samples collected from the bioavailability study of Metronidazole 0.75% cream and gel, on the first skin setup, presented a similar concentration-time profile as observed in previous chapters. The concentration of drug observed in the lateral diffusion probes at both the skin samples was below LLOQ. From the retrodialysis study, on the second skin sample, upon perfusion of metronidazole solution (100 µg/mL in LR) at a flow rate of 0.5 uL/min, we observed the concentration to reach equilibrium at the beginning of the third hour, and the perfusion was continued until the eight hours. An average of 8.9 µg (n=4) of the drug was infused into the dermis during that 5 hours of perfusion at equilibrium. On termination of the infusion process, the drug concentration in the dermis, captured by the microdialysis process, exhibited a first-order decay (Figure 7.3) with the elimination rate constant $\lambda_z = 0.21$ (0.06), corresponding to an average half-life of 3.44 (0.99) hr.

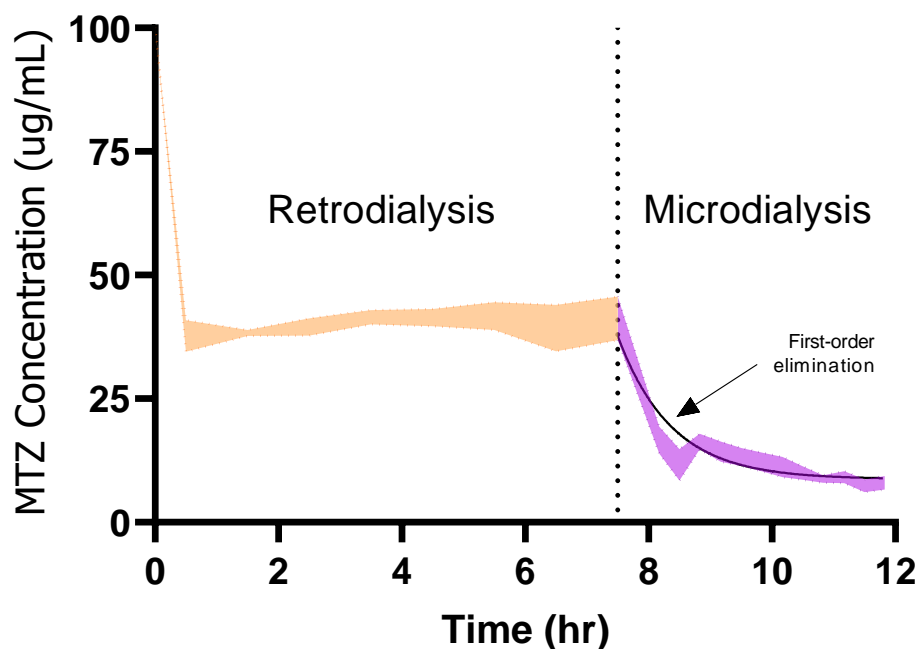


Figure 7.3: Overall dialysate concentration-time data from the retrodialysis-microdialysis process. The orange shaded area is the error band of loss of perfusate from all probes in the retrodialysis process. The loss was at equilibrium between 2.5 and 7.5 hr. The vertical dotted line represents the end of drug perfusion in the dermis by retrodialysis and marks the beginning of recovery sampling by microdialysis. The purple shaded area is the error band of recovery of the drug from all the probes. The initial drop in concentration at around 9th hr is assumed to be due to lag time in recovery of the probe. Elimination rate constant estimated from the terminal phase beyond 10 hr of dermis tissue sampling, an overall mono-exponential equation was fitted, purple solid line. (n=3)

7.3.2 Dermis Unit Impulse Response (dUIR)

The total drug infused into the dermis and terminal elimination (λ_z) value calculated from retrodialysis and microdialysis process respectively was used in the calculation of dermal clearance and volume of distribution estimations (Table 7.1). The inverse of the volume of distribution was used for A value calculation for each probe and then the mean of all A values was used in the dUIR. The dUIR equation thus is as following:

$$dUIR = 6.99e^{-0.21t}$$

Equation 7.7: Dermis Unit Impulse (dUIR) calculated from the individual probes used for deconvolution of ex vivo bioavailability data.

Table 7.1: Estimated and derived parameters from retrodialysis and microdialysis in ex vivo pig skin. (Mean \pm SD, n=4)

Parameter	Dose	AUC	λ_z	Cl	Vd	A
	<i>ug</i>	<i>ug*hr/mL</i>	<i>1/hr</i>	<i>ml/hr</i>	<i>ml</i>	
Mean (SD)	8.90	294.33	0.21	0.03	0.15	6.99
	(0.20)	(4.24)	(0.06)	(0.00)	(0.04)	

7.3.3 Ex vivo in vivo correlation (EVIVC) development

The bioavailability data of Metronidazole 0.75% Cream and Gel topical formulation performed on the pig in vivo was kindly provided by Kuzma (10) and was compared to the ex vivo pig skin study, as described in the method section (Figure 7.3). The concentration over time-scale expressed in the in vivo bioavailability profile is magnified by three orders of magnitude in ex vivo bioavailability data. The Mean (SEM) Cmax for Metronidazole cream in vivo and ex vivo are 41.27 (10.73) ng/ml and 204.31 (39.90) ug/mL respectively. Similarly, the Mean (SEM) Cmax for gel formulation in vivo and ex vivo are 15.10 (9.61) ng/mL and 165.82 (25.97) ug/mL. The difference in thickness of the skin at different locations within Yucatan minipig and domestic Yorkshire pig breed has been reported (72–74), and from our ultrasound images, we have observed similar differences between the back (dorsal side) of the Yucatan minipig and belly skin (ventral part of pig) of Yorkshire domestic pig. This difference in thickness of skin between the breeds is surely a contributing factor for the difference in permeation profile.

Using the dUIR obtained in the in vivo and ex vivo studies, their individual PK profiles were deconvolved. The λ_z of in vivo study was reported as 0.47 1/hr and was observed as 0.21 1/hr in ex vivo pig skin. The cumulative absorption (CA) over time for in vivo studies was gradual, and

on the other hand a bi-phasic CA was observed in ex vivo, where after an initial rush in the flux the rate changes after around the 5th hour duration (Figure 7.4).

The difference in both the extent and the rate of absorption between the two studies was observed. Thus, to generate a point-to-point correlation the ex vivo scale was scaled to match the in vivo profile. Due to the vast difference in magnitude, the CA in each case was converted to max value 1 and fractional cumulative value (fCA) was respectively generated at every time point. Figure 7.5 demonstrate a common disparity in the trend of mean fractional absorption with respect to time in both cream and gel formulation in either study and a general need to bring the ex vivo (orange) profile close to in vivo (purple) profile for a point to point comparison was warranted.

Time-scaling by calculating dissolution in vivo and applying the mean permeation time (MPT) of the dose observed in in vivo to the ex vivo permeation, we observed a point-to-point match of the two profiles. Figure 7.6 demonstrates the Levy plot construction before time scaling, and after time scaling with the Hill dissolution method and Weibull dissolution method. The application of the Weibull method gave a better slope and Rsq value for the time-to-time matching on the Levy plot for both gel and cream. Hill dissolution for cream (Rsqu=0.9879, Slope=1.0665), and gel (Rsqu=0.9865, Slope= 1.0411); Weibull dissolution for cream (Rsqu=0.9990, Slope=1.0026) and gel (Rsqu=0.9969, Slope=1.0039) respectively.

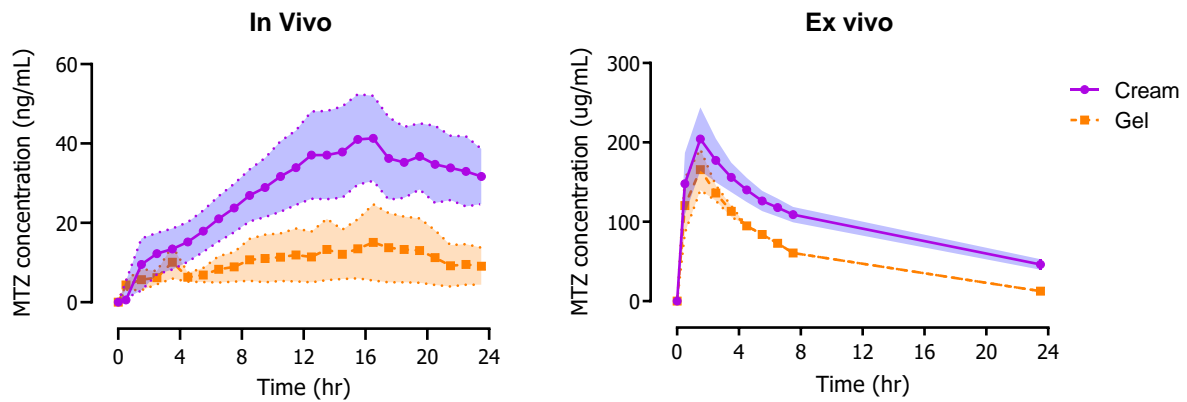


Figure 7.4: Bioavailability profile of MTZ in the dermis after topical administration of cream and gel formulation in vivo (left), and ex vivo (right) at a dose of 10 mg/cm². Purple- profile after treatment with MTZ 0.75% topical cream and, Orange- profile after treatment with MTZ 0.75% topical gel. Data presented in Mean (SEM).

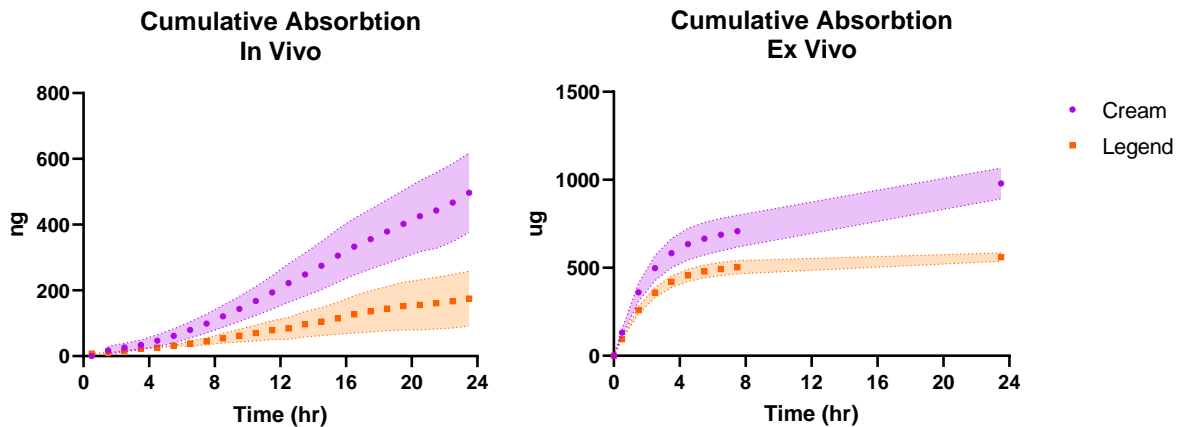


Figure 7.5: Cumulative absorption profile of MTZ in the dermis in vivo (left), and ex vivo (right) at a dose of 10 mg/cm². Purple- profile after treatment with MTZ 0.75% topical cream and, Orange- profile after treatment with MTZ 0.75% topical gel. Data presented in Mean (SEM).

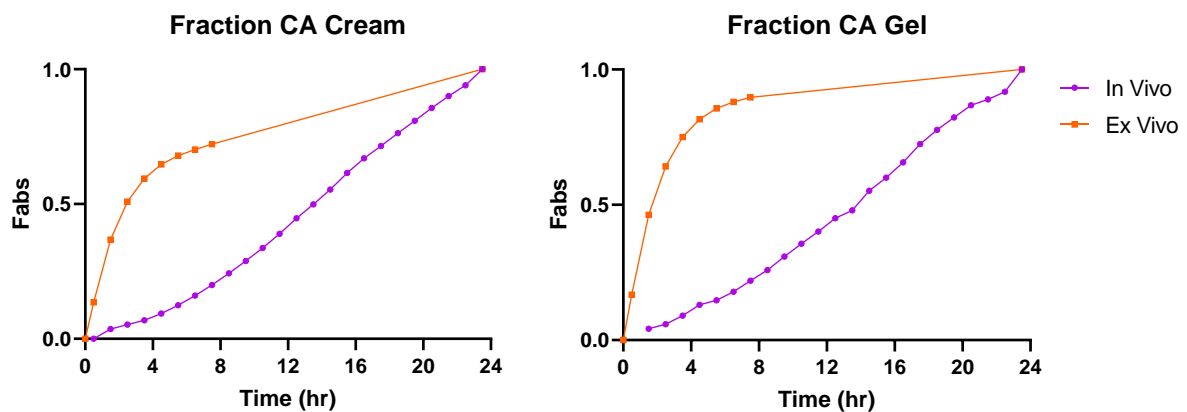


Figure 7.6: Mean Cumulative absorption profile of MTZ in dermis expressed in fraction (Fabs) for cream (left) and gel (right) formulation. Purple- profile was observed in in vivo pig, and Orange- profile was observed in ex vivo pig skin.

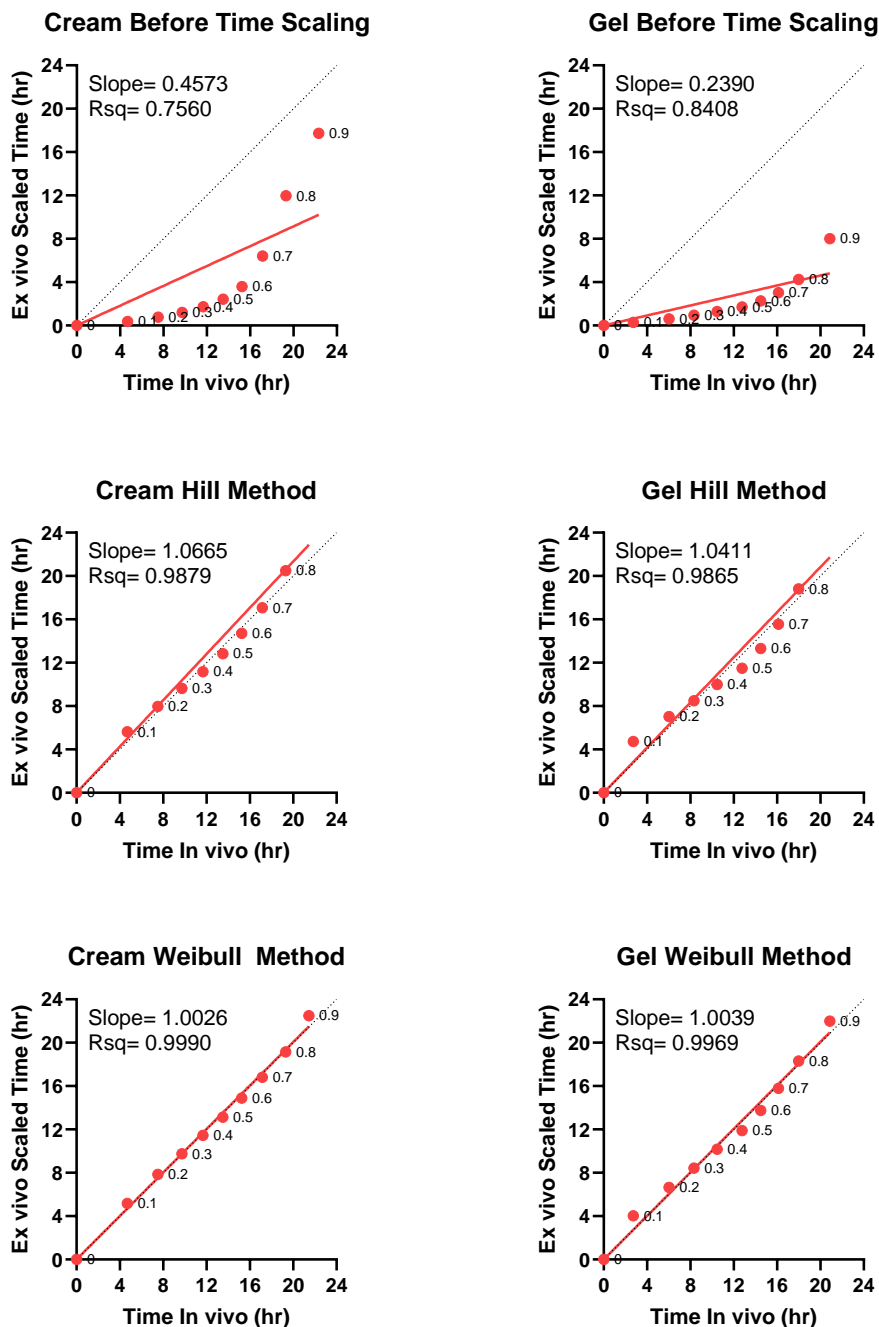


Figure 7.7: Levy plot constructed for point-to-point comparison of Tin vivo (Time In Vivo) as independent variable and Tin vitro (Ex Vivo Scaled-Time) as the dependent variable. The top row indicates the mapping of cream and gel formulation and the bottom row for Gel formulation before time-scaling, the slope and Rsq values indicate poor correlation. The middle row indicates Levy Plot after time-scaling the ex vivo timeline with Hill absorption equation (equation 8.8), the Slope and Rsq values were improved with time-scaling. The bottom row demonstrates the Levy plot after time-scaling with the Weibull absorption equation (equation 8.9). The Rsq of the mapped time point is linear ($Rsq > 0.99$) in both cream and gel. The slopes were closer to 1.00.

7.3.4 Extrapolation of ex vivo data to in vivo PK profile and validation

The regression values of scaled time obtained from Levy plot construction using the Weibull dissolution formula were used to generate corresponding CA values ex vivo. These values were scaled down using a permeation factor of 2000 for Cream and 3200 for Gel to match the in vivo extent of in vivo PK profile. Figure 7.7 demonstrates the mapping of ex vivo Cumulative absorption data to the in vivo cumulative absorption profile.

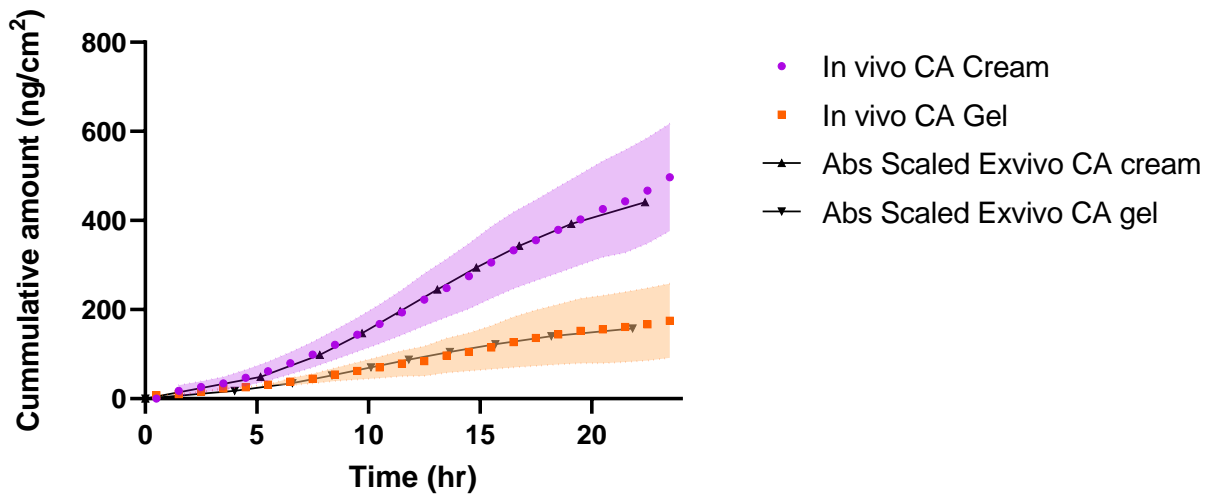


Figure 7.8: Observed and mapped Cumulative Absorption Curve. Purple- The purple dot and shaded region denote the Mean (SEM) of cumulative absorption of MTZ cream in vivo pig, Orange – the orange square, and shaded region denotes the Mean (SEM) of cumulative absorption of MTZ gel in vivo pig. The black down arrow and up arrow with connecting lines denotes the mapped cumulative absorption of MTZ cream and gel extrapolated from ex vivo data.

Convolution of the above mapped CA of ex vivo cream/gel profile with the ex vivo dUIR function generated the predicted in vivo profile from ex vivo data (Figure 7.8). The PK parameters observed from NCA of the predicted profile resulted in fold error of 1.03 for C_{max} of cream, 0.98 for C_{max} of gel, and 0.94 for AUC of cream, 0.90 for AUC of gel. The model developed presented a point-to-point prediction of the anticipated in vivo profile; however, it started deviating from

23rd hour for Cream and 22nd for Gel. The regression analysis obtained from the Levy plot failed to capture any data point beyond these time values, resulting in a drop in the T/R value for AUC.

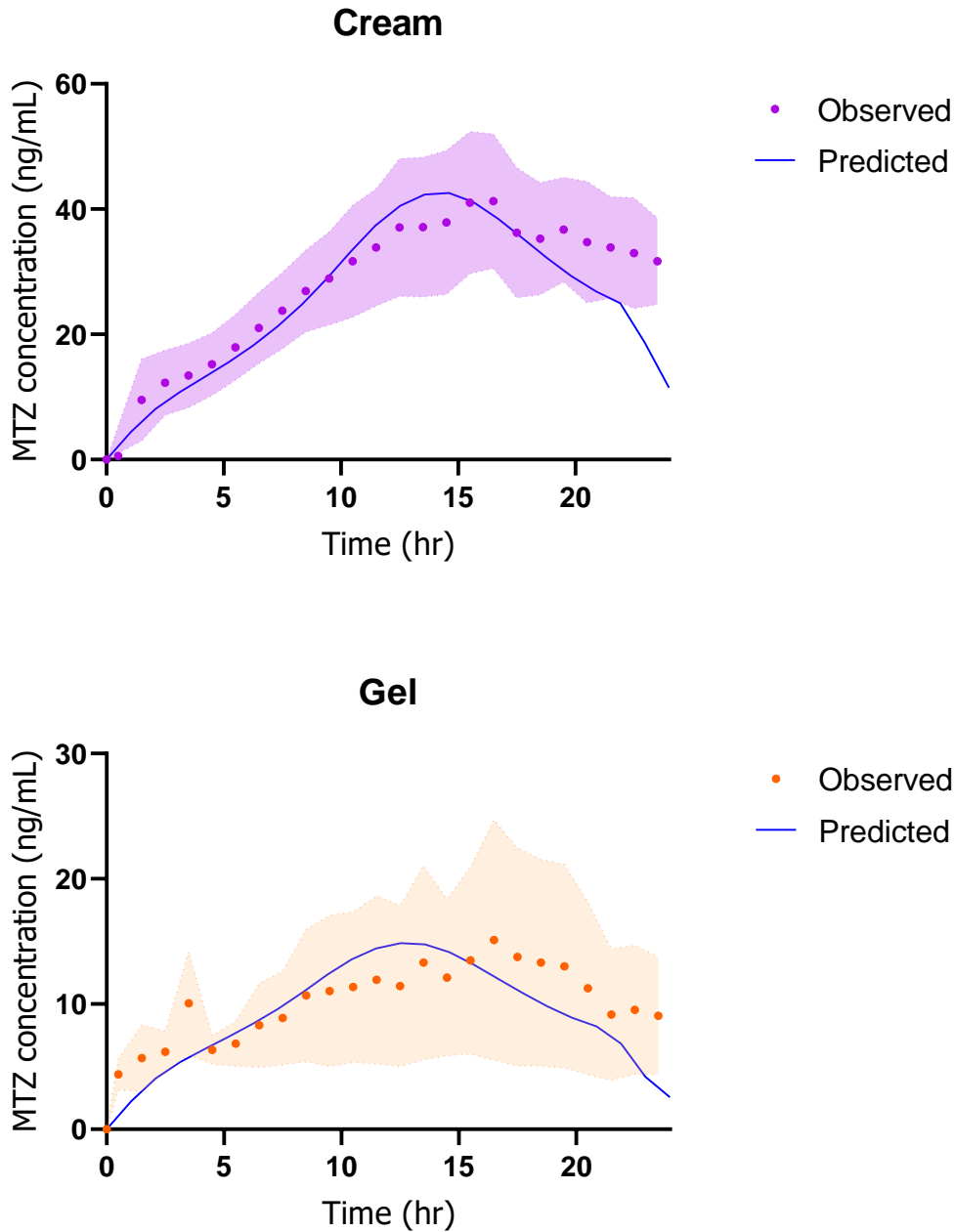


Figure 7.9: Predicted vs Observed concentration-time profile. Purple- The purple dot and shaded region denote the observed Mean (SEM) of cumulative absorption of MTZ cream in vivo pig, Orange – the orange square, and shaded region denotes the observed Mean (SEM) of cumulative absorption of MTZ gel in vivo pig. The blue continuous line denotes the predicted concentration-time profile extrapolated from ex vivo data for cream and gel in respective graphs.

7.4 Discussion

In the previous chapters, our goal was to develop an ex vivo dermal microdialysis model that will manifest a bioavailability profile of topically applied drugs, similar to its in vivo counterpart. We have achieved satisfactory data from pig skin ex vivo. In this chapter, we have explored the possibilities to extrapolate the data from the ex vivo study to in vivo with some certainties. To study the absorption independent drug disposition in the skin, it was challenging to introduce the drug directly into the dermis without changing the microenvironment of the same. Through the dermal retrodialysis method, we have successfully infused a very high concentration of drug into the skin ex vivo. The advantage of the process is that a certain amount of the drug was introduced into the dermis tissue without adding any external fluid or vehicle to the tissue itself (as would be expected in subcutaneous infusion or bolus injection). In a way, we have avoided any external variables that will disturb or obscure the PK measurements.

Despite the infusion of a very high dose of metronidazole solution (100 µg/ml), the lateral diffusion probe did not pick any signal from the adjacent infusion sites. Not only, signals obtained from individual probes were independent of any bias, but also we could derive two other possible outcomes of this observation: (a) if there was any lateral diffusion in the dermis it did not travel enough to extend up to a very optimistic distance of 2 cm to be detected in the lateral diffusion probes, previously reported up to 1.2 cm beyond application site (75,76), (b) the diffusion of active molecules were down the gradient towards the next layer of cells in the dermis. The latter hypothesis could be better understood if two probes were introduced horizontally at different depths in the dermis.

During the initial feasibility trials, to optimize the variables of the retrodialysis study, we have explored the effect of the flow rate of perfusate (0.5 and 1.0 µL/min) and the concentration

of perfusate (50, 100, and 200 $\mu\text{g/mL}$). The loss decreased with increased flow rate; this observation is consistent with in vitro microdialysis observations (refer to section 3.3.3). Each skin sample tested gave different loss values within a range, this may be contributed to the inter-donor skin's microstructure; however, the percentage loss was constant across different perfusate concentrations. At the flow rate was 0.5 $\mu\text{L/min}$ the average loss ranged from 45 to 65% of the initial perfused concentration. A similar loss in retrodialysis was found in pig skin in vivo. This consistent equilibrium behavior of the retrodialysis process across in vivo and ex vivo pig skin confirms a steady-state situation was reached. To attain the steady-state concentration, generally, it would require about 5 half-lives of the drug in the dermis (77). Although we have observed an early equilibrium state, this does not affect our experimental design as our goal was only to load the dermis tissue with a quantifiable amount of drug and to derive the elimination parameters from the terminal declining phase.

Introduction of metronidazole in the skin by retrodialysis was previously used by Kuzma to study the dermal disposition of the drug in vivo. In his studies, he has observed a mono-exponential decay and the elimination rate constant was $\lambda_z=0.47$ 1/hr; whereas the mono-exponential decay constant in this ex vivo study was $\lambda_z=0.21$ 1/hr. The higher exponential decay may have been contributed by the continuous clearance of the drug from the skin by the microvasculature. A follow-through ex vivo study had helped us understand the extent to which these micro vasculatures affect the clearance of the drug from the dermis. The three-order magnitude increase in the bioavailability profile of the formulations from in vivo to ex vivo could be due to two reasons, (a) in the ex vivo tissue the barrier function is compromised leading to higher permeation values supported by the higher TEWL value observed, (b) reduced elimination due to lack of microvasculature.

In a traditional IVIVC involving oral dosing, the fraction dissolved in vitro is compared to the in vivo input rate which is a function of in vivo dissolution (70). For topical formulations, two concerns need to be addressed before attempting to design a correlation- (a) the dissolution term is required to be adopted as absorption/permeation, (b) the amount absorbed/permeated is seldom a major fraction of the dose. Also, due to the observed difference in rate and extent of absorption between ex vivo and in vivo systems, a comparison of the actual fraction of dose absorbed will be inadequate for developing a correlation. In a similar situation, where the formulations in vitro and in vivo presented dissimilar time scales (78), the problem was resolved by modeling the relationship between the times at which the same fraction of the max dissolution was achieved. Similarly, we have considered the cumulative absorption at the last time point as 1 and converted the entire cumulative range as a fraction.

Conventionally, for topical and transdermal products, we correlate permeation profile in vitro with the deconvoluted in vivo absorption profile (79,80). This is the first report where we have tried to correlate the dermal bioavailability profile on pig skin in vivo and ex vivo with the aid of real-time dermal drug concentration estimation using microdialysis. Here both the experimental models resulted in PK profiles, and dermal Unit Impulse Response was of dire importance to deconvolute the drug absorption profile. The retrodialysis-microdialysis process was beneficial in replacing the traditional UIR determination by IV injection. The application of an appropriate release function (Weibull dissolution) helped us to unlock the most vital key - the Mean permeation time (MPT). The MPT indeed attributed to the mathematical conversion of the time function of live in vivo skin to excised ex vivo skin.

Mathematical conversion of ex vivo rate and extent, and its sequential mapping with the in vivo profile, offered us a matching cumulative absorption over time curve profile (Figure 7.7).

Consequently, the predictability, the attribute of a mathematical model that defines its usefulness in real life, was established by convolution of the predicted CA profile to a predicted PK profile.

A one-on-one comparison of the observed and predicted PK profile is recommended by the FDA guidance for IVIVC. There is enough space for the investigator as a variety of methods are possible and potentially acceptable. Methodology for the evaluation of IVIVC predictability is an active area of investigation and a correlation should predict in vivo performance accurately and consistently. We have attained predictability within the accepted (percent prediction error (% PE) of 10% or less for C_{max} and AUC). The study presented here was a beneficial learning experience and a scientific exploration where the validity of the approach must be further investigated. Once fully understood, ex vivo bioavailability assay by dermal microdialysis can be used confidently as a surrogate for in vivo bioavailability/bioequivalence of topical dermal drug products.

7.5 Conclusions

In the present chapter, we have successfully introduced the drug into the dermis and estimated the absorption independent elimination kinetics parameters. Deconvolution of the absorption profile of the drug from the different topical formulations was possible from these elimination parameters. Both the studies were performed on the skin from a single subject and same location, thereby any bias of skin variability was avoided. In the later part of the chapter, we have compared the estimated ex vivo profiles with an available in vivo data set and developed a mathematical correlation between the two profiles. A point-to-point correlation has been demonstrated with the potential to predict in vivo drug kinetic profile from the extrapolation of ex vivo outcomes. In the future, the model would be used for external predictability and we can

foresee this comparison could play a pivotal role in replacing the burden of extensive experiments on animal subjects during early preclinical research.

Chapter 8: Conclusion and General Discussions

With the increasing demand for dermal tissue monitoring technologies, such as dermal microdialysis (dMD), dermal open-flow microperfusion (dOFM), imaging by Raman spectroscopy, there is a constant need for human and animal subjects for product performance testing. Especially, the application of these cutting-edge technologies on animals during preclinical evaluations could be expensive and inconvenient. In the work presented here, we hypothesized to decrease this burden of animal testing by introducing the performance testing on excised skin by dermal microdialysis. We have laid down experimental design, proved our concepts through a data-driven approach, and optimized the conditions required to perform the tests.

The central component of the dermal microdialysis process is the microdialysis probe. While different configurations and speciation of the probes are commercially available, we decided to use our in-house Gambro AN 69 probe with a 1.7 cm exchange window, based on our previous experience for metronidazole recovery. Making the probes in-house provides us the flexibility to manufacture them only when we require, this not only prevented the timely deterioration of the polymeric exchange membrane but also helped lower the cost per experiment and inventory.

The wide availability of reported data on the similarity of the pig skin to human skin motivated us to explore the use of excised skin from pigs for the ex vivo dermal microdialysis study. Human cadaver skin and excised pig skin from commercial sources are stored at freezing temperatures. There are conflicting reports from various research groups on the proper storage temperature for the skin (27); however, studies with fresh skin remain the gold standard in such assays. A statistics by OECD in 2019 reported the United States as the fifth largest consumer of pork meat in the world (81); with nearly a hundred million pigs slaughtered in a year, there would be a stiff amount of fresh pig skin available at slaughterhouses or local meat shop. Fresh skin samples of any dimension or specification could be made available from these sources to design a suitable experiment. We have explored one such avenue to source fresh domesticated Yorkshire

pig skin explant to design and conduct bioavailability study of commercial products of Metronidazole 0.75% topical formulations using dermal microdialysis. In our initial studies, we have compared the feasibility of using frozen pig skin (excised in-house at different temperatures: -20 °C, -40 °C, -80 °C, and flash-freeze by liquid nitrogen) with freshly sourced skin explant from a local meat shop. Thawing of frozen skin at ambient lab temperature takes a couple of hours and subsequently increases the hydration of the surface layer to the extent where the permeation of the drug is too high. Comparatively, the thawing step was not required for the outsourced skin and it was ready for downstream processing.

Reports of microdialysis for dermal tissue fluid sampling are widely available but we were interested to design and test a first-of-its-kind ex vivo skin model to discriminate between formulations and establish it as a routine bioequivalence tool. After the probe and microdialysis system performance was characterized in vitro, the method was transferred to the skin explant for dermal tissue fluid monitoring. The physiological differences between living and excised skin were anticipated early in the study and trials were planned to reduce the physiological differences to a minimum. One critical aspect of the study was to keep the skin performance similar throughout the study. Measuring the performance of the skin would be complex, hence we intended to keep the skin visibly the same until the end of the study, especially when the skin tends to dry with time and bent inwards toward the stratum corneum side. One novel approach was undertaken, a full-thickness skin without a subcutaneous fat layer was placed on a wicking material that constantly provided hydration from the ventral side of the skin. The experimental plan led to an over hydrated system causing the negative control to present a larger exposure profile in the dermis. In the alternate approach, where a skin flap (full-thickness skin with the subcutaneous fat layer) was used, the dermal microdialysis sampling provided a bioavailability profile of both the test and the negative control similar to available literature data. This best-fit

method was eventually optimized and tested for dose-response linearity with satisfactory outcomes.

The ex vivo skin explant of our study is comparable to a vasoconstricted system. Here the absence of a dynamic circulatory system not only makes the skin dry over time but also fails to provide thermoregulation. Superficial addition of heat on the skin is deemed to alter the thermodynamics of formulation hence affect the permeation kinetics. An alternate approach to mimic thermoregulation was explored; simply, the heat was provided to the skin from the bottom using a regulated heating system. The ex vivo skin system in conjugation with dermal microdialysis sampling was expected to give a significant increase in the permeation profile when compared between ambient laboratory conditions and physiological temperature. However, the fold increase in the AUC values after 24 hrs of microdialysis sample from the dermis suggests that the model is not sensitive to respond to changes in temperature. Mimicking the thermoregulation provided no added benefit to the ex vivo dermal microdialysis system; rather, the process became labor-intensive. It added several extra hours of pre-experimental set-up time; regardless, at the cost of thermal degradation of the subcutaneous fat layer. After 24 hours of sampling duration, the skin was visually different, shrunk 10% in each dimension, and warped at the surface making the whole sampling technique unreliable. Due to the aforementioned reasons, we have decided to use the ex vivo skin model in routine bioavailability studies at ambient laboratory temperatures at around 25 °C.

The ex vivo pig skin microdialysis method was developed with the intention to employ the model in bioequivalence studies of topically applied pharmaceutical products. Comparing the commercially available RLD and approved generic of Metronidazole 0.75% cream from the microdialysis data, the log-normal ratio of T/R for AUC and C_{max} was found within the FDA limits although skewed towards the lower boundary of the 90% confidence interval. The window of

variation (width of the confidence interval) was 24% and 27% for AUC and Cmax respectively. Generally speaking, narrow CI is an indicator of tighter values and is often observed in larger population sizes. In our experimental results, we have observed narrow CI width even when we had a small population size. One possible implication is that the method gives very consistent outputs; however, we would like to accept the results with caution. We firmly believe, increasing the sample size to a larger number, the power and the statistical confidence in the result can be improved.

Yet again, the fact that reference and test formulations can be tested simultaneously, the experimental population size required to establish bioequivalence for TDDPs can be reduced. It is efficient on time and resources and mimics more closely the permeability behavior observed in vivo. The lack of signal in the lateral diffusion rejects any possible cross-talk of dMD probes and indicates the probes implanted underneath a designated formulation application site is specifically measuring their local bioavailability. This current experimental setup may provide a convenient, reliable, cost-effective, table-top, and quantitative approach to routinely evaluate the percutaneous drug permeability of TDDP.

Lastly, we were driven by curiosity to explore the predictability of in vivo PK profile from our current ex vivo bioavailability outcomes. In this exercise, we have mathematically mapped the two profiles with a point-to-point correlation similar to a Level A IVIVC. During this explorative study we had overcome the challenge to introduce the drug to the dermis directly without disturbing the interstitial fluid, quantified absorption independent elimination kinetics, understood the drug disposition and the effect of the microvasculature on the clearance of the drug from the dermis. This simple study was indeed very fruitful in understanding the drug kinetics and dynamics within the dermis tissue.

Dermal microdialysis *ex vivo* can be potentially employed to expand the knowledge of dermis pharmacokinetics. It can be instrumental in small explorative investigations, as well as in larger populations for BA/BE studies. *Ex vivo*, in combination with *in vivo* dermal microdialysis has the potential to become a powerful tool in the future. In addition, dermal microdialysis can provide a link between dermis concentration-time profiles and permeation profiles generated in IVPT studies. While there were several assumptions made in this work, the models proposed in this study can be tested with other compounds with a suitable study design to refine and optimize this tool.

References

1. Kuzma BA, Senemar S, Ramezanli T, Ghosh P, Raney SG, Stagni G. Evaluation of local bioavailability of metronidazole from topical formulations using dermal microdialysis: Preliminary study in a Yucatan mini-pig model. *European Journal of Pharmaceutical Sciences*. 2021;159:105741. doi:10.1016/j.ejps.2021.105741
2. Ault JM, Riley CM, Meltzer NM, Lunte CE. Dermal Microdialysis Sampling in Vivo. *Pharmaceutical Research: An Official Journal of the American Association of Pharmaceutical Scientists*. 1994;11(11):1631-1639. doi:10.1023/A:1018922123774
3. Baumann KY, Church MK, Clough GF, et al. Skin microdialysis: Methods, applications and future opportunities - An EAACI position paper. *Clinical and Translational Allergy*. 2019;9(1):1-13. doi:10.1186/s13601-019-0262-y
4. Schmook FP, Meingassner JG, Billich A. Comparison of human skin or epidermis models with human and animal skin in in-vitro percutaneous absorption. *International Journal of Pharmaceutics*. 2001;215(1-2):51-56. doi:10.1016/S0378-5173(00)00665-7
5. Swindle MM, Makin A, Herron AJ, Clubb FJ, Frazier KS. Swine as Models in Biomedical Research and Toxicology Testing. *Veterinary Pathology*. 2012;49(2):344-356. doi:10.1177/0300985811402846
6. Ranamukhaarachchi SA, Lehnert S, Ranamukhaarachchi SL, et al. A micromechanical comparison of human and porcine skin before and after preservation by freezing for medical device development. *Scientific Reports*. 2016;6. doi:10.1038/srep32074
7. Metronidazole - DrugBank. <https://www.drugbank.ca/drugs/DB00916>
8. Lamp KC, Freeman CD, Klutman NE, Lacy MK. Pharmacokinetics and pharmacodynamics of the nitroimidazole antimicrobials. *Clinical Pharmacokinetics*. 1999;36(5):353-373. doi:10.2165/00003088-199936050-00004
9. Food and Drug Administration, Center for Drug Evaluation and Research. *Guidance for Industry: Statistical Approaches to Establishing Bioequivalence*; 2001. Accessed July 8, 2020. <https://www.fda.gov/media/70958/download>
10. Kuzma B, Senemar S, Stagni G. Estimation Of In Vivo Skin Permeation (Flux) And Cumulative Amount Input of Metronidazole Formulations in Mini-pigs' Dermis. In: *GRS/GRC – Skin Barrier Function of Mammalian Skin*. ; 2019.
11. Ng KW, Lau WM. Skin deep: The basics of human skin structure and drug penetration. In: *Percutaneous Penetration Enhancers Chemical Methods in Penetration Enhancement: Drug Manipulation Strategies and Vehicle Effects*. Springer Berlin Heidelberg; 2015:3-11. doi:10.1007/978-3-662-45013-0_1
12. Prausnitz MR, Elias PM, Franz TJ, et al. *Skin Barrier and Transdermal Drug Delivery*; 2012.
13. Benson HAE. Skin Structure, Function, and Permeation. In: *Topical and Transdermal Drug*

- Delivery*. John Wiley & Sons, Inc.; 2012:1-22. doi:10.1002/9781118140505.ch1
14. *Notice-Draft Guidance for Industry on Topical Dermatological Drug Product NDA's and ANDA's—In Vivo Bioavailability, Bioequivalence, In Vitro Release and Associated Studies; Availability*; 1998. Accessed May 1, 2020. <http://www.hcfa.gov/>
 15. *Draft Guidance for Industry on Topical Dermatological Drug Product NDA's and ANDA's In Vivo Bioavailability, Bioequivalence, In Vitro Release and Associated Studies*.; 1998. Accessed April 29, 2020. <https://www.govinfo.gov/content/pkg/FR-1998-06-18/pdf/98-16141.pdf>
 16. N'Dri-Stempfer B, Navidi WC, Guy RH, Bunge AL. Improved bioequivalence assessment of topical dermatological drug products using dermatopharmacokinetics. *Pharmaceutical Research*. 2009;26(2):316-328. doi:10.1007/s11095-008-9742-9
 17. Baker DE. *Department of Health and Human Services, Food and Drug Administration Guidance for Industry on Special Protocol Assessment; Availability*. Vol 67.; 2002. www.fda.gov/cber/guidelines.htm.
 18. FY2016 Regulatory Science Report: Topical Dermatological Drug Products | FDA. Accessed April 30, 2020. <https://www.fda.gov/industry/generic-drug-user-fee-amendments/fy2016-regulatory-science-report-topical-dermatological-drug-products>
 19. Vlig M, Boekema BKHL, Ulrich MMW. Porcine models. In: *Biomaterials for Skin Repair and Regeneration*. Elsevier; 2019:297-330. doi:10.1016/b978-0-08-102546-8.00010-8
 20. Dorsett-Martin WA. Rat models of skin wound healing: A review. *Wound Repair and Regeneration*. 2004;12(6):591-599. doi:10.1111/j.1067-1927.2004.12601.x
 21. Meyer W, Schwarz R, Neurand K. The skin of domestic mammals as a model for the human skin, with special reference to the domestic pig. *Current problems in dermatology*. 1978;7:39-52. doi:10.1159/000401274
 22. Gore A V., Liang AC, Chien YW. Comparative biomembrane permeation of tacrine using Yucatan minipigs and domestic pigs as the animal model. *Journal of Pharmaceutical Sciences*. 1998;87(4):441-447. doi:10.1021/js970359u
 23. Qvist MH, Hoeck U, Kreilgaard B, Madsen F, Frokjaer S. Evaluation of Gottingen minipig skin for transdermal in vitro permeation studies. *European Journal of Pharmaceutical Sciences*. 2000;11(1):59-68. doi:10.1016/S0928-0987(00)00091-9
 24. Hammarlund-Udenaes M. Microdialysis as an Important Technique in Systems Pharmacology—a Historical and Methodological Review. *AAPS Journal*. 2017;19(5):1294-1303. doi:10.1208/s12248-017-0108-2
 25. Chefer VI, Thompson AC, Zapata A, Shippenberg TS. Overview of Brain Microdialysis. *Current Protocols in Neuroscience*. 2009;47(1):7.1.1–7.1.28. doi:10.1002/0471142301.ns0701s47
 26. Baumann KY, Church MK, Clough GF, et al. Skin microdialysis: Methods, applications and

- future opportunities - An EAACI position paper. *Clinical and Translational Allergy*. 2019;9(1):1-13. doi:10.1186/s13601-019-0262-y
27. Abd E, Yousuf S, Pastore M, et al. Skin models for the testing of transdermal drugs. *Clinical Pharmacology: Advances and Applications*. 2016;Volume 8:163-176. doi:10.2147/CPAA.S64788
 28. Ault JM, Lunte CE, Meltzer NM, Riley CM. Microdialysis Sampling for the Investigation of Dermal Drug Transport. *Pharmaceutical Research: An Official Journal of the American Association of Pharmaceutical Scientists*. 1992;9(10):1256-1261. doi:10.1023/A:1015892914649
 29. Leveque N, Muret P, Makki S, Mac-Mary S, Kantelip JP, Humbert P. Ex vivo Cutaneous Absorption Assessment of a Stabilized Ascorbic Acid Formulation Using a Microdialysis System. *Skin Pharmacology and Physiology*. 2004;17(6):298-303. doi:10.1159/000081115
 30. Döge N, Hönzke S, Schumacher F, et al. Ethyl cellulose nanocarriers and nanocrystals differentially deliver dexamethasone into intact, tape-stripped or sodium lauryl sulfate-exposed ex vivo human skin - assessment by intradermal microdialysis and extraction from the different skin layers. *Journal of Controlled Release*. 2016;242:25-34. doi:10.1016/j.jconrel.2016.07.009
 31. Holmgaard R, Benfeldt E, Nielsen JB, et al. Comparison of open-flow microperfusion and microdialysis methodologies when sampling topically applied fentanyl and benzoic acid in human dermis ex vivo. *Pharmaceutical research*. 2012;29(7):1808-1820. doi:10.1007/s11095-012-0705-9
 32. Critical Path Initiative | FDA. Accessed July 10, 2020. <https://www.fda.gov/science-research/science-and-research-special-topics/critical-path-initiative>
 33. Lionberger RA. FDA critical path initiatives: Opportunities for generic drug development. *AAPS Journal*. 2008;10(1):103-109. doi:10.1208/s12248-008-9010-2
 34. Shippenberg TS, Thompson AC. Overview of Microdialysis. doi:10.1002/0471142301.ns0701s00
 35. Hsiao JK, Ball BA, Morrison PF, Mefford IN, Bungay PM. Effects of Different Semipermeable Membranes on In Vitro and In Vivo Performance of Microdialysis Probes. *Journal of Neurochemistry*. 1990;54(4):1449-1452. doi:10.1111/j.1471-4159.1990.tb01982.x
 36. Cremers TIFH, de Vries MG, Huinink KD, et al. Quantitative microdialysis using modified ultraslow microdialysis: Direct rapid and reliable determination of free brain concentrations with the MetaQuant technique. *Journal of Neuroscience Methods*. 2009;178(2):249-254. doi:10.1016/j.jneumeth.2008.12.010
 37. Stagni G, O'Donnell D, Liu YJ, Kellogg DL, Shepherd AMM. Iontophoretic current and intradermal microdialysis recovery in humans. *Journal of Pharmacological and Toxicological Methods*. 1999;41(1):49-54. doi:10.1016/S1056-8719(99)00027-1

38. Shippenberg TS, Thompson AC. Overview of Microdialysis. *Current Protocols in Neuroscience*. 1997;00(1):7.1.1-7.1.22. doi:10.1002/0471142301.ns0701s00
39. Larsson CI. The use of an "internal standard" for control of the recovery in microdialysis. *Life Sciences*. 1991;49(13). doi:10.1016/0024-3205(91)90082-M
40. Lai J, Maibach HI. Experimental Models in Predicting Topical Antifungal Efficacy: Practical Aspects and Challenges. *Skin Pharmacology and Physiology*. 2009;22(5):231-239. doi:10.1159/000235827
41. Food and Drug Administration. *Draft Guidance for Industry on Topical Dermatological Drug Product NDA's and ANDA's—In Vivo Bioavailability, Bioequivalence, In Vitro Release and Associated Studies.*; 1998. Accessed April 29, 2020. <https://www.govinfo.gov/content/pkg/FR-1998-06-18/pdf/98-16141.pdf>
42. Raney SG, Franz TJ, Lehman PA, Lionberger R, Chen ML. Pharmacokinetics-Based Approaches for Bioequivalence Evaluation of Topical Dermatological Drug Products. *Clinical Pharmacokinetics*. 2015;54(11):1095-1106. doi:10.1007/s40262-015-0292-0
43. *MEDICARE PRESCRIPTION DRUG, IMPROVEMENT, AND MODERNIZATION ACT OF 2003.*; 2000.
44. Kuzma B, Senemar S, Ramezanli T, Ghosh P, Raney SG, Stagni G. Evaluation of Local Bioavailability of Metronidazole from Topical Formulations using Dermal Microdialysis: Preliminary Studies in Yucatan Mini-Pig. In: *AAPS PharmSci 360.* ; 2018. doi:10.13140/RG.2.2.32378.54725
45. Narasimha Murthy S. Characterizing the Critical Quality Attributes and In Vitro Bioavailability of Acyclovir and Metronidazole Topical Products. In: *Topical Dermatological Generic Drug Products: Overcoming Barriers to Development and Improving Patient Access.* The Food and Drug Administration (FDA); 2017.
46. Benfeldt E, Hansen SH, Vølund A, Menné T, Shah VP. Bioequivalence of topical formulations in humans: Evaluation by dermal microdialysis sampling and the dermatopharmacokinetic method. *Journal of Investigative Dermatology*. 2007;127(1):170-178. doi:10.1038/sj.jid.5700495
47. Boelsma E, Anderson C, Karlsson AMJ, Ponc M. Microdialysis technique as a method to study the percutaneous penetration of methyl nicotinate through excised human skin, reconstructed epidermis, and human skin in vivo. *Pharmaceutical Research*. 2000;17(2):141-147. doi:10.1023/A:1007505011474
48. Holmgaard R, Benfeldt E, Nielsen JB, et al. Comparison of open-flow microperfusion and microdialysis methodologies when sampling topically applied fentanyl and benzoic acid in human dermis ex vivo. *Pharmaceutical research*. 2012;29(7):1808-1820. doi:10.1007/s11095-012-0705-9
49. Tettey-Amlalo RNO, Kanfer I, Skinner MF, Benfeldt E, Verbeeck RK. Application of dermal microdialysis for the evaluation of bioequivalence of a ketoprofen topical gel. *European*

Journal of Pharmaceutical Sciences. 2009;36(2-3):219-225.
doi:10.1016/j.ejps.2008.09.002

50. Cross SE, Roberts MS. Use of in vitro human skin membranes to model and predict the effect of changing blood flow on the flux and retention of topically applied solutes. *Journal of Pharmaceutical Sciences.* 2008;97(8):3442-3450. doi:10.1002/jps.21253
51. Lboutounne Y, Silva J, Pazart L, Bérard M, Muret P, Humbert P. Microclimate next to the skin: influence on percutaneous absorption of caffeine (ex-vivo study). *Skin Research and Technology.* 2014;20(3):293-298. doi:10.1111/srt.12118
52. Scheuplein RJ. Analysis of Permeability Data for the Case of Parallel Diffusion Pathways. *Biophysical Journal.* 1966;6(1):1-17. doi:10.1016/S0006-3495(66)86636-5
53. Blank IH, Scheuplein RJ, Macfarlane DJ. Mechanism of Percutaneous Absorption: III. The Effect of Temperature on the Transport of Non-Electrolytes Across the Skin. *Journal of Investigative Dermatology.* 1967;49(6):582-589. doi:10.1038/jid.1967.184
54. Yin Q, Wang R, Yang S, et al. Influence of Temperature on Transdermal Penetration Enhancing Mechanism of Borneol: A Multi-Scale Study. *International Journal of Molecular Sciences.* 2017;18(1):195. doi:10.3390/ijms18010195
55. Hao J, Ghosh P, Li SK, Newman B, Kasting GB, Raney SG. Heat effects on drug delivery across human skin. *Expert Opinion on Drug Delivery.* 2016;13(5):755-768. doi:10.1517/17425247.2016.1136286
56. Akomeah F, Nazir T, Martin GP, Brown MB. Effect of heat on the percutaneous absorption and skin retention of three model penetrants. *European Journal of Pharmaceutical Sciences.* 2004;21(2-3):337-345. doi:10.1016/j.ejps.2003.10.025
57. Andersen IL, Egil Bøe K, Hove K, Andersen IL, Hove KE, Behavioural K 2000. *Behavioural and Physiological Thermoregulation in Groups of Pregnant Sows Housed in a Kennel System at Low Temperatures.*
58. Soerensen DD, Pedersen LJ. Infrared skin temperature measurements for monitoring health in pigs: A review. *Acta Veterinaria Scandinavica.* 2015;57(1):5. doi:10.1186/s13028-015-0094-2
59. Scheuplein RJ. Mechanism of percutaneous adsorption. I. Routes of penetration and the influence of solubility. *The Journal of investigative dermatology.* 1965;45(5):334-346. doi:10.1038/jid.1965.140
60. Roberts M, Mohammed Y, Namjoshi S, et al. Correlation of physicochemical characteristics and in vitro permeation test (IVPT) results for acyclovir and metronidazole topical products FDA Workshop on Bioequivalence Testing of Topical Drug Products. In: *Topical Dermatological Generic Drug Products: Overcoming Barriers to Development and Improving Patient Access.* The Food and Drug Administration (FDA); 2017. <https://www.fda.gov/media/110256/download>

61. Administration, Food and Drug C for DE and R. *Guidance for Industry-Bioequivalence Studies with Pharmacokinetic Endpoints for Drugs Submitted Under an ANDA.*; 2013. Accessed January 28, 2021. <http://www.fda.gov/Drugs/GuidanceComplianceRegulatoryInformation/Guidances/default.htm>.
62. Sharareh Senemar, Benjamin Kuzma, Tannaz Rameznali, Priyanka Ghosh, Sam Raney, Grazia Stagni. Evaluating the Bioequivalence of Topical Dermatological Drug Products containing Metronidazole using Dermal Microdialysis: Preliminary Studies in Rabbit. In: *AAPS PharmSci* 360. ; 2019. Accessed February 23, 2021. https://virtual.aaps.org/pdfviewer/web/viewer.html?file=https%3A//virtual.aaps.org/aaps/download/poster%3Fcm_id%3D284235
63. Bodenlenz M, Augustin T, Birngruber T, et al. Variability of Skin Pharmacokinetic Data: Insights from a Topical Bioequivalence Study Using Dermal Open Flow Microperfusion. doi:10.1007/s11095-020-02920-x
64. Khan GM, Frum Y, Sarheed O, Eccleston GM, Meidan VM. Assessment of drug permeability distributions in two different model skins. *International Journal of Pharmaceutics*. 2005;303(1-2):81-87. doi:10.1016/j.ijpharm.2005.07.005
65. Meidan VM, Roper CS. Inter- and intra-individual variability in human skin barrier function: A large scale retrospective study. *Toxicology in Vitro*. 2008;22(4):1062-1069. doi:10.1016/j.tiv.2008.01.009
66. Dąbrowska AK, Spano F, Derler S, Adlhart C, Spencer ND, Rossi RM. The relationship between skin function, barrier properties, and body-dependent factors. *Skin Research and Technology*. 2018;24(2):165-174. doi:10.1111/srt.12424
67. Derraik JGB, Rademaker M, Cutfield WS, et al. Effects of Age, Gender, BMI, and Anatomical Site on Skin Thickness in Children and Adults with Diabetes. Brandner JM, ed. *PLoS ONE*. 2014;9(1):e86637. doi:10.1371/journal.pone.0086637
68. Holmgaard R, Benfeldt E, Sorensen JA, Nielsen JB. Chronological Age Affects the Permeation of Fentanyl through Human Skin in vitro. *Skin Pharmacology and Physiology*. 2013;26(3):155-159. doi:10.1159/000348876
69. Kaur P, Jiang X, Duan J, Stier E. Applications of In Vitro-In Vivo Correlations in Generic Drug Development: Case Studies. doi:10.1208/s12248-015-9765-1
70. Food and Drug Administration, Center for Drug Evaluation and Research (CDER). *Guidance for Industry Extended Release Oral Dosage Forms: Development, Evaluation, and Application of In Vitro/In Vivo Correlations*. Vol 20857. Tel; 1997. Accessed March 1, 2021. <http://www.fda.gov/cder/guidance/index.htm>
71. Wagner JG, Nelson E. Per cent absorbed time plots derived from blood level and/or urinary excretion data. *Journal of Pharmaceutical Sciences*. 1963;52(6):610-611. doi:10.1002/jps.2600520629

72. Sumena KB, Lucy K, Chungath JJ, Ashok N, Harshan K. Morphology of the Skin in Large White Yorkshire Pigs. *Indian Journal of Animal Research*. 2010;44(1):55-57.
73. Branski LK, Mittermayr R, Herndon DN, et al. A porcine model of full-thickness burn, excision and skin autografting. *Burns*. 2008;34(8):1119-1127. doi:10.1016/j.burns.2008.03.013
74. Eggleston TA, Roach WP, Mitchell MA, Smith K, Oler D, Johnson TE. Comparison of Two Porcine (*Sus scrofa domestica*) Skin Models for In Vivo Near-Infrared Laser Exposure.
75. Schicksnus G, Müller-Goymann CC. Lateral Diffusion of Ibuprofen in Human Skin during Permeation Studies. *Skin Pharmacology and Physiology*. 2004;17(2):84-90. doi:10.1159/000076018
76. Gee CM, Nicolazzo JA, Watkinson AC, Finnin BC. Assessment of the Lateral Diffusion and Penetration of Topically Applied Drugs in Humans Using a Novel Concentric Tape Stripping Design. *Pharmaceutical Research*. 2012;29(8):2035-2046. doi:10.1007/s11095-012-0731-7
77. Hill S. Pharmacokinetics of drug infusions. *Continuing Education in Anaesthesia Critical Care & Pain*. 2004;4(3):76-80. doi:10.1093/bjaceaccp/mkh021
78. Costello C, Rossenu S, Vermeulen A, Cleton A, Dunne A. A time scaling approach to develop an in vitro-in vivo correlation (IVIVC) model using a convolution-based technique. *Journal of Pharmacokinetics and Pharmacodynamics*. 2011;38(5):519-539. doi:10.1007/s10928-011-9206-4
79. Patel H, Joshi A, Joshi A, Stagni G. Transdermal Delivery of Etoposide Phosphate II: In Vitro In Vivo Correlations (IVIVC). *Journal of Pharmaceutical Sciences*. 2016;105(7):2139-2145. doi:10.1016/j.xphs.2016.04.022
80. Yang Y, Manda P, Pavurala N, Khan MA, Krishnaiah YSR. Development and validation of in vitro-in vivo correlation (IVIVC) for estradiol transdermal drug delivery systems. *Journal of Controlled Release*. 2015;210:58-66. doi:10.1016/j.jconrel.2015.05.263
81. OECD. Meat consumption (indicator). Published 2021. Accessed March 31, 2021. doi:10.1787/fa290fd0-en

Author's Bio

Summary

I am a methodical, ambitious and always evolving researcher with proven leadership skills. I have a versatile expertise in Pharmaceutical manufacturing, Preclinical pharmacological evaluations (including in vivo, in vitro and ex vivo experimentation), Formulation BA/BE evaluation, Bioanalysis (small and large molecules as per ICH bioanalytical guidelines), and Pharmacokinetic modeling and simulation. I enjoy collaborating with scientists from different disciplines and always on the look to expand my skillset and solve newer challenges.

Work Experience

Research Scientist, Formulation Development

Jan 2021 onwards

Solaris Pharma Corporation, Bridgewater, New Jersey.

- Formulated reverse engineered retinoids based and pain management products intended for regulatory filings. Developing topical formulations to treat skin carcinoma, herpes singles, and anesthetics.
- Undertook exhibit batches for ANDA application.
- Formulation experience in semi-solid products- cream, gel, lotion, jelly and aerosol.
- Prepared FDA product briefing documents, product specifications, manufacturing and stability protocols.

Ph.D Intern

May 2019-Aug 2019

Regeneron Pharmaceuticals, Inc., Tarrytown, New York.

- Involved in collaborative project between Analytical Chemistry Group and Formulation Development Group.
- Development and validation of mass spectrometry- based analytical method as per USFDA guidelines to accurately measure the concentrations of monoclonal antibodies (mAbs) in co-mixture products using tryptic digestion.
- Techniques learnt- sample handling of mAbs, reduction, tryptic digestions, in-silico MRM precursor-daughter fragment prediction and simulation, optimization of MS/MS

Senior Officer at Product Development Laboratories

Sept 2009-Aug 2012

Sun Pharma, Paonta Sahib, HP, India.

- Supervisor in-charge of core activity area of Product Development Laboratory
 - Planning, execution and monitoring of trial, scale-up, exhibit, registration and tech transfer batches as per regulatory guidelines.
 - Sound knowledge in commercial dry/wet granulation, Wurster process (granulation and coating), tablet compression and coating, capsule filling, softgel encapsulation, etc.
 - Proficient in various formulation techniques, troubleshooting, in-process analysis, interpretation of analytical data, and compilation of reports.
 - Compilation of manufacturing protocols and reports for trial, scale-up, exhibit and process validation batches.
 - Key responsible personnel in inventory procurement, facility maintenance, man-power management, proper documentation and cGMP compliance of dedicated processing area
 - Initiation and handling of process deviations, change controls and investigation, CAPA.
 - SOP creation and review
 - Implementation of Quality management software, viz- Document Compliance Manager, TrackWise and Learning Management System.
-

Technical skills & key accomplishments

- Dermal microdialysis studies: To estimate dermal bioavailability in dermis interstitial tissue from topical drug applications and determination of bioequivalence.
- Permeation assay: In-vivo, In-vitro and Ex-vivo permeation assay of drugs from topical, transdermal and intradermal administration of drugs in rabbit and pig models.
- Modelling and simulations: Non-compartmental analysis to characterize PK parameters using Winnonlin. Ability to work independently on in-silico modelling and simulation using SimCyp platforms.
- Mass Spectrometry: development and validation of LC-UV and MS/MS techniques for detection of small and large molecules in co-mixtures.
- Cardiovascular safety assessment: by QT prolongation in rat model and expertise in various pharmacological screening.

Education

Ph.D., Pharmaceutical Sciences

2015-2020

Long Island University, Brooklyn, NY

- Advisor: Grazia Stagni, Ph.D.
- Thesis: "Ex vivo Dermis Microdialysis: A Tool for Bioequivalence Testing of Topical Dermatological Drug Product (Demonstration of Proof of Concept and Testing)"
- Other Projects: Fabrication, characterization and performance evaluation of drug loaded dissolving microneedle patches.
- Instrumental efficiency: HPLC, LC-MS/MS, Microdialysis, Franz Diffusion Cell, DSC, TGA, Texture analyzer.
- Notable courses: Advanced Biopharmaceutics / Pharmacokinetics, Mathematical Modeling, PBPK Modeling and Simulation, Biostatistics, Drug Metabolism & Disposition, Methods of Pharmaceutical Analysis, Dosage Form Design.

Master's in Pharmaceutical Sciences

2012-2014

Jadavpur University, Kolkata, WB, India

- Advisor: Sanmay Karmakar, Ph.D.
- Thesis: "An improvised QTc interval study model for predictive cardio-safety assessment".
- Other Projects: Evaluation of upregulation/downregulation of Ikr ion-channel in heart tissue with modulation in biological parameters.
- Instrumental efficiency: Electrocardiography (ECG), Nanodrop, Fluorescence microscopy, rtPCR
- Notable courses: Advanced Biopharmaceutics / Pharmacokinetics, Experimental Pharmacology, Biochemistry

Bachelor of Pharmacy

2005-2009

West Bengal University of Technology, Kolkata, WB, India

Publications & Conference Presentations

- Ex Vivo Dermis Microdialysis: Method Development and Testing (Poster - AAPS PharmSci360 2020).
- Fabrication and Characterization of a Microneedle Patch Prepared by Air-Pressure Assisted Filling and Drying (Poster - AAPS Annual meeting 2017)
- QT Prolongation by Ranitidine in Hypokalemia and Arrhythmogen Provoked Rat Heart (2017). Vascular Diseases and Therapeutics (DOI: 10.15761/VDT.1000125.)
- Beverage Induced Enhanced Bioavailability of Carbamazepine and its Consequent Effect on The Antiepileptic Activity and Toxicity (2014). Journal of Food and Drug Analysis (DOI: <http://dx.doi.org/10.1016/j.jfda.2014.07.012>)

Summary of Expertise

- Deep understanding and proven ability to work independently in the field pharmaceuticals, biopharmaceuticals, physiology-based pharmacokinetics (PBPK), mathematical modeling (compartmental and non-compartmental) and bioanalytics.
- Used Phoenix WinNonlin to perform PK analysis (NCA and compartment modeling), bioequivalence (ABE and RSABE), dose-response relationship, estimated permeation independent local disposition of drug, establish unit impulse response, absorption predictions, PK-PD development and IVIVC calculation.
- Used SimCyp to simulate the systemic exposure of test drug with known CYP3A4 competitive inhibitors. Created substrate profile from available published data and validated in-silico data with clinical findings. Working knowledge with enzymes and transporters.
- 3 years of industrial experience at a GMP setting in solid oral & topical product development and assisted in regulatory filing. Ability to expand to newer formulation techniques.
- Ability to implement design-of-experiment and modern tools to optimize formulation target profile and characterize quality parameters.
- 7 years of experience in H/UPLC based bioanalytical development with equivalent pharmacology and pharmacometric-based-drug development and evaluation process.
- Ability to design quantitative and translational pharmacokinetic experiments and design MS-based bioanalytical methods for small and large molecules.
- Relevant therapeutic area of work: transdermal, cardiovascular.
- Proficiency in software platforms: PhoenixWinNonlin, Simcyp, PK-Sim, Prism GraphPad, Thermo Xcalibur, Agilent MassHunter, Waters Empower, Skyline.

Professional affiliations, Awards and Leadership skills

- Served as Chair-elect (2017) and Chair (2018), AAPS Student Chapter at LIU – Brooklyn.
- Lead a team of talented graduate students to earn the prestigious AAPS Student Chapter of The Year (SCOTY 2019)
- Awarded Rho Chi Honor for academic excellence (2017)
- Organized the NIPTE conference 2018 at LIU-Brooklyn
- American Association of Pharmaceutical Scientists (AAPS) member

LinkedIn

<https://www.linkedin.com/in/mdasifali/>
